



NTNU – Trondheim
Norwegian University of
Science and Technology

Developing molecular tools for the genetic manipulation of *Nannochloropsis*

Oxana Chernyavskaya

Biotechnology (5 year)

Submission date: July 2014

Supervisor: Martin Frank Hohmann-Marriott, IBT

Co-supervisor: Rahmi Lale, IBT

Norwegian University of Science and Technology
Department of Biotechnology

Abstract

The main aim of the master project was the establishment of the efficient protocols for the genetic manipulation (nuclear transformation and chloroplast transformation) of *Nannochloropsis oceanica* CCMP1779. *Nannochloropsis* is a heterokont algae and a potential producer of biofuel and high value lipids, as it can accumulate significant amount of triacylglycerols.

Cell concentration is an essential parameter for establishing an electroporation protocol. Therefore, a convenient method for the determination of cell concentration was established. Determination of cell concentrations by hemocytometer, flow cytometer and optical density at 750 nm (OD_{750nm}) were compared with one another. Satisfactory correlation between flow cytometer and OD_{750nm} as an indicator of cell growth was established by preparing the accurate standard curves. It was revealed that the maximum cell density that could be reliably determined by the flow cytometer was 5.85×10^6 cells/mL corresponding to an OD_{750nm} value of 0.1169. It was evaluated under what conditions cells could be harvested and stored and counted at a later point. A storage protocols that used glutaraldehyde and snap-freeze in liquid nitrogen decreased the number of counted cells by less than 4 and 3% respectively, compared to the number of cells counted in fresh samples.

To achieve nuclear transformation of *N. oceanica* CCMP1779, the plasmid pSELECT100 was used. As this plasmid contains a hygromycin resistance cassette, the hygromycin concentration that prevented growth of untransformed wild type cells on agar plates was assessed. These experiments revealed that hygromycin concentration of 30-50 $\mu\text{g/mL}$ resulted in no growth. Consequently, the selective medium for the screening of transformants contained 50 $\mu\text{g/mL}$ hygromycin.

Parameters that result in efficient nuclear transformation, such as harvesting cell concentrations, cell washing steps, voltage and resistance applied under electroporation, incubation of the transformed cells, and addition of the carrier DNA, were investigated. The experiments revealed that growing the cells up to an exponential phase concentration of $2-4 \times 10^6$ cells/mL resulted in competent for transformation cells. The highest transformation efficiency achieved at the experiment was 4.08×10^{-5} colonies/cells/ μg , which was a higher efficiency compared to the available transformation protocols. A voltage of 1800 volts and resistance of 500 Ohm and a relative low amount of the transformation plasmid DNA ($\sim 1 \mu\text{g}$) resulted in the highest transformation efficiencies.

Genetic manipulation of the chloroplast genome by biolistic transformation (particle bombardment) has been established in several microalgae. As no published protocols exist for

the chloroplast transformation of *Nannochloropsis*, the initial steps to develop a protocol, which are based on integrating an antibiotic resistance cassette into the chloroplast genome, were made.

A wide range of antibiotics was evaluated to establish which antibiotic inhibits cell growth at a low concentration, in addition to availability of antibiotic resistance cassette in the lab at the Department of Biotechnology. Growth experiments on agar plates supplemented with different antibiotics (ampicillin, apramycin, chloramphenicol, cycloheximide, gentamycin, G418 neomycin, hygromycin, kanamycin, spectinomycin, and tetracaine) at different concentrations revealed that chloramphenicol inhibits growth at $\geq 20 \mu\text{g/mL}$. Consequently, agar-solidified selective medium containing chloramphenicol at a concentration of $40 \mu\text{g/mL}$ was used to select for cells transformed by particle bombardment.

Modern DNA sequence assembly (Gibson Assembly) was carried out to generate a plasmid (pLit_chlL_chlor) that carried the chloramphenicol resistance gene flanked by sequences of the *chlL* gene that is native to *N. oceanica* CCMP1779. The choice of the gene was based on the assessment that heterokont algae also encode a gene within the nucleus catalyzing the same reaction (i.e. conversion of protochlorophyllide to chlorophyllide). This makes the deletion of the *chlL* gene unimportant for the cell growth under constant light supply.

The transformation of the chloroplast genome with the plasmid pLit_chlL_chlor was performed with biolistic delivery technology using tungsten microparticles coated with the plasmid DNA. The technique was previously reported being more efficient for plastid transformation by homologous recombination. The screening of the potential transformants on the selective medium resulted in appearance of few colonies indicating the successful transformation. However, the incubation of the cell colonies in the selective liquid medium did not result in any cell growth, leaving the confirmation of the successful insertion of the chloramphenicol resistance cassette as an experiment of future research.

Sammendrag

Målet med dette prosjektet har vært å etablere protokoller for effektiv genetisk manipulering av mikroalgen *Nannochloropsis oceanica* CCMP1779 via transformasjon (både til det nukleære genomet og til kloroplastgenomet). *Nannochloropsis* er en heterokont alge og også en potensiell produsent av biodrivstoff og lipider, ettersom disse algene er i stand til å akkumulere relativt store mengder triacylglyceroler.

Å vite den nøyaktige cellekonsentrasjon er viktig for å få etablert en protokoll for genetisk transformasjon via elektroporering. Derfor har en del av prosjektet dreid seg om å finne en effektiv metode for nøyaktig bestemmelse av cellekonsentrasjon. Cellekonsentrasjonsmålinger utført med både hemocytometri, flow-cytometri og optisk densitet målt ved 750 nm (OD_{750nm}), ble sammenlignet med hverandre. Standardkurver ble lagd både ved hjelp av flow-cytometri og spektrofotometri (OD_{750nm}), og disse dataene ble kombinert til en korrelasjonskurve som viste en god korrelasjon mellom de to datatypene. Den høyeste cellekonsentrasjonen som kan måles ved flow-cytometri med noenlunde pålitelighet, ble anslått til å være 5.85×10^6 celler/mL. Denne cellekonsentrasjonen hadde en korresponderende OD_{750nm} verdi på 0.1169. Det ble i tillegg gjort en evaluering på under hvilke forhold celler kan høstes, lagres og telles for senere forsøk. Protokoller for fiksering av celler med glutaraldehyd og nedfrysing i flytende nitrogen, viste seg å redusere antall celler med henholdsvis 4 og 3%, sammenliknet med ubehandlet cellekultur. Disse resultatene viste at det er mulig å lagre algeceller uten et alt for stort tap.

For å transformere *N. oceanica* CCMP1779 celler, ble transformasjonsplasmidet pSELECT100 brukt. Ettersom dette plasmidet inneholder resistans-genet for hygromycin, ble det utført en analyse av forskjellige hygromycinkonsentrasjoner, for å evaluere hvilke konsentrasjoner som inhiberte vekst av uttransformerte vill-type-celler. Disse eksperimentene viste at hygromycinkonsentrasjoner på 30-50 $\mu\text{g/mL}$ var i stand til å inhibere cellevekst. Derfor ble det brukt 50 $\mu\text{g/mL}$ hygromycin i seleksjonsmediet for å effektivt kunne skille transformanter fra celler som ikke hadde mottatt resistansgener via transformasjon.

Parametere som har vist seg å kunne påvirke resultater av nukleær transformasjon ble undersøkt. De undersøkte parameterne inkluderte cellekonsentrasjon ved høsting, vask av cellene, spenning og resistans brukt under elektroporering, forhold for inkubering av transformerte celler (inkludert lysstyrke, temperatur og vekstmedia) og bruk av bærer-DNA. Eksperimentene viste at celler som ble gjort kompetente mens de var i eksponentiell vekstfase ($2-4 \times 10^6$ celler/mL) ga høyest rate av vellykket transformasjon. Den høyeste transformasjonseffektivitet som ble oppnådd i løpet av prosjektet var på 4.08×10^{-5} kolonier/celler $\times\mu\text{g}$ (der μg indikerer mengde transformasjonsplasmidet brukt). Dette er også den høyeste transformasjonseffektiviteten som tidligere er rapportert i studier av transformasjon

av *Nannochloropsis* via elektroporering. Spenning på 1800 volt og resistans på 500 ohm brukt i kombinasjon med en relativt liten mengde transformasjonsplasmid-DNA (~1 µg) resulterte i den mest effektive transformasjonen.

Genetisk manipulasjon av kloroplastgenomet via biolistisk transformasjon har blitt rapportert for flere typer mikroalger. Ettersom det enda ikke finnes noen publisert protokoll for kloroplasttransformasjon i *Nannochloropsis*, ble det i dette masterprosjektet startet forarbeid for å få utarbeidet en slik protokoll. Dette arbeidet ble innledet ved å integrere gener for antibiotikaresistans i *Nannochloropsis*' kloroplastgenom.

Et bredt spekter av antibiotikatyper ble evaluert for å bestemme lav konsentrasjon av hvilke antibiotika ville inhiberer cellevekst og resistensgenet av hvilke var tilgjengelig på lab i Bioteknologi Departement. Veksteksperimentet ble utført på agar-plater tilsatt ulike konsentrasjoner av forskjellige typer antibiotika (ampicillin, apramycin, kloramfenikol, cycloheximid, gentamycin, G418 neomycin, hygromycin, kanamycin, spectinomycin og tetracain). Disse forsøkene avslørte at kloramfenikol inhiberer cellevekst ved konsentrasjoner på ≥ 20 µg/mL. Som følge av resultatene på disse eksperimentene ble en konsentrasjon på 40 µg kloramfenikol/mL brukt i seleksjonsmediet for å selektere celler som ble transformert via biolistisk transformasjon.

Moderne DNA-sekvens-sammensetning (Gibson Assembly) ble gjennomført for å konstruere et plasmid (pLit_chlL_chlor) som inneholder genet for kloramfenikolresistens flankert av DNA-sekvenser fra *chlL*-genet til *N. oceanica* CCMP1779. *chlL*-genet ble valgt på grunnlag av at heterokonte alger har et nukleært gen som koder et protein som katalyserende den samme reaksjonen som *chlL* gjør (omdannelse av protochlorophyllid til chlorophyllid). Dette gjør at *chlL*-genet kan unnværes hvis celleveksten skjer under konstant belysning.

Transformasjon av kloroplastgenomet i *Nannochloropsis* med plasmidet pLit_chlL_chlor ble gjennomført med biolistisk teknologi ved bruk av wolfram partikler dekket med plasmid-DNA. Teknikken er tidligere rapportert å være den mest effektive for kloroplasttransformasjon via homolog rekombinasjon. Seleksjon av potensielle transformanter ble gjort ved å bruke seleksjonsmedium, og transformasjonen viste seg å resultere i dannelse av noen få cellekolonier. Ved forsøk på å overføre cellekolonier til flytende seleksjonsmedium som inneholdt samme konsentrasjon av kloramfenikol, ble ingen cellevekst observert. Derfor vil spørsmålet om hvorvidt kloramfenikolresistensgenet faktisk ble integrert i kloroplastgenomet til *Nannochloropsis*, være et mulig fremtidig forskningsprosjekt.

Acknowledgements

This project has been carried out at the Faculty of Natural Sciences and Technology, Department of Biotechnology, NTNU, at the research group of Photosynthesis & Bioenergy. I would like to express a great appreciation to my Associate Professor Martin Frank Hohmann-Marriott for being a tremendous support for me during my master project. Your constant optimism and interest in my project infected me and helped me through long and hard evenings at the lab when nothing seemed to work. Your encouragement kept me motivated.

I would also like to thank my second supervisor, PhD student Alice Mühlroth for having enormous patience and tolerance for me. You have really contributed to my development as a scientist during several months of my master practice. You were running with me in between the labs and floors at the departments, constantly teaching me new techniques and the way of becoming an independent researcher. You have never given up on me. I will always appreciate you as my first mentor.

I am also grateful to my co-workers from the research group, especially PhD students Gunvor Røkke and Jacob Lamb for contributing with their knowledge and experience to different aspects of my research. Especially, I want to thank Gunvor Røkke and another master student Ksenia Gulyaeva for their complete support and belief in my success. You have been there for me cheering me up with our conversations.

I want to thank the rest of Photosynthesis & Bioenergy research group for being such good co-workers, and bringing that amazing atmosphere to our partnership during the period of my master project. I realized how important it is to have a great chemistry at the working place and how it contributes to a work performance. One thing I am sure about is that I will miss it a lot.

I am grateful to Professor Olav Vadstein for giving me an opportunity being one of few with access to BD Accuri C6 flow cytometry located at his lab. It made my experiments possible and gave me a chance to learn a new technology as it is important to keep up with development in the field of biotechnology.

Finally yet importantly, I would like to thank my mother for her enormous support and encouragement during my six years at NTNU and especially during my master project. We crossed this finish line together. I would not have made it without you.

Contents

Abstract	1
Sammendrag	3
Acknowledgements	5
Contents	6
Chapter I: <i>Nannochloropsis</i>	10
The Potential of <i>Nannochloropsis</i>	11
Genome Manipulation	13
Oil Production	15
Chapter II - Correct Cell Count Estimation: Introduction	17
Flow cytometry	17
The setups of flow cytometer	18
Result analysis	19
Goal	19
Materials and Methods	19
Growth conditions	19
Correlation between cell count and OD values	21
Results and Discussion	22
Growth conditions	22
Cell count correlation with OD _{750nm}	24
Cell count loss induced by fixation and snap-freeze	27
Establishment of cell density limits for flow cytometry	28
Conclusion	31
Chapter III – Cell Growth Assay: Introduction	33
Goal	34
Materials and Methods	34
Results and Discussion	36
Hygromycin (experiment # 2)	36
Chloramphenicol (experiment # 3)	37
Initial experiment # 1	39
Comparison of cell sensitivity to <i>N. oceanica</i> and <i>N. gaditana</i>	41
Conclusion	44
Chapter IV – Transformation by Electroporation: Introduction	46
Genetic transformation	46
Electroporation	46

Difficulties	49
Goal	49
Materials and Methods	50
Transformation plasmid pSELECT100	50
Plasmid verification	51
Cutting with SmaI	51
DNA sequencing	51
Plasmid amplification methods	51
Electroporation protocol	53
Screening method	55
Transformation added carrier DNA.....	57
Results and Discussion	58
Plasmid verification	58
pSELECT100 DNA sequencing	59
Amplification of pSELECT100.....	60
Electroporation	60
Screening method	63
Transformation added carrier DNA.....	70
Transformation efficiency	73
Conclusion	75
Chapter V: Introduction	77
Gibson Assembly.....	77
Plasmid insertion by homologous recombination	79
<i>chlL</i> gene.....	79
<i>psbY</i> gene.....	80
The gap region between <i>ycf54</i> and <i>secA</i> genes.....	80
Antibiotic resistance	82
Chloramphenicol	82
Goal	82
Materials and Methods	83
Primer design	83
Amplification of the fragments.....	85
Gibson Assembly.....	86
Results and Discussion	87
Conclusion	91

Chapter VI – Biolistic Transformation: Introduction	93
Biolistic transformation	94
Goal	96
Materials and Methods	97
Cell culture	97
Preparation of microcarriers	97
Preparation of microcarriers for biolistic transformation	97
Preparation of Particle Delivery System	98
Microparticles bombardment.....	98
Results and Discussion	99
Conclusion	101
Future Research	102
Cell growth	102
Colony PCR.....	103
GFP	103
The need for an appropriate promoter	104
Biolistic transformation	104
Bacterial Magnetic Particles	105
Gene knock-out.....	105
References	107
Appendix	114
Appendix A – Chapter II: Correct Cell Concentration Estimation	114
Appendix B – Chapter III: Cell Growth Assay (Antibiotic Susceptibility)	119
Appendix C – Chapter IV: Transformation by Electroporation	120
Appendix D – Chapter V: Gibson Assembly	131

Chapter I

Nannochloropsis

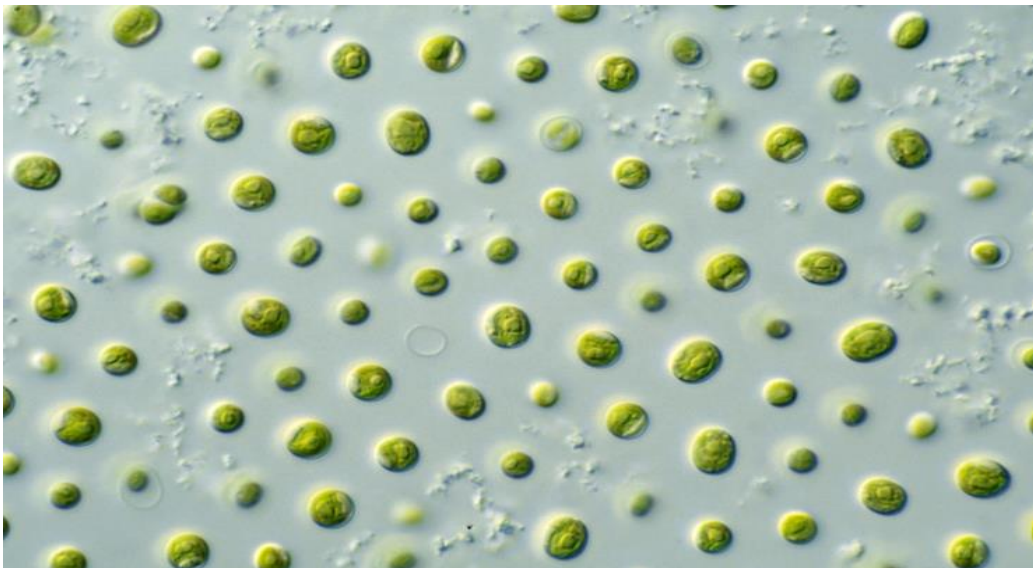


Photo: The Commonwealth Scientific and Industrial Research Organization (CSIRO)

Chapter I: *Nannochloropsis*

Nannochloropsis is a genus of eukaryotic algae and includes currently six species (*N. gaditana*, *N. granulata*, *N. limnetica*, *N. oceanica*, *N. oculata*, *N. salina*). The genus *Nannochloropsis* was first mentioned by Hibberd in 1981 (Hibberd D. J. 1981). *Nannochloropsis* species are heterokonts having their plastids derived by secondary endosymbiosis. The occurrence of secondary symbiosis included transfer of photosynthetic plastids into other eukaryotic supergroups. Consequently, almost all cytoplasmic structures including nuclear genome, of the endosymbiotic algae have disappeared. However, the plastids due to their importance in carrying out photosynthesis have been preserved (Kroth P. G. 2007). As an example, diatoms, brown algae, eustigmatophytes (*Nannochloropsis*), and most dinoflagellates contain plastids derived from red algae (Janouskovec J. et al. 2010). That explains the presence of four enveloping membranes to the plastids of *Nannochloropsis* where the outer two are continuous with endoplasmic reticulum (ER). That functions as a barrier between the lumen of ER and the primary chloroplast where the thylakoid membranes are found (Vieler A. et al. 2012). Together these compartments (chloroplast and endoplasmic reticulum) forms a nucleus-plastid continuum (NPC). The maintenance of this physical connection between the nucleus and the chloroplast occurs throughout the cell cycle (Murakami R. et al. 2009).

As aforementioned, *Nannochloropsis* species belong to the family of Eustigmatophyceae. Eustigmatophyceae is a small group including seven genera and twelve species of eukaryotic algae from different habitats, including freshwater, marine environment (*Nannochloropsis*), and soil. All eustigmatophyceae are unicellular, of coccoid shape and possess cell walls consisting of polysaccharides (Hoek C. et al. 1998). Specifically, the *Nannochloropsis* species are small, non-motile spheres without expressing any specific morphological feature. Cells of different *Nannochloropsis* species cannot be distinguished by light-microscopy as their size ranges between 2-4 μm (Fawley K. P. et al. 2007). The overview over taxonomic classification of *Nannochloropsis* is presented in table 1.1.

Table 1.1: Scientific classification of microalgae *Nannochloropsis*.

Domain	Eukaryota
Kingdom	Chromalveolata
Phylum	Heterokontophyta
Class	Eustigmatophyceae
Family	Eustigmataceae
Genus	<i>Nannochloropsis</i>

The Potential of *Nannochloropsis*

One of the present most challenging goals of the society is finding sufficient supplies of clean energy with global stability and economics depending on it. Fossil used at the present denote 70 % of the total global energy requirements, including transportation, domestic heating, and manufacturing (Gouveia L. et al. 2008). Therefore, the potential demand for biofuel is significant, especially when considering the reduction of gaseous emissions causing climatic changes. Biodiesel is usually produced from oleaginous crops such as rapeseed, palm, and soybean. However, photosynthetic algae, both microalgae and macroalgae have been considered as an efficient source of biofuels for decades (Sheehan J. et al. 1998) and have been compared to terrestrial plants (Dismukes et al. 2008). Specifically, eukaryotic microalgae are considered desirable due to their capacity to accumulate significant amounts of triacylglycerol (TAG) and starch. Consequently, the oil can be extracted and processed into transportation fuels, though the technology for this process is yet to be optimized (Gouveia L. et al. 2008, Radakovits R. et al. 2010).

The advantageous metabolic attributes of microalgae include:

- fast growth and high biomass production efficiencies
- high photosynthetic conversion rate
- capability to produce a variety of biofuels (TAG , starch)
- capability to grow in different environments permitting the use of non-arable and non-potable water
- no need for large quantities of water compared to higher plants
- possible daily harvesting
- season-independent growth (Campbell C. J. 1997, Chisti Y. 2008)

Though microalgae are considered a promising base for biofuel production, recent studies show that economics for biofuel production need to be significantly improved. Due to modern techniques, which include new genetic tools, such as established transformation protocols for both nuclear and plastid transformation, available genome sequences, and analytical techniques, the process of manipulating metabolic pathways has become precise and efficient for the scientists (Radakovits R. et al. 2010). Yet some deficiencies in advanced molecular tools for most eukaryotic microalgae prevent the rapid development of microalgae as a source of biofuel (Kilian O. et al. 2011). In addition to molecular techniques the improvement of cultivation techniques, cell harvesting and extraction methods also lead to the successful establishment of biofuel. Problems, such as contamination in ponds, poor light penetration in too dense cultures, and problems with cold flow properties of the biodiesel derived from microalgae are to be

eliminated (Dunn R. O. 2011). The optimization of productivity by cultivation methods and identification of strains with features required for potential biofuels production are the main goals for engineering solutions (Radakovits R. et al. 2010).

The most costly processing step in biofuel production using microalga as feedstock would be harvesting/dewatering and extraction of the biomass itself. A possible solution to the problem might be the genetic manipulation of cells until the point where cells start to secrete the compounds directly into the growth medium. However, more knowledge of transport systems and secretion pathways is required. A limitation in use of natural secretion pathways might be the aforementioned contamination of the cultivation system. This again might influence the compounds secreted by the microalgae as they can be used as a source of nutrients (Radakovits R. et al. 2010).

Microalgae have advantages compared to various crops and their biodiesel production, and are predicted to become one of the Earth`s most desirable and important renewable feedstock due to their unique photosynthetic features (Chisti Y. 2008). In fact, the production of biodiesel from microalgae can be 10-20 times higher than that obtained from oleaginous seed or vegetable oils (Tickell J. et al. 2000, Chisti Y. 2007). Table 1.2 presents oil production by various oleaginous organisms including microalgae.

Table 1.2: Oil yield measured in liter per hectare of six higher plants compared to oil yield given by microalgae (Chisti Y. 2007).

Crop	Oil Yield (L/ha)
Corn	172
Soybean	446
Canola	1190
Jatropha	1892
Coconut	2689
Palm	5950
Microalgae	136900

However, the microalgae-based biofuel production needs models for the further development of fundamental insights into the production of biomass and biofuel. Numerous studies have been conducted to detect candidates for the most efficient oil production. The screening of various species (e.g. *Nannochloropsis* sp., *Chlorella vulgaris*, *Spirulina maxima*, *Neochloris*

oleabundans, *Scenedesmus obliquus* and *Dunaliella tertiolecta*) was performed in order to investigate their oil quality and quantity. Both *Neochloris oleabundans* (fresh water microalga) and *Nannochloropsis* sp. (marine microalga) possess promising features for production of raw materials and biofuel, due to their high oil content (29.0 and 60% respectively) in nitrogen deprived conditions (Gouveia L. et al. 2008, Bondioli P. et al. 2012). The potential of *Nannochloropsis* as a production platform for biofuels caused increased interest and motivated detailed studies of various *Nannochloropsis* species (e.g. *Nannochloropsis oceanica* (Pan K. et al. 2011)).

Genome Manipulation

Since the first successful nuclear transformation of *Chlamydomonas*, the transformations of large number of other eukaryotic microalgae has been developed and adjusted for various species. Different transformation techniques have evolved since then – electroporation, microparticle bombardment (biolistic transformation), glass beads, *Agrobacterium tumefaciens* – still having a number of limitations and factors influencing the transformation stability and efficiency (Leon R. et al. 2007). The first successful chloroplast transformation was performed by biolistic transformation of *Chlamydomonas reinhardtii* in 1988 (Purton S. 2007). Microalgae have been used as model organism not only for their high oil productivity but also for studies of photosynthesis, flagellar function, nutrients content and expression of therapeutic proteins. However, the *Nannochloropsis* genus has awakened large interest and therefore motivation in the field of transgenic microalgae.

The ability of microalgae to produce high amount of biomass and their metabolic efficiency to accumulate compounds of interest (such as TAG and starch), decide the organism's production rate of biofuels. There are some technical limitations inherent to small- and large-scale microalgal photobioreactors, which negatively affect biomass accumulation. In addition, photosynthetic efficiency of the microalgae can be negatively affected by salt concentration, pH, light intensity and temperature. Some of these limitations may be overcome by the development and establishment of genetic approaches for achieving new cell properties, such as higher tolerance to stress factors. Genetic approaches may help to decrease the time needed for desired traits to develop themselves as has happened with agriculture crops cultivated for thousands of years. Genetic engineering therefore opens a door for bypassing this time demand for the selection process (Radakovits R. et al. 2010).

Microalgae *Nannochloropsis* possess haploid genome, and this provides a great opportunity for genetic manipulations by homologous recombination (HR), which in turn provides an abundant prospect for the future development of systematic functional genomics and improvement in the

field of biotechnology (Kilian O. et al. 2011). The presence of haploid genome was discovered by generating knock-outs in only a single transformation step. This suggested that *Nannochloropsis* was indeed haploid as diploid organisms would require successive rounds of transformation in order to achieve homozygous knock-out strains (Galloway R. E. 1990, Cruz A. et al. 1991). *Nannochloropsis* is considered to be a robust industrial alga and a good candidate for the production of biomass and other valuable products (Kilian O. et al. 2011). In summary, qualities giving *Nannochloropsis* a potential of being such a promising source for biofuel include:

- haploidy of the cells
- high transformation efficiency
- transformation by HR
- ability to grow in mass culture (Kilian O. et al. 2011).

The knowledge of species-specific characteristics including the genetic information is essential for optimizing biofuels production. As an example, the oil production can be improved by determining the difference sets of genes relevant for fatty acid biosynthesis. The genetic manipulation of these genes may contribute to an increased biomass yield. Access to genome information will not only contribute to a functional analysis of individual genes of *Nannochloropsis*, but genomic information will also result in future development of the organisms into a feedstock for industrial purposes. The gene replacement in *Nannochloropsis*, which already has been reported for *N. oceanica* (Kilian O. et al. 2011), is another process that will facilitate achieving future goal of renewable bioenergy (Vieler A. et al. 2012).

Nannochloropsis and other microalgae do not accumulate lipids efficiently during logarithmic growth. The storage of lipids will start at the point where organism is experiencing an environmental stress, such as nitrogen deprivation. Under these conditions, cells will attempt to store the energy in the form of lipids in order to survive poor culture conditions (Hu Q. et al. 2008). The attempts to inhibit beta-oxidation, the degradation of lipids, might prevent the loss of fatty acids, though the cell growth and survival will be affected. Inhibiting beta-oxidation could be a method to increase the lipid production but only for microalgae grown in photobioreactors due to continuous light supply (Austin A. , Radakovits R. et al. 2010).

In addition to improve the quantity of the lipid, while controlling their quality is also an essential step for producing biofuel efficiently. As enzymes control fatty acid length and number of unsaturated bonds, genetic engineering can be applied to directly manipulate the quality of fatty acids (Radakovits R. et al. 2010).

Oil Production

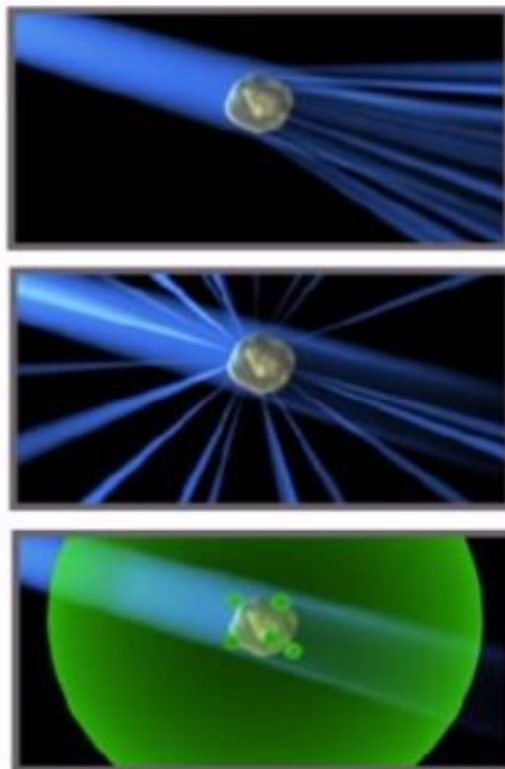
The high potential of microalgae for producing biomaterials and lipids has raised large interest in utilizing microalgae for production of biofuels that replace fossil fuels. Many microalgae are able to store more than half of their dry weight biomass as lipids growing photoautotrophically (Hu Q. et al. 2008). The produced lipids include triacylglycerols and other valuable pharmaceutical compounds (Pulz O. et al. 2004). Heterokonts of genus *Nannochloropsis* have the ability to accumulate high amounts of cellular oil and is already in industrial use for the production of lipid-based products.

Nannochloropsis species have demonstrated a potential for lipid production. In a study with 30 various strains screened and compared, the *Nannochloropsis* species achieved 60% lipid content by biomass in nitrogen-deprived environment compared to 30% under normal conditions. Microalgae grown in open photobioreactor under nitrogen deprivation showed an increase in lipid content, reaching from 117 mg/L/day (in nutrient sufficient medium) up to 204 mg /L/day (Rodolfi L. et al. 2009).

Not only has the quantity of the lipids changed under nitrogen-deprived conditions, but also their chemical composition. In a nitrogen-depleted environment, the concentrations of triacylglycerols will increase while polar glycerolipids, free fatty acids, and diacylglycerols will decrease to some extent. In fact, this increase of triacylglycerols has higher rate than the decrease of other mentioned compounds, indicating that cells synthesize new triacylglycerols rather than just converting the other existing lipids into triacylglycerols (Simionato D. et al. 2013). One study showed that it is not the increased synthesis of fatty acids itself that causes storage of cellular oil, but up-regulation of genes responsible for the assembly of triacylglycerols, that decides the final oil content inside the cells. Therefore, it is up-regulation of triacylglycerol assembly genes rather than genes of fatty acids synthesis, which determine the amount of triacylglycerols production (Li J. et al. 2014).

Chapter II

Correct Cell Count Estimation (Flow Cytometry)



Davidson Institute of Science Education
Flow Cytometry Tutorials, Introduction (video image)

Chapter II - Correct Cell Count Estimation: Introduction

Flow cytometry

Flow cytometry is a technology originally developed to perform analysis of cellular populations with higher precision than any cell counter can perform. Modern flow cytometry technology is also an efficient measurement system for studying many different parameters of cell cultures. Some of recent flow cytometers are able to record 32 various parameters at 200,000 events/s and sort up to 100,000 cells/s into 6-way sorting (Picot J. et al. 2012).

Modern flow cytometry is a laser-based technology applied for multiple biological and physical studies over a heterogeneous cell culture. The studies include the determination of cell numbers, physical cell sorting by their populations, and detection of various biomarkers. Other research applications investigate immune-phenotype, DNA analysis (supposing correct staining dye added), cell proliferation, shape, size and fluorescence (Picot J. et al. 2012). Another advantage of using flow cytometry emerges when the cell size gets too small to be distinguished with light microscope (as when cell size gets down to 2-3 μm) (Marie D. et al. 2005). The usage of various nucleic acid-specific stains as e.g. SYBR Green has also helped detection and counting of heterotrophic bacteria. The stains binds to nucleic acid and therefore provides a picture regarding intact DNA (whole genome) content and dead cells with destroyed nuclei (Marie D. et al. 2005).

Flow cytometry data are obtained when cell suspension is driven into a narrow stream of fluid (10-20 μm wide), and passes one or more powerful laser beams. When the cell is encountered, light is scattered in different angles according to the size and shape of a cell. Hundreds of thousands of cells can be drawn through the stream, and parameters are recorded with high accuracy (Picot J. et al. 2012). Small angles, which give forward scatter (FSC - 180 degrees) are correlated and are relative to the size of the particles/cells. Light scattered at larger angles (side scatter – SSC) provides more complex information about the shape and the surface character of the particles/cells (Marie D. et al. 2005).

Furthermore, if the cell/particle contains a fluorescent compound that has an absorption spectrum corresponding to the excitation source (as e.g. chlorophyll *a* that absorbs blue light efficiently) its fluorescence emission will be collected by a lens and passed through different optical filters. At this point the excitation light will be removed leaving only emission light for the detection (Marie D. et al. 2005).

Detectors (photodiode and photomultiplier tubes) will collect, amplify, and convert the light signals (photons) from cell fluid stream to an electric signal. The signal is then digitalized,

recorded and analyzed by a specific software connected to the flow cytometer instrument (Picot J. et al. 2012).

Consequently, the flow cytometer can be summarized into three main constitution parts: the first is the fluidic system that allows the cell suspension to be drawn in a narrow fluid stream permitting the cells pass one by one for the precise detection. The second is the excitation source and optical emission detection system, which the cells pass by, and the third is the electronic system, which digitalizes the signals to be analyzed by specific computer software.

The setups of flow cytometer

The BD Accuri™ C6 flow cytometer used in the master project is equipped with both 24- and 96-well plates where several parallel sample can be analyzed automatically with different procedures. The volume of a sample needed for the analysis ranges between 0.5 and 1 mL. The level of automation of this flow cytometry is therefore an advantage as there is no need for an operator during data acquisition.

The time and the speed at which the cell suspension runs through the stream passing the lasers can be adjusted and depends on the pressure of the analyzer. The higher the pressure - the higher the velocity and the lower is the precision of the measurements. Therefore, choice of parameters is always a compromise between time used for the analysis and its quality. The most optimal setups are determined after comparison of various samples.

The phenomenon called *coincidence* occurs when two cells are counted as one event. The reason for such occurrence may be a simultaneous passage of two cells through the excitation beam or short distance between the cells. Coincidence will cause imprecise and decreased cell count determination. To prevent this phenomenon it is necessary to reduce flow rate or make a dilution of the samples. It is also important to select the appropriate threshold depending on the characteristics by which the cell counting is desired. Beyond the threshold point, the events (cells) will not be counted and analyzed. The threshold setup is hence critical for the quality of the records sought after by the scientists (Marie D. et al. 2005).

The BD Accuri™ C6 flow cytometer used in the master project is equipped with 488 and 640 nm solid-state lasers, and can analyze up to six parameters (FSC, SSC, and four fluorescence filters) (BD Biosciences).

- Forward scatter (FSC) – sortation by size of the cells
- Side scatter SSC – sortation by shape of the cells
- Filters – FL1 (533 ± 30 nm), FL2 (565 ± 40 nm), FL3 (670 nm), FL4 (675 ± 25 nm)

Result analysis

Data can be interpreted at different plots and charts displayed by the analysis software. Different types of plots include histograms for cell count presentation, dot-plots, and sky-plots for other cell culture measurements. Parameters for both x- and y-axes can be chosen and changed for a better interpretation. The determination of different areas of the plots gives a percentage of this chosen population compared to the total amount of the population analyzed. After simple mathematical calculations, the concentration of the cell culture can be determined. The chlorophyll fluorescence or the forward scattering signal can be used to determine the cell population. By choosing the correct threshold values for these signals, flow cytometry provides the possibility of detecting contaminations. Staining of nucleic acid with appropriate dye makes difference in genome size detectable.

Goal

The aim of using flow cytometry was the determination of the correlation between cell concentration and corresponding optical density (OD_{750nm}) values as a growth indicator, measured by Tecan Infinite® 200 Pro Multimode Reader. As the main goal of the master project was establishment of an efficient transformation of *Nannochloropsis oceanica* CCMP1779 cells by electroporation, the cell concentration at the harvesting time point played an important role, and could be assessed by the flow cytometry. The correct cell concentration at the time point of harvest is fundamental parameter for achieving an efficient transformation. To determine the cell concentration quick, the accurate standard curves between flow cytometry-measured cell concentrations and corresponding OD_{750nm} were created. For comparison, the cell count was determined by the manual, time-consuming hemocytometer and by the automatized flow cytometer. The preservation methods, such as fixation with glutaraldehyde and snap-freezing with liquid nitrogen were tested in order to investigate a potential cell count loss determined by flow cytometry.

Materials and Methods

Growth conditions

Initially, *Nannochloropsis oceanica* CCMP1779 cells obtained from the National Center for Marine Algae and Microbiota (NCMA, former CCMP, <https://ncma.bigelow.org/>) were cultivated in two distinct media where seawater was filtered through 0.2 mm disposable filter and autoclaved afterwards. The seawater was since enriched with either f/2 medium or Cell-Hi

NC solution obtained commercially from Varicon Aqua Solutions. To prepare f/2 medium, 1 mL of NaNO_3 (stock solution 75 g/L – final concentration 0.075 g/L), 1 mL of NaH_2PO_4 (24 g/L – 0.024 g/L), 0.1 mL of both $\text{CuSO}_4 \cdot 5\text{H}_2\text{O}$ (9.8 g/L – 0.98 mg/L), $\text{Na}_2\text{MoO}_4 \cdot 2\text{H}_2\text{O}$ (6.3 g/L – 0.63 mg/L), $\text{ZnSO}_4 \cdot 7\text{H}_2\text{O}$ (22.0 g/L – 2.2 mg/L), $\text{CoCl}_2 \cdot 6\text{H}_2\text{O}$ (10 g/L – 1 mg/L), and $\text{MnCl}_2 \cdot 4\text{H}_2\text{O}$ (180 g/L – 18 mg/L), 1 mL of biotin (0.1 g/L – 0.1 mg/L), and 0.1 mL of cyanocobalamin (1 g/L – 1 mg/L) were added to 1 L of seawater. First the cell were grown under constant light intensity of $80 \mu\text{E m}^{-2} \text{s}^{-1}$ with supply of air through a bubbling system at 30°C . After obtaining a growth standard curve using hemocytometry, the decision to utilize another growth system was taken. New growth conditions excluded the bubbling system, but achieved aeration by a rotation system induced by a Heidolph® Rotamax 120 Orbital Shaker mimicking wavelike movements (see figure 2.1). The cells were grown under constant light intensity of $100 \mu\text{E m}^{-2} \text{s}^{-1}$ at 23°C .

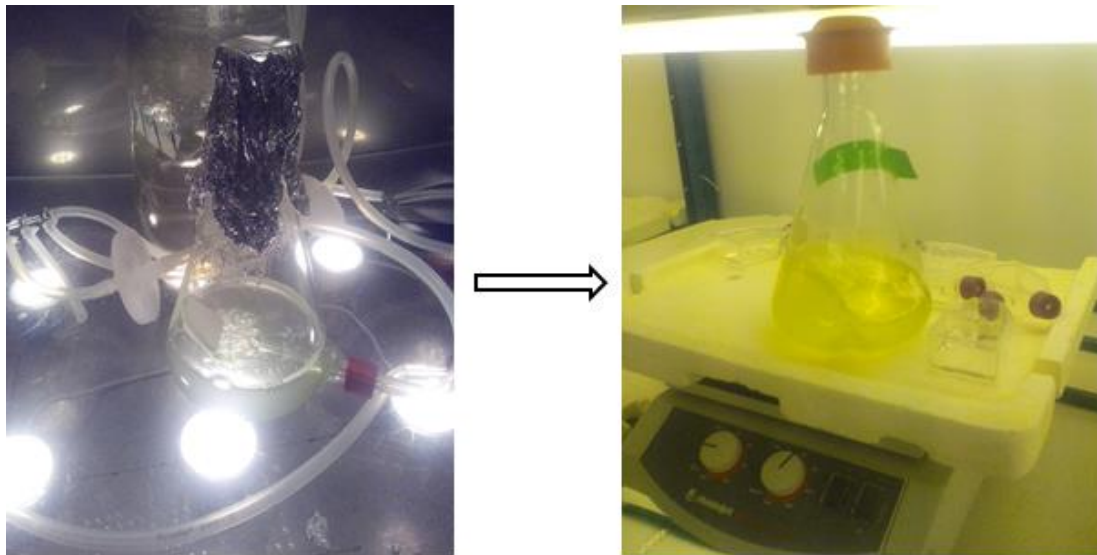


Figure 2.1: **Growth condition of the *N. oceanica* CCMP1779 cells.** Initially, growth conditions of *N. oceanica* CCMP1779 included supply of air through a bubbling system at temperature of 30°C and constant light intensity of $80 \mu\text{E m}^{-2} \text{s}^{-1}$. After establishment of the standard growth curve, the cultivation was performed under different growth conditions using continuous rotation at Heidolph® Rotamax 120 Orbital Shaker at 23°C and light intensity of $100 \mu\text{E m}^{-2} \text{s}^{-1}$.

The growth coefficient k was determined using the standard formula, where N – cell concentration at certain point of time, N_0 – initial cell concentration, t – time, k – growth coefficient:

$$N = N_0 e^{kt} \quad \rightarrow \quad k = \frac{\ln(N/N_0)}{t}$$

Correlation between cell count and OD values

Initially, determining the correlation between cell count by hemocytometer and BD Accuri™ C6 flow cytometer was used to establish the association between physical and automatized cell counting systems. Afterwards, the estimation of the correlation between cell count by BD Accuri™ C6 flow cytometer and OD at 750 nm (OD_{750nm}) values by Tecan Infinite® 200 Pro Multimode Reader could be established therefore interpreting OD_{750nm} values as a growth indicator.

For this purpose dilution series of *N. oceanica* CCMP1779 culture were prepared in triplicates and the cell count was performed by both of the counting methods, hemocytometer and flow cytometer. Hemocytometry was conducted by counting the fixated with lugol-solution (2% iodine) cells in four different squares at both, the upper and the bottom field of a 0.1 mm deep Burker`s chamber. The average determination of the cell number was determined by the formula (Grigoryev Y. 2013):

$$\text{Total cells/mL} = \frac{\text{Total cells counted}}{\# \text{ of Squares}} \times 10,000 \text{ cells/mL} \times \text{Dilution factor}$$

Cell count of 0.5 mL of prepared cell sample triplicates were performed with BD Accuri™ C6 flow cytometer. Before usage of the flow cytometer, the instrument was adjusted with milliQ water and 6- and 8-peak rainbow calibration particles. The flow cytometer was equipped with a solid state laser (excitation light of 488 nm), a forward angle light scatter (FSC, 0° ± 13°) and a side light scatter (SSC, 90° ± 13°). Additionally, the flow cytometer contained 4 fluorescence filters: FL1 533 ± 15 nm (488 ex.), FL2 585 ± 20 nm (488 ex.), FL3 670 nm (488 ex.) and FL4 675 ± 12.5 nm (650 ex.) (Marie D. et al. 2005).

The settings for flow cytometer analysis were following:

- Speed (µL/min) – medium
- Time (min) – 2
- Culture volume drawn (µL) – 69
- Threshold – eliminate events less than 30000 on forward scatter (FSC)
- Cell count measurements were recorded by detecting the signals of fluorescence filter FL3 (670 nm) (FL3 values along x-axis and “Count” along y-axis). All values were converted to logarithmic scale for a data recording.
- Washing step – 1 cycle (flushing the nozzle once between every sample run)
- Agitation step – 1 cycle (agitation of the samples between every sample run)

Further, OD values of the same samples were measured by Tecan Infinite® 200 Pro Multimode Reader (cuvette and plate reader, Switzerland) with absorbance value of 750 nm (OD_{750nm}).

Different storage methods including fixation with glutaraldehyde and snap-freezing using liquid nitrogen for storing the samples over a longer duration at -80°C were tested. The final concentration of the glutaraldehyde in cell culture was 0.1-1% (stock solution 50% glutaraldehyde). Same flow cytometer settings were used for determination of cell count loss after snap-freeze with liquid nitrogen. Snap-freezing were performed twice with thawing the samples in between.

Results and Discussion

Growth conditions

The initial growth conditions for *N. oceanica* CCMP1779 included incubation at 30°C and continuous light at intensity of 80 $\mu\text{E m}^{-2} \text{s}^{-1}$ with supply of air through a bubbling air system. Initially, cells were grown in both liquid medium, f/2 and Cell-Hi CN. The difference in growth rate was observed as cell cultures were sampled after a certain amount of time, and the cells were counted with hemocytometer with daily result records (see table 2.1).

Table 2.1: *N. oceanica* CCMP1779 cells were initially grown in f/2 medium and Cell-Hi CN medium, at 30°C, constant light intensity of 80 $\mu\text{E m}^{-2} \text{s}^{-1}$ and continuous supply of air through a bubbling system. The cell cultures were sampled approximately every 24 h for establishment of a standard growth-time curve according to the growth medium. Cell samples for f/2 day # 5 and for Cell-Hi CN day # 7 are missing due to technical problems with hemocytometer on those days.

Days	Hours	Medium type	
		Cell-Hi CN	f/2
0	0	5,00×10 ⁵	5,00×10 ⁵
1	23	5,30×10 ⁵	4,40×10 ⁵
2	47.5	5,54×10 ⁵	6,24×10 ⁵
3	71	7,85×10 ⁵	7,69×10 ⁵
4	94	1,46×10 ⁶	1,05×10 ⁶
5	118	2,60×10 ⁶	-
6	141	3,20×10 ⁶	2,04×10 ⁶
7	167	-	2,60×10 ⁶
8	185	2,85×10 ⁶	2,61×10 ⁶

Cell count records are missing at day # 5 and day # 7 for cells growing in f/2 medium and Cell-Hi CN medium, respectively. This occurrence is due to technical problems with hemocytometer on those days. Missing data resulted in gaps in the growth-time standard curves but the pattern of sigmoidal growth curve is obvious (see figure 2.2).

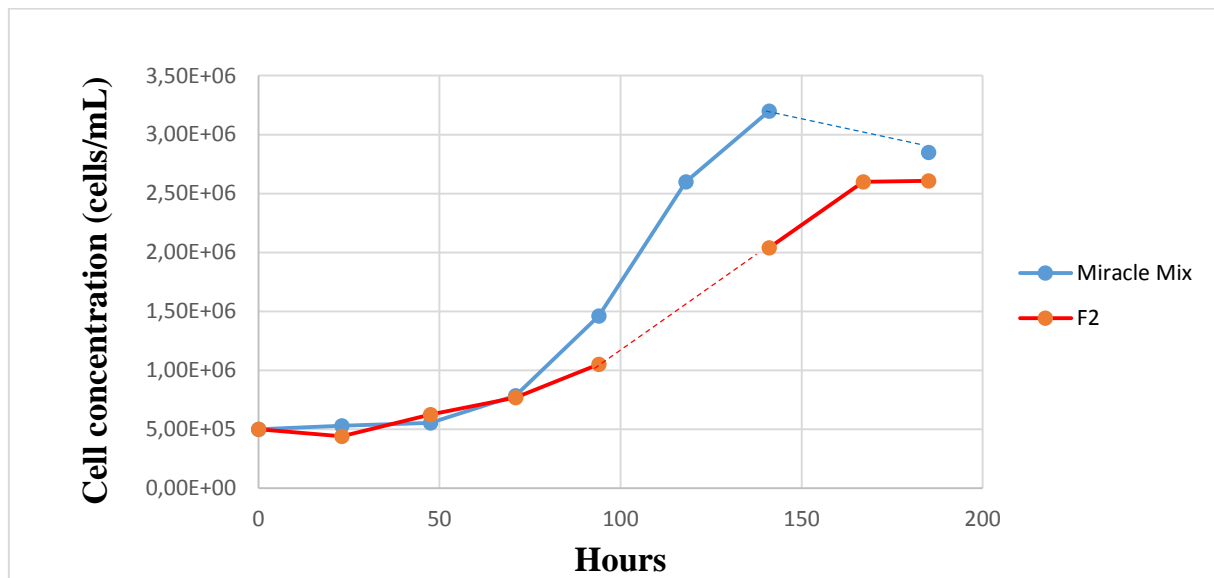


Figure 2.2: **Growth of *N. oceanica* CCMP1779 in f/2 medium and Cell-Hi CN medium.** The standard growth curves obtained after cultivating the *N. oceanica* CCMP1779 cells in f/2 medium (red curve) and Cell-Hi CN medium (blue curve) at 30°C, constant light intensity of 80 $\mu\text{E m}^{-2} \text{s}^{-1}$ and continuous supply of air through a bubbling system. Both curves are fitting the sigmoidal curve describing three phases of cell growth, lag, exponential and stationary phases. Cell growth in Cell-Hi CN medium is more efficient compared to f/2 medium. The dash lines indicates the missing data due to technical problems with hemocytometer those days.

Based on these records, the growth coefficient was determined for both growth media. The growth coefficient was determined being equal 0.017 and 0.020 for cells growing in f/2 medium and Cell-Hi CN medium, respectively. The obvious advantage of Cell-Hi CN as a growth medium led to decision to grow *N. oceanica* cells consigned for transformation in this type of medium. Though cell growth in both media was considered being not efficiently progressive at initial growth conditions, still cells in Cell-Hi CN medium reached a higher stationary phase compared to f/2 medium. Graphs presented in figure 2.2 indicate that it took around 50 h to double the cell concentration, while previous doubling time for *Nannochloropsis* reported in the range of ~14-16 h (Kilian O. et al. 2011). Based on growth condition previously reported for *Nannochloropsis* (Rocha J. M. S. et al. 2003, Sandnes J. M. et al. 2005, Converti A. et al. 2009, Ras M. et al. 2013) the growth conditions were changed to enhance the cell growth.

After growth conditions were changed (see Materials and Methods – Growth conditions), growth coefficient for cells in Cell-Hi CN medium increased and reached the value of 0.026, indicating that the new conditions were advantageous for the cell growth. Lower incubation

temperature and rotational shaking instead of air-supplying bubbling system prevented cell sedimentation observed at initial cell culture growth and resulted in more efficient cell growth. Faster growing cells are likely to be more competent for transformation techniques as stressed cells are likely to have thicker cell walls influencing the transformation efficiency.

Cell count correlation with OD_{750nm}

A dilution series of a *N. oceanica* culture was created and analyzed with the spectrophotometer Tecan Infinite® 200 Pro Multimode Reader in order to establish a correlation to the cell count. These samples were then analyzed by BD Accuri™ C6 flow cytometry. Cell count results of one of eleven *N. oceanica* CCMP1779 samples analyzed in parallel provided by flow cytometer software are presented in figure 2.3. It was initially suspected the presence of a cell culture contamination represented by the first peak. However, the analysis of the Cell-Hi CN medium alone under the same flow cytometer settings showed the same peak (see figure 2.3). Therefore, it was concluded that the ingredients of Cell-Hi CN medium affect the results by the software analysis, due to culture medium particles that are counted using the fluorescence filter FL3 signal.

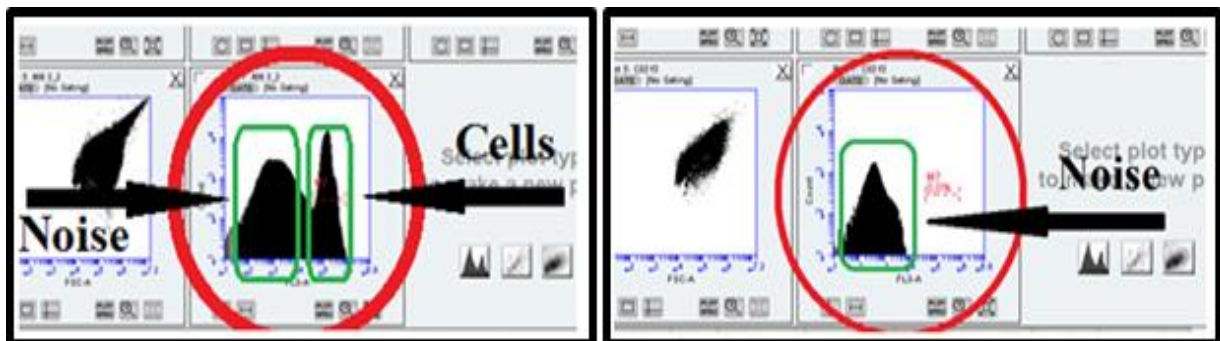


Figure 2.3: Data screenshot of BD Accuri™ C6 flow cytometer software indicating two separate populations of cells after a *N. oceanica* cell sample run. The histogram plot is shown in logarithmic scale with signals recorded and interpreted of FL3-A fluorescence filter on x-axis and count values on y-axis. The second data screenshot shows data after pure Cell-Hi CN medium was analyzed. The histogram plot is shown in logarithmic scale with signals recorded and interpreted of FL3-A fluorescence filter on x-axis and count values on y-axis. The peak on the histogram plot of Cell-Hi CN medium is of the same shape and indicates the same fluorescence signal intensity as the corresponding histogram of *Nannochloropsis* culture does, indicating no presence of contamination.

As Cell-Hi CN medium content is a trade secret, no more analysis could be conducted to conclude the nature of the medium components and establish which minerals or trace metals were affecting the result. Another reason for the occurrence of such a clear signal peak could be a background noise due to small air bubbles, salt crystals and other minerals of saltwater. The background noise is impossible to avoid and makes up only 5% of the counted events, therefore the operator should always be critical in reading and analyzing the data.

To estimate correlation between OD_{750nm} values measured by Tecan Infinite® 200 Pro Multimode Reader and cell concentration values determined by BD Accuri™ C6 flow cytometer, dilution series of *N. oceanica* CCMP1779 were prepared. In addition, cell amount of each sample was counted by hemocytometer in order to see how all three measurements correlated to each other.

First, the correlation between two cell count methods – time-consuming hemocytometer and the automatized flow cytometer was established (see figure 2.4 and table A.1, appendix A). The relationship between hemocytometer and flow cytometer cell count values was efficiently precise with correlation coefficient reaching the value close to 1 ($R^2 = 0.9824$). This indicates the reliance on flow cytometry as a suitable, less time-consuming cell counting system.

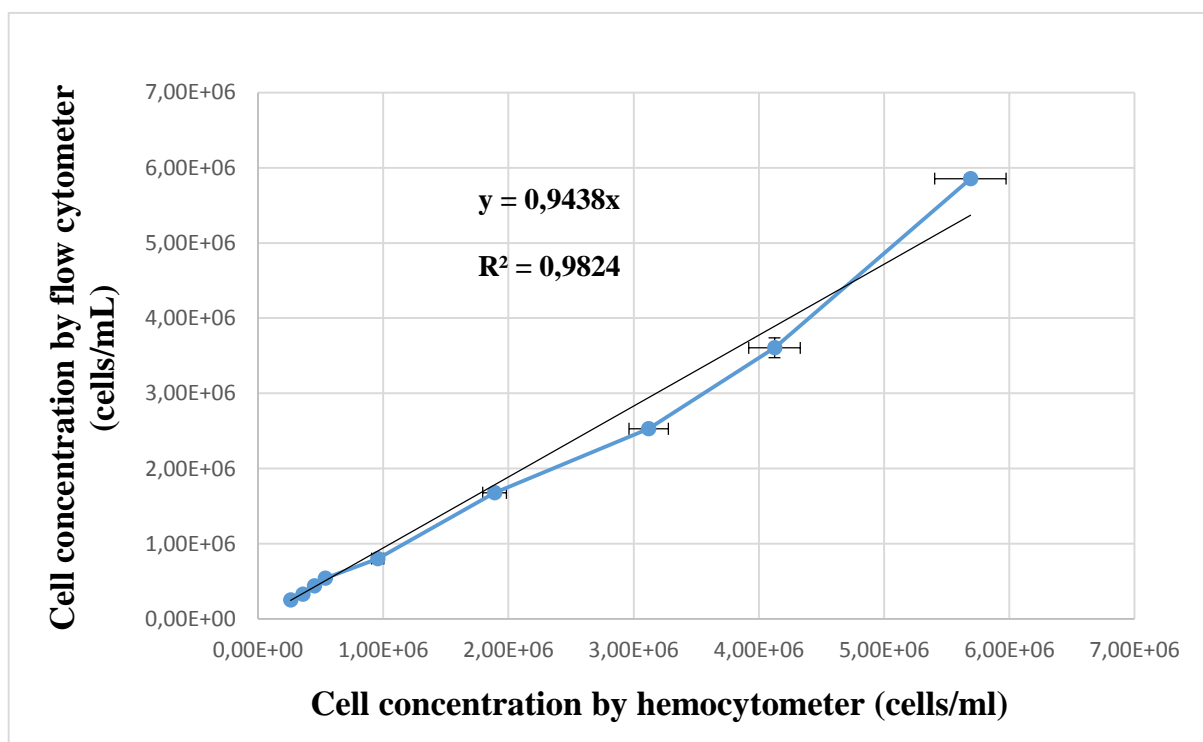


Figure 2.4: **Correlation between *N. oceanica* cell counts performed with hemocytometer and flow cytometer.** *N. oceanica* cells grew until they reached the exponential phase concentration ($\sim 2 \times 10^6$ cells/mL). The dilution series in triplicate was prepared, and cell count was performed via hemocytometer and flow cytometer. Setups of flow cytometer included excitation at 488 nm, detection of fluorescence of the sample cells with FL3 filter (670 nm), threshold 30000 FSC, medium velocity (69 $\mu\text{L}/\text{min}$) for 2 min run. Correlation between cell counts performed on hemocytometer and flow cytometer was established with correlation coefficient $R^2 = 0.9824$, revealing the almost perfect correlation between these two counting methods. The standard deviations are given for both cell concentration determined by hemocytometer and flow cytometer.

After the precise correlation of the hemocytometer and flow cytometer based-measurements, the standard curve between cell count values and OD_{750nm} values was determined (see figure 2.5, table A.2, A.3, A.4, and A.5, appendix A). The linear trend lines were drawn and correlation coefficients calculated. The correlation coefficients for both correlations are approaching 1,

indicating the almost perfect correlation ($R^2 = 0.9728$ for flow cytometry and $R^2 = 0.9962$ for hemocytometry).

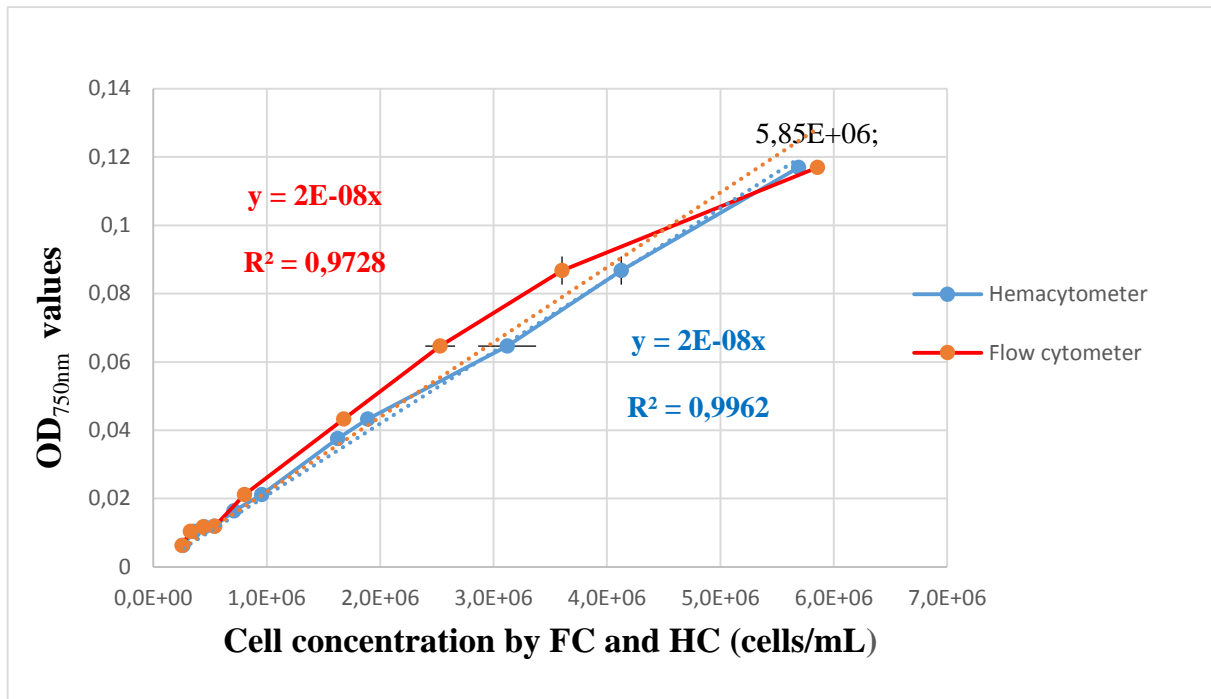


Figure 2.5: **Correlation between *N. oceanica* cell counts measured with flow cytometer (FC) and hemocytometer (HC) corresponding to OD_{750nm} values.** Correlation between cell numbers measured with hemocytometer and flow cytometer and corresponding OD_{750nm} values of the same cell samples measured by Tecan Infinite® 200 Pro Multimode Reader was established. The correlation coefficients are close to 1 indicating almost a precise correlation between the two direct cell counting methods and OD_{750nm} values. The presented standard deviations for both OD_{750nm} values, cell count values by hemocytometer and flow cytometer are insignificant for most of the values revealing the preciseness of the methods.

The reason to a slightly decreased cell count value for flow cytometry compared to hemocytometry at the values higher than 2.0×10^6 cells, might be due to the coagulation of the flow cytometer's nozzle, through which the cell sample was drawn. If the cell culture is too dense and the speed with which the sample is drawn through is too high, the coincidence phenomenon may occur.

On the correlation graphs both linear trend lines were drawn with intersection being equal zero. In this case, the correlations with OD_{750nm} seem to be precise for both of the methods for cell counting. However, the correlation equation used for determination of harvesting cell concentration for genetic transformations, were calculated with intersection point of trend line not being equal zero. The comparison of trend lines drawn through the zero intersection point, and trend line fitting to the correlation lines without the zero intersection restriction is presented in table 2.2.

Table 2.2: The difference between both linear correlation equations and correlation coefficients (R) when the trend lines for the graphs describing the correlations established between flow cytometry/hemocytometry counting methods and OD_{750nm}, are drawn through the intersection value being equal/unequal zero.

Intersection point	Linear correlation equation		Correlation coefficient (R)	
	Hemocytometry	Flow cytometry	H.cytometry	F. cytometry
= 0.00	$y = 2E-08x$	$y = 2E-08x$	0,9972	0,9728
≠ 0.00	$y = 2E-08x + 0,0024$	$y = 2E-08x + 0,0047$	0,9986	0,9808

There is not a large difference between correlation coefficient of both methods, making correlation equation suitable for determination of cell concentration related to OD_{750nm} values and confirming that the flow cytometry is indeed a reliable technique for cell counting.

Cell count loss induced by fixation and snap-freeze

For many experiments, it is useful to collect samples during the experiment and then count cells after the completion of the experiment. Two cell storage methods, which do not change the cell count number, were evaluated. Flow cytometry was applied to establish the effect of cell storage on cell count number. Cell count loss after glutaraldehyde (0.1 – 1%) fixation and snap freezing with liquid nitrogen is presented in the table 2.3 (see table A.6, A.7, and A.8, appendix A). There is no large decrease in counted cells after fixation with glutaraldehyde and snap-freezing with liquid nitrogen. However, the importance of thawing cell samples prior to analysis in a graduate way (first on ice in the fridge, then on ice at room temperature) was significant.

Table 2.3: The *N. oceanica* cells grew until they reached an exponential growth phase (~2×10⁶ cells/mL). The cell sample triplicates were prepared and 0.5 mL of each sample were analyzed via BD Accuri C6 flow cytometer for cell count determination. Further, the cells were fixated with glutaraldehyde (0.1 – 1%) and the cell loss was determined via flow cytometer under the same settings. Snap-freezing of the cell samples was performed using liquid nitrogen. Slow thawing and the subsequent cell count were performed. Cell samples were snap-frozen once more for further determination of cell count loss by flow cytometer under the same settings.

Condition	Average cell loss percentage
Glutaraldehyde fixation	3.0% ± 1.6%
Glutaraldehyde fixation + snap-freeze (liquid N ₂)	2.3% ± 2.0%
Glutaraldehyde fixation + snap-freeze 2× (liquid N ₂)	2.9% ± 2.2%

The cell count loss, though inefficient, was yet observed after glutaraldehyde (0.1 - 1%) fixation and snap-freeze with liquid nitrogen. The potential cause of such behavior could be cell bursting as thawing of the cell samples between conducted snap-freeze was performed in a faster way than suggested. Coagulation of the cells could occur while fixation with glutaraldehyde. This in its turn could cause wrong data recording through the flow cytometer nozzle. The unsuccessful fixation of some cells in the samples could lead to cell disintegration.

Establishment of cell density limits for flow cytometry

The maximal cell density that can be measured and analyzed by the flow cytometer was determined. A dilution series of a very concentrated *Nannochloropsis* cell suspension revealed that. Application of the BD Accuri™ C6 flow cytometer to these samples were performed with the same collection parameters (see Materials and Methods) used in the initial experiment. The cell concentrations and corresponding OD_{750nm} values are displayed in figure 2.6 (see table A.9 and A.10, appendix A). The cell count values start to decrease dramatically as the breaking point value of 2.19×10^7 cells/mL is crossed.

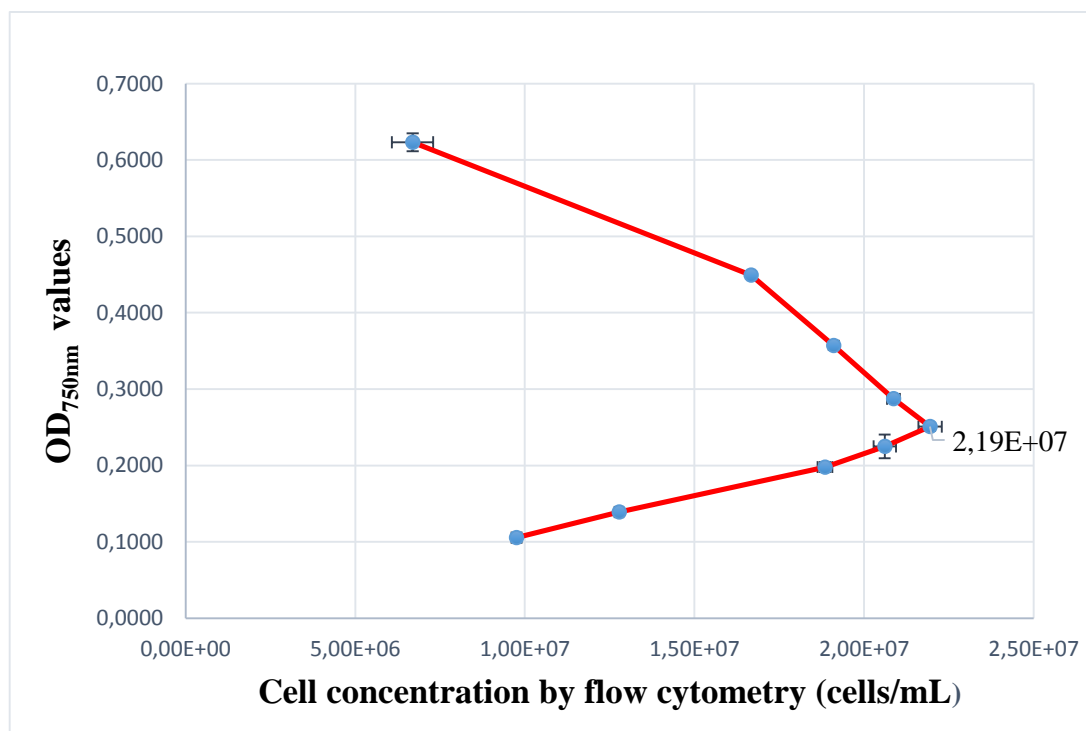


Figure 2.6: **Correlation between cell count measured by flow cytometry and corresponding OD_{750nm} values.** Correlation between cell count of new cell dilution series of highly concentrated *N. oceanica* cell culture measured by BD Accuri™ C6 flow cytometry and OD_{750nm} values measured by Tecan Infinite 200 Pro, was established. The breaking point value of the cell concentration is equal 2.19×10^7 cells/mL. After reaching this point, the cell concentration measured by flow cytometry decreases drastically. The standard deviations are given for both cell concentrations and OD_{750nm} values and is insignificantly low for both.

As the OD measurements can be expected to be accurate at least to an OD of 0.5, the disparity of cell count measured by flow cytometry (figure 2.6) indicates the inability of flow cytometer to measure cell samples with concentrations exceeding 2.19×10^7 cell/mL (breaking point value). This assessment is supported by the observation of decreased volume of the cell sample sucked through flow cytometer's nozzle at higher densities. For each cell sample with concentration higher than 2.19×10^7 cells/mL the thin nozzle was clogged by the high amount of cells causing a decrease in cell count. Therefore, making suitable dilution of samples of high cell concentrations prior running the cell samples on the flow cytometer is an essential part in working with the instrument.

To gain further insights into the suitable range of cell density measurements graphs 2.5 and 2.6 were merged (see figure 2.7).

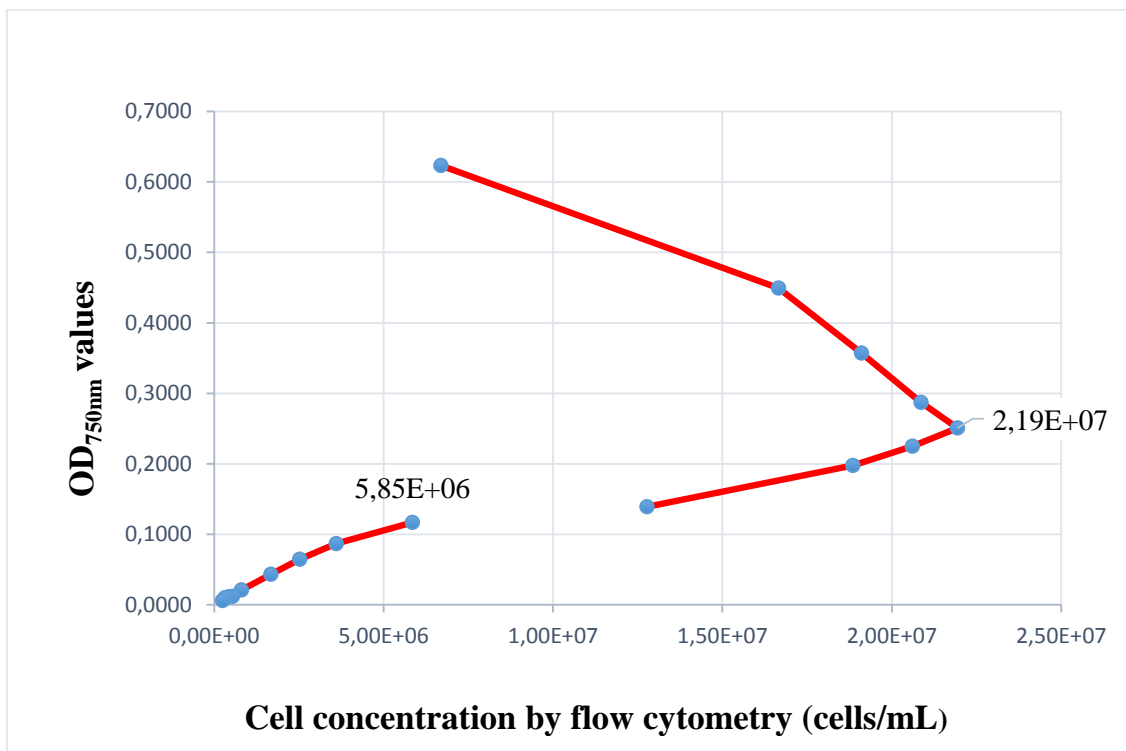


Figure 2.7: **Correlation between *N. oceanica* cell count by flow cytometer and corresponding OD_{750nm} values (two correlations described in figure 2.5 and 2.6 merged).** The left line indicates the initial experiment with highest cell concentration being equal 5.85×10^6 cells/mL (see figure 2.5). The second line represents the subsequent experiment with cell dilution series of a very dense *N. oceanica* culture (see figure 2.6). The highest cell concentration value measured by BD Accuri C6 flow cytometer was $\sim 2.19 \times 10^7$ cells/mL indicating inability of the flow cytometer measuring higher values, as they decrease drastically while OD_{750nm} is still increasing. The standard deviation of both cell count values and OD_{750nm} are presented in the figures 2.5 and 2.6

Figure 2.7 indicates a linear correlation of OD_{750nm} and flow cytometer at low cell concentrations. However, this linear relationship cannot be extrapolated to higher cell concentrations. The deviation of the relationship between OD_{750nm} measurements and cell counts was visualized by calculating anticipated cell numbers using the known dilution factor (see figure 2.8 and table A.9, appendix A).

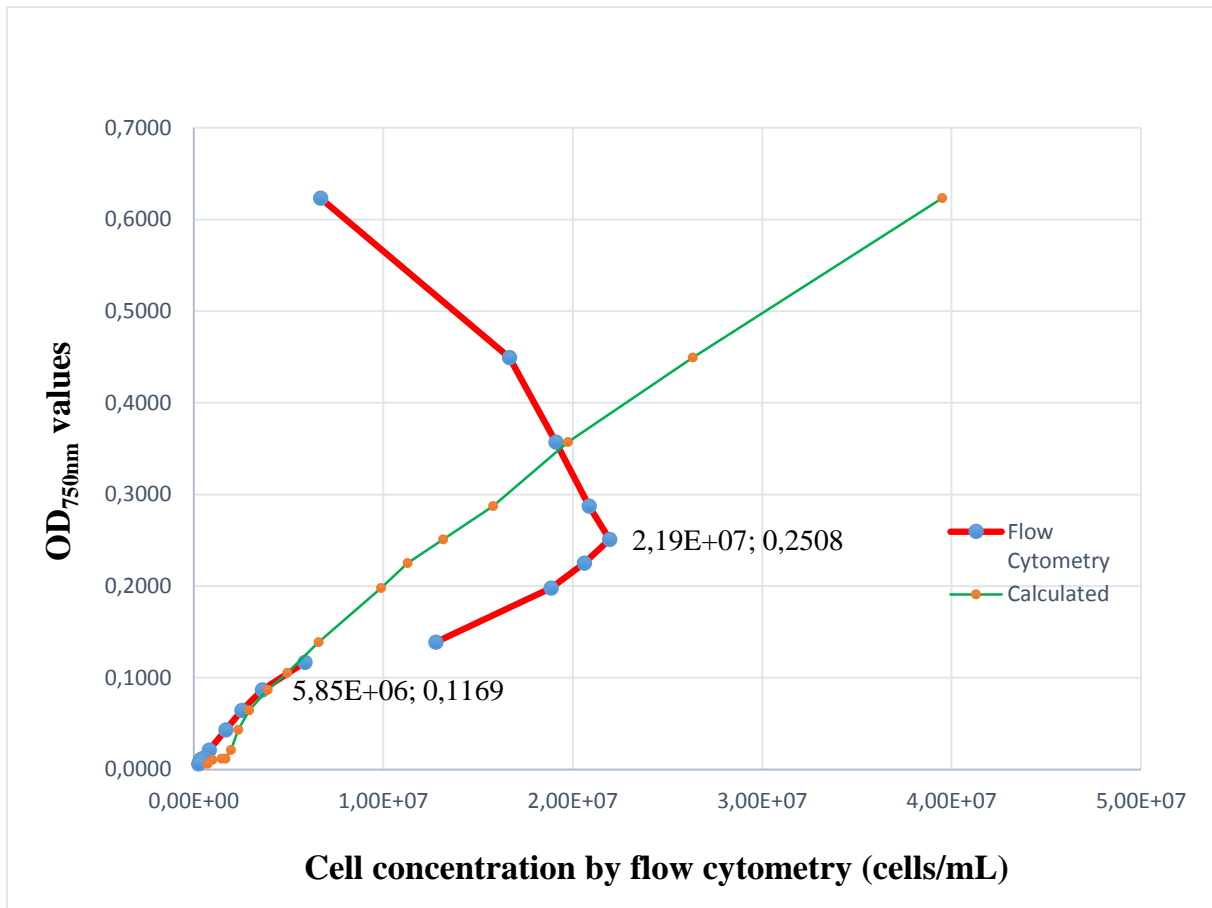


Figure 2.8: **Comparison of the correlations between cell concentration by flow cytometer and corresponding OD_{750nm} values with values of theoretical cell concentrations and OD_{750nm} values.** The graph includes three curves describing two correlations between *N. oceanica* cell counts and corresponding OD_{750nm} values. The left red line represents correlation between cell counts by flow cytometry ranging between 2.52×10^5 – 5.85×10^6 cells/mL and OD_{750nm}. The right red line is representing the correlation between cell counts by flow cytometer under the same settings as the first correlation ranging from 1.28×10^7 – 6.69×10^6 cells/mL and OD_{750nm}. The highest value measured by flow cytometer is 2.19×10^6 cells/mL. The thin green line indicates the correlation between OD_{750nm} values and theoretically determined cell numbers using dilution factors. The correlation lines diverge after the cell concentration value of 5.85×10^6 cells/mL is achieved.

The theoretical correlation line (green) follows almost perfectly the correlation line established by the first experiment with cell count values reaching the value of 5.85×10^6 cells/mL (left red line). However, the right correlation line representing denser cell samples is overall lower (up to a cell density of 2.19×10^7 cells/mL) compared to theoretical correlation line. This pattern indicates that flow cytometer's analysis of the cell samples with concentration above 5.85×10^6 cells/mL is imprecise. The difference between the high cell density correlation line and theoretical correlation line indicates large differences between calculated/theoretical cell count

values with ones measured by flow cytometry. Consequently, it is concluded that cell concentration of 5.85×10^6 cells/mL is the highest cell density that allows the precise assessment of concentration by flow cytometry.

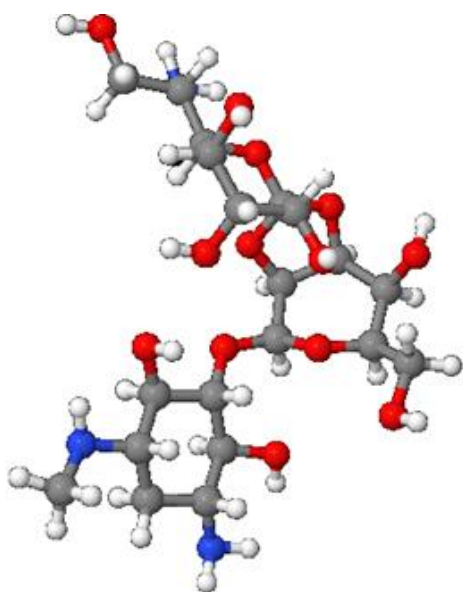
Conclusion

The determination of correct cell concentration is an essential parameter for optimization of *N. oceanica* cells transformation (see chapter IV – Transformation by Electroporation). The aim of the experiments presented in this chapter was the determination of cell concentration using different assessment techniques (hemocytometer, flow cytometer, OD_{750nm}). The flow cytometer stands out as a very time efficient and reliable method to assess cell densities. The conducted experiments reveal that cell concentration of up to 5.85×10^6 cells/mL (correlated with OD_{750nm} value of 0.1169) can be reliably determined by the flow cytometer (see figure 2.8). Therefore, at the determination of the cell concentration using the correlation established between flow cytometer measurement and OD_{750nm} values as a cell growth indicator, a dilution of the cell samples is required if a cell sample reaches an OD_{750nm} value of 0.1169 or higher.

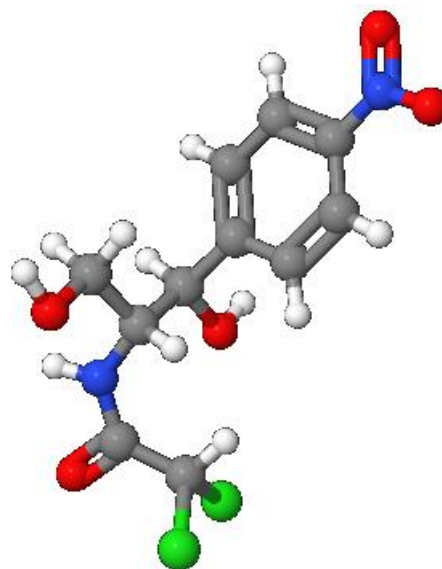
Chapter III

Cell Growth Assay

(Antibiotic Susceptibility)



Hygromycin B molecule structure
Image by ChemSpider



Chloramphenicol molecule structure
Image by ChemSpider

Chapter III – Cell Growth Assay: Introduction

Antibiotics have different targets ranging from cell wall or cell membrane synthesis (loracarbef, meropenem), essential enzymes (bacitracin, enoxacin, mafenide), or protein synthesis (gentamycin, kanamycin, neomycin, tetracycline, chloramphenicol) (Berkow R. 1999).

In addition to its use to fight diseases, antibiotics are also frequently used in research involving microorganisms. In spite of some arguments against the use of antibiotics, as they can lead to poor culturing techniques, spontaneous mutations and masking of resistant bacteria, the use of antibiotics has become an essential method for elimination of contamination from cell culture (Vieler A. et al. 2012, Meenakshi A. 2013). In addition, the use of antibiotics in the cell medium gives the ability to select the growth of cells with desired qualities that have been generated by molecular biology techniques. Therefore, antibiotic resistance genes are applied as selection markers for genomic transformation of cells. Cells that managed to acquire and incorporate a desired gene or mutation that is linked to the presence of the resistance cassette will grow on the selective medium with antibiotic as they become resistant to it (Vieler A. et al. 2012).

In the experiments presented in this chapter, hygromycin and chloramphenicol are used in the selective media to obtain *Nannochloropsis oceanica* CCMP1779 cells transformed with hygromycin resistance cassette and chloramphenicol resistance cassette via nuclear and chloroplast transformation, respectively.

The mechanism of action of hygromycin includes strong inhibition of protein synthesis by interfering with aminoacyl-tRNA recognition and inhibition of ribosomal translocation during elongation step of protein translation (Cabanas M. J. et al. 1978). Hygromycin inhibited the cell growth at 25 µg/mL reported by previous experiments (Vieler A. et al. 2012). To verify that this concentration is sufficient to select the resistance, a wider range of hygromycin concentrations was investigated.

Chloramphenicol affects protein synthesis as well, but the mechanism is somewhat different from hygromycin. Chloramphenicol binds to a receptor site on the ribosome and inhibits peptidyl transferase, the enzyme responsible for amino acid transfer to a growing peptide chain. Protein formation by this action is therefore limited (Antimicrobial Resistance Learning Site 2011).

In addition to the binding constants of an antibiotic to its target enzyme, the rate, at which molecule penetrates the cells and its retention within a cell will determine the sensitivity of the organism to different antibiotics. These parameters can be different between species and even strains and therefore a detailed assessment of suitable antibiotics and antibiotic concentrations was conducted. As reported by recent studies, certain cell wall composition to *N. oceanica*

results in an efficient entry of antibiotics and therefore increased cell sensitivity. This makes *N. oceanica* a desirable laboratory model organism (Vieler A. et al. 2012).

Goal

The aim of the growth assay was the establishment of lethal antibiotics doses for *Nannochloropsis oceanica* wild type cells. This determination was essential for preparation of selective media for screening of the transformants. As nuclear transformation was performed with plasmid pSELECT100 containing hygromycin resistance cassette, the selective medium contained hygromycin. For chloroplastic transformation with plasmid pLit_chlL_chlor containing chloramphenicol resistance cassette, the selective media contained chloramphenicol. In addition to hygromycin and chloramphenicol, the range of other antibiotic types was tested. In addition to *N. oceanica* growth influenced by antibiotics, the survival of *N. gaditana* cells were also tested in this growth assay. The results for both species were compared with each other.

Materials and Methods

Cell cultures of *N. oceanica* and *N. gaditana* were grown in the Cell-Hi CN medium at temperature 23°C with constant illumination at $100 \mu\text{E m}^{-2} \text{s}^{-1}$ and constant shaking on a Heidolph® Rotamax 120 Orbital Shaker (see Chapter II - Materials and methods - Growth conditions).

Agar plates of 9 cm diameter were used for the plating out of the cell culture. The agar medium contained seawater added Cell-Hi CN (1 mL to 1 L seawater) and antibiotic concentrations of following range: 5, 10, 50, 100 and 300 $\mu\text{g/mL}$. The antibiotics used for the growth assay and their respective stock solution concentrations are listed in table 3.1 (experiment # 1).

Table 3.1: Antibiotics and their stock solution concentrations used in the cell growth assay (experiment #1).

Antibiotic	Stock solution concentration (mg/mL)
Ampicillin	50
Apramycin	30
Chloramphenicol	30
Cycloheximide	30
Gentamycin	30
G418 Neomycin	30
Hygromycin	50
Kanamycin	50
Spectinomycin	50
Tetracaine	30

For determination of the lethal antibiotic concentration for wild type cells of *N. oceanica* and *N. gaditana*, the cell growth on hygromycin-containing plates with narrow range of concentrations including 10, 20, 30, 40, 50, 60, 70, 80, and 100 $\mu\text{g/mL}$ was tested (experiment # 2).

Based on the initial growth test results, which identified the suitable concentrations of chloramphenicol, another growth assay with chloramphenicol was conducted that included narrower range of chloramphenicol concentrations (10, 20, 30, 40, 50, and 60 $\mu\text{g/mL}$) (experiment # 3).

For the growth tests the cell suspensions (3 μL) of both *N. oceanica* and *N. gaditana* species were spotted on antibiotic-containing with Cell-Hi CN medium plates at different cell concentrations ($\text{OD}_{750\text{nm}}$ of 1.0, 0.1, 0.055, 0.01 and 0.0055, corresponding to the cell numbers between 4.98×10^7 to 4.0×10^4 cells/mL, see table B.1, appendix B). Only cells of *N. oceanica* were used to test for lethal hygromycin concentrations (experiment # 2). The incubation of the cultures were performed under the same conditions as for the cell cultures` growth (see Materials and Methods). After two weeks of incubation, the results were recorded.

For determining the lethal antibiotic concentrations, the spotted cell concentration at 2.52×10^6 cells/mL ($\text{OD}_{750\text{nm}}$ of 0.055) was used, as higher concentrations might cause spontaneous mutations giving a feature of being able to grow on environment containing antibiotic. Intensity of the cell colonies of some cell growth experiments was analyzed by customer built Plate Imager analyzing the cell density on the agar-solidified medium in order to digitalize the visualized results.

Results and Discussion

The results of the cell growth experiments are presented according to their importance for the project.

Hygromycin (experiment # 2)

The cell growth and sensitivity results were obtained by visually comparing the plates with various antibiotic concentrations. The cell growth test for determination of the lethal concentration of hygromycin (range from 10–100 $\mu\text{g}/\text{mL}$) for *N. oceanica* wild type resulted in the cell growth visualized in figure 3.1. The cell growth inhibition was already observed at hygromycin concentration of 30 $\mu\text{g}/\text{mL}$ (therefore, the pictures of plates with higher hygromycin concentration were not included).

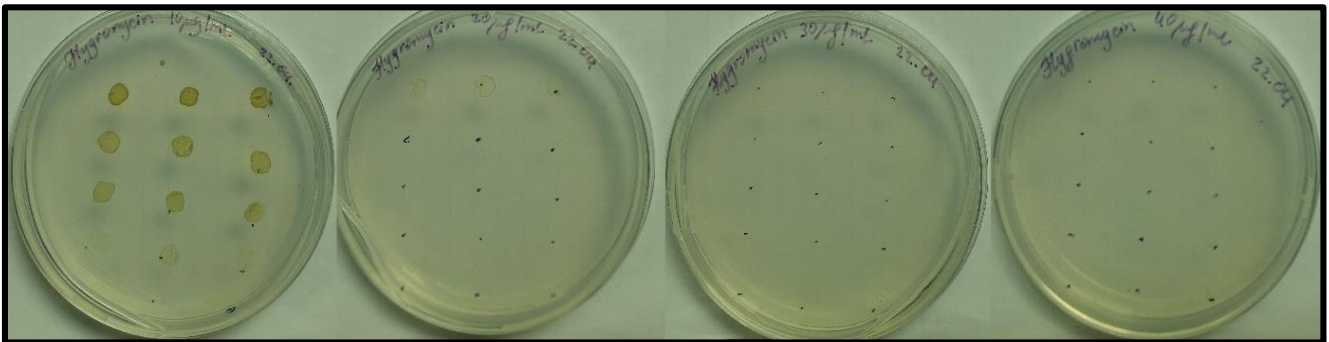


Figure 3.1: **Cell growth of *N. oceanica* CCMP1779 on various hygromycin concentrations.** The *N. oceanica* wild type were growing at 23°C and constant light intensity of 100 $\mu\text{E m}^{-2} \text{s}^{-1}$ including continuous rotational shaking. 3 μL *N. oceanica* cells of different concentrations ranging from 4.98×10^7 to 4.0×10^4 cells/mL (top to bottom) were plated out onto plates with various hygromycin concentration ranging from 10 – 100 $\mu\text{g}/\text{mL}$ (this picture presents concentration range up to 40 $\mu\text{g}/\text{mL}$). Cells were spotted three times each. The cell growth inhibition was already observed at low concentrations of 30 $\mu\text{g}/\text{mL}$.

The actual lethal dosage of hygromycin may be lower than 30 $\mu\text{g}/\text{mL}$, as only the growth of the most dense cell sample (4.98×10^7 cells/mL) could be observed at 20 $\mu\text{g}/\text{mL}$ hygromycin. This indicates that a larger number of cells helps in overcoming antibiotic toxicity or a higher occurrence of spontaneous mutations that make cells resistant to the antibiotic. As this part of the growth assay were conducted to investigate the lowest lethal concentration of hygromycin for *N. oceanica* wild type, the selective medium for the cells transformed with plasmid pSELECT100 should therefore contain hygromycin concentration of ≥ 30 $\mu\text{g}/\text{mL}$ to allow the selection of the cells with successful insertion of the hygromycin resistance cassette after transformation by electroporation. To ensure a stable transformation and according to the electroporation protocol from Vieler et al. (2012), where the agar-solidified selective medium included a hygromycin concentration of 50 $\mu\text{g}/\text{mL}$ (Vieler A. et al. 2012), it was decided that

the same concentration would be used in our studies (see chapter IV – Transformation by Electroporation).

Chloramphenicol (experiment # 3)

The first part of establishing the cell sensitivity to chloramphenicol included *N. oceanica* and *N. gaditana* cell growing on just four different chloramphenicol concentrations 5, 10, 50, and 100 $\mu\text{g}/\text{mL}$ (a part of the experiment # 1). The cell growth on agar-solidified selective medium with chloramphenicol from the initial experiment is shown on the figure 3.2.

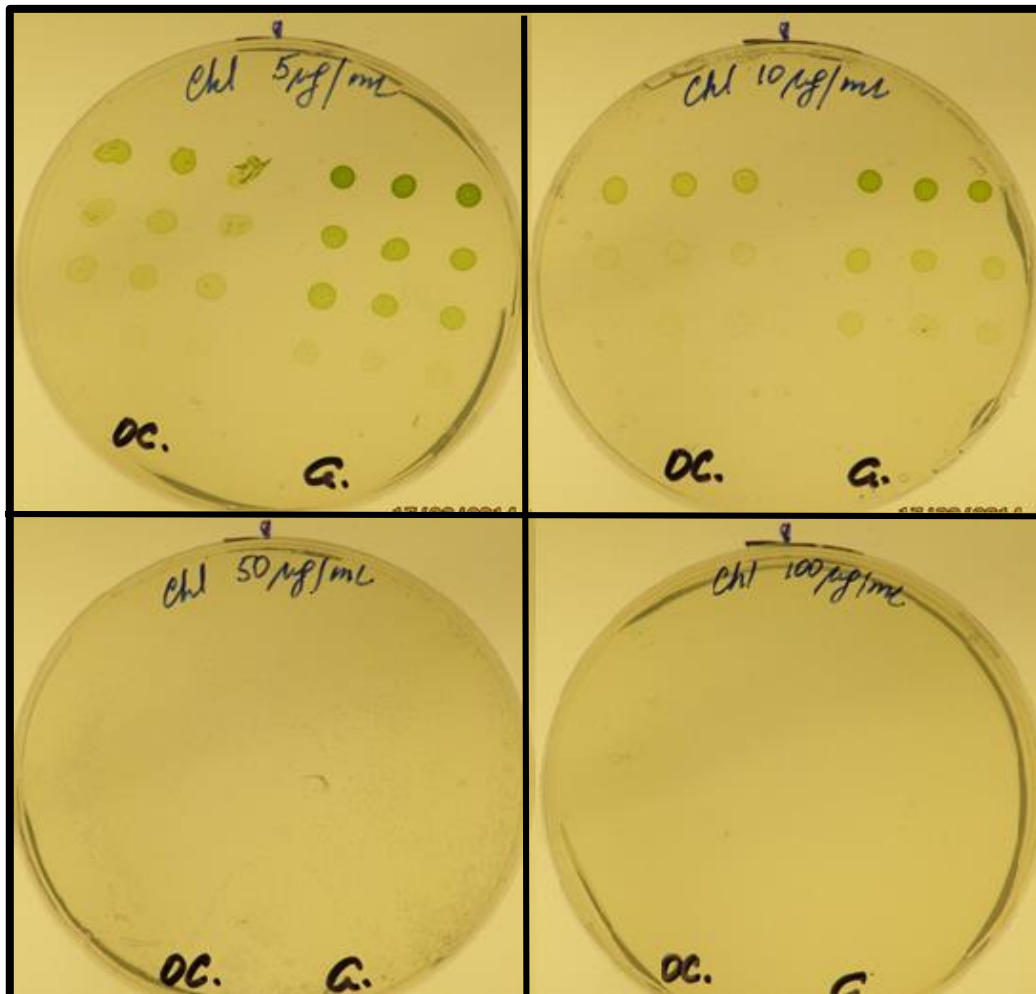


Figure 3.2: Cell growth of *N. oceanica* and *N. gaditana* on various chloramphenicol concentrations (a part of the experiment # 1). *N. oceanica* and *N. gaditana* wild type cells were growing at 23°C and constant light intensity of 100 $\mu\text{E m}^{-2} \text{s}^{-1}$ including continuous rotational shaking. *N. oceanica* (abbreviated OC.) and *N. gaditana* (abbreviated G.) cell samples of different concentrations ranging from 4.98×10^7 to 4.0×10^4 cells/mL were spotted 3 μL onto agar-solidified Cell-Hi CN medium added different chloramphenicol concentrations of 5, 10, 50 and 100 $\mu\text{g}/\text{mL}$. Cells were spotted three times each. The inhibition of the cell growth of both *N. oceanica* and *N. gaditana* was observed at antibiotic concentration of 50 $\mu\text{g}/\text{mL}$. The intensity of the cell colonies to *N. gaditana* indicated less sensitivity to chloramphenicol compared with *N. oceanica*.

Figure 3.2 indicates absence of cell growth (for both *N. oceanica* and *N. gaditana*) at a chloramphenicol concentration of 50 $\mu\text{g}/\text{mL}$. The cell growth at that point is already completely

inhibited. For determination of the precise lethal dosage for the wild type cells at the antibiotic concentration range of 10–50 $\mu\text{g}/\text{mL}$, an additional growth test was performed. At this experiment, a wider range of concentration was analyzed: 10, 20, 30, 40, 50, 60, 70, 80, and 100 $\mu\text{g}/\text{mL}$. Figure 3.3 represents the results of *N. oceanica* and *N. gaditana* cell growth with the aforementioned chloramphenicol concentrations (experiment # 3).

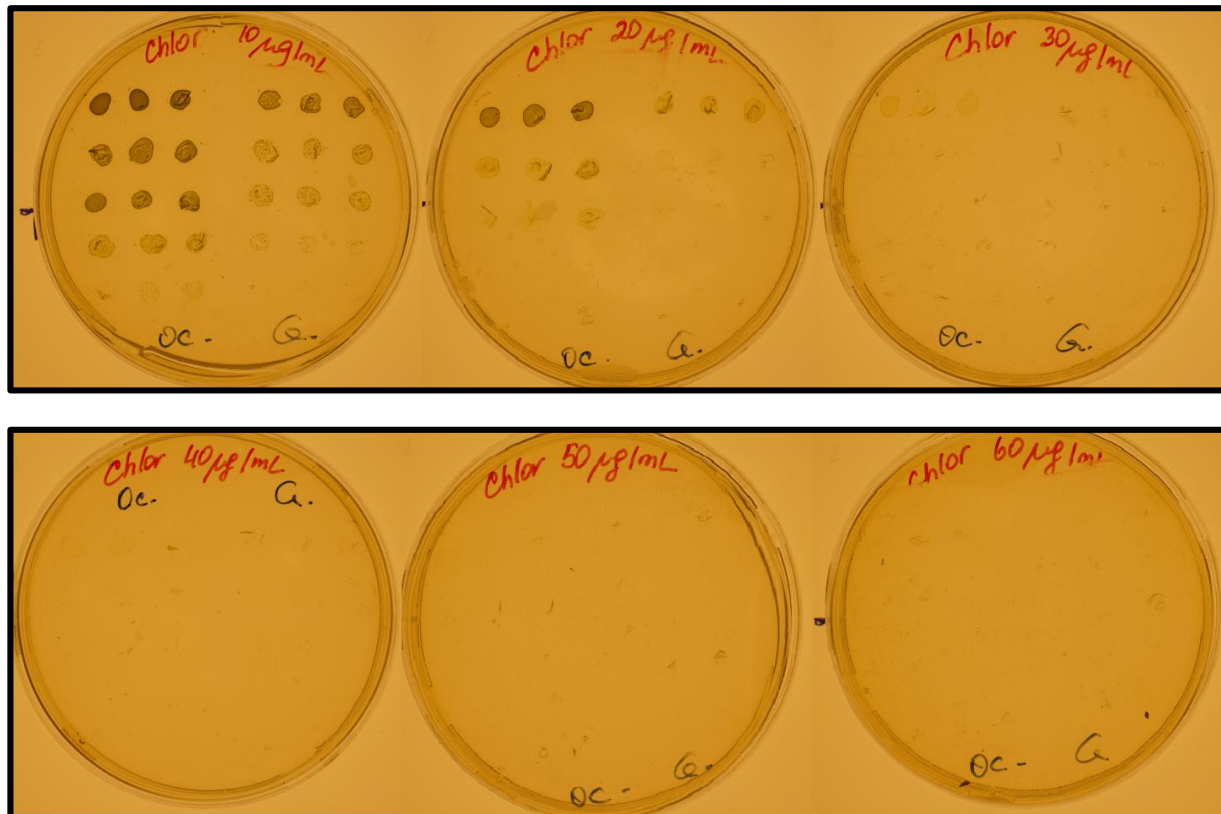


Figure 3.3: Cell growth of *N. oceanica* and *N. gaditana* on various chloramphenicol concentrations (experiment # 3). *N. oceanica* and *N. gaditana* wild type cells were growing at 23°C and constant light intensity of $100 \mu\text{E m}^{-2} \text{s}^{-1}$ including continuous rotational shaking. *N. oceanica* (abbreviated OC.) and *N. gaditana* (abbreviated G.) cell samples of different concentrations ranging from 4.98×10^7 to 4.0×10^4 cells/mL (top to bottom) were spotted 3 μL onto agar-solidified Cell-Hi CN medium added different chloramphenicol concentrations of narrower range from 10 to 100 $\mu\text{g}/\text{mL}$. Cells were spotted three times each. The inhibition of cell growth of both *N. oceanica* and *N. gaditana* was observed at antibiotic concentration of 40 $\mu\text{g}/\text{mL}$. At this experiment, the sensitivity of *N. gaditana* to the antibiotic seemed to decrease compared to sensitivity of *N. oceanica* at the previous experiment (experiment # 1, see figure 3.2).

A chloramphenicol concentration of 40 $\mu\text{g}/\text{mL}$ inhibited the growth of *N. oceanica* cells. This concentration of chloramphenicol was somewhat lower than the concentration tolerated by all *Nannochloropsis* strains reported in previous growth tests (100 $\mu\text{g}/\text{mL}$) (Vieler A. et al. 2012). However, the *N. oceanica* as mentioned previously, is somewhat less tolerant to high dosages of antibiotics compared to e.g. *N. gaditana* (see Introduction). Therefore, the chloramphenicol concentration of 40 $\mu\text{g}/\text{mL}$ was still used to prepare the selective medium for *N. oceanica* cell

after chloroplast transformation with transformation plasmid pLit_chlL_chlor containing chloramphenicol resistance cassette.

Initial experiment # 1

The determination of sensitivity to antibiotics of both *N. oceanica* and *N. gaditana* species was investigated in more detail using nine antibiotics (see table 3.1, figure 3.4 and summary table 3.2). The tables in figure 3.4 display the OD_{750nm} of the cell samples spotted on the plates (concentrations ranging from 4.98×10^7 to 4.0×10^4 cells/mL). Each table responds to a certain antibiotic type and its various concentrations.

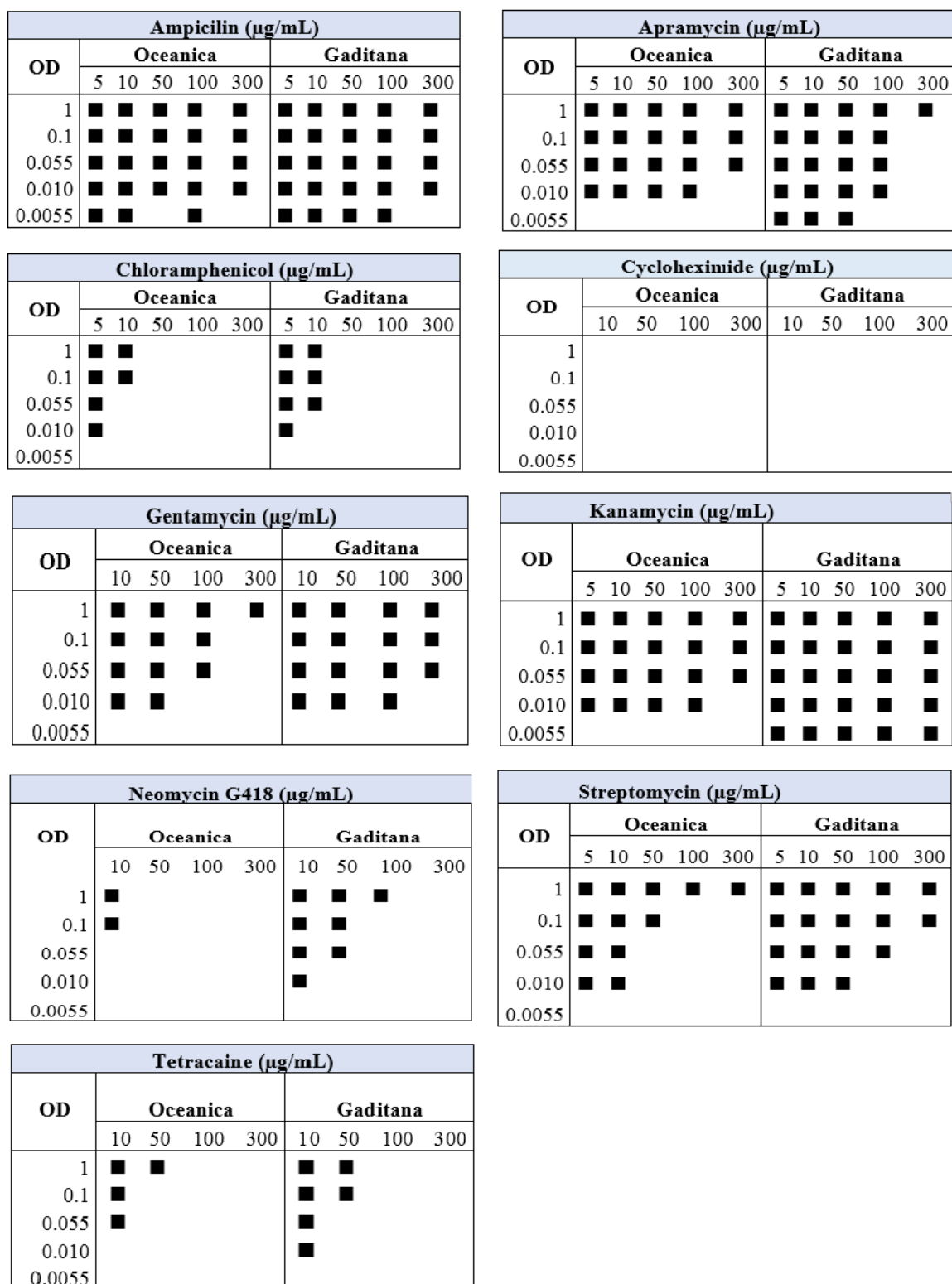


Figure 3.4: Comparison of effect of nine antibiotics on the growth of *N. oceanica* and *N. gaditana* cells (experiment # 1). *N. oceanica* and *N. gaditana* wild type cells were growing at 23°C and constant light intensity of 100 µE m⁻² s⁻¹ including continuous rotational shaking. The antibiotic concentrations are shown in µg/mL and range from 10 to 300 µg/mL. Growth characteristics were determined by spotting 3 µL of the cell suspension of different concentrations ranging from 4.98×10⁷ to 4.0×10⁴ cells/mL onto agar-solidified Cell-Hi CN medium added specific type of antibiotic at different concentrations. The positive cell growth is marked with black rectangle at certain cell and antibiotic concentration. In general, *N. gaditana* seemed to be less sensitive to all antibiotics compared to *N. oceanica*.

Table 3.2 **Comparison of the effect of nine antibiotics on *N. oceanica* and *N. gaditana* cell growth (summary of figure 3.4).** The antibiotic concentrations ranged from 10 to 300 µg/mL. Growth characteristics were determined by spotting 3 µL of the *N. oceanica* and *N. gaditana* cell suspensions of different concentrations ranging from 4.98×10^7 to 4.0×10^4 cells/mL on agar-solidified Cell-Hi CN medium added certain type of antibiotic at certain concentration. The table shows the antibiotic concentration at which the cell growth is inhibited.

Antibiotic	Lethal antibiotic concentration (µg/mL)	
	<i>N. oceanica</i>	<i>N. gaditana</i>
Ampicillin	≥ 300	≥ 300
Apramycin	≥ 300	300
Gentamycin	300	≥ 300
Cycloheximide	10	10
Chloramphenicol	10	50
Neomycin G418	10	100
Kanamycin	≥ 300	≥ 300
Streptomycin	50	300
Tetracaine	50	50

In general, it seems like the most harmless antibiotics for both *N. oceanica* and *N. gaditana* cells are ampicillin, apramycin, gentamycin and kanamycin (see figure 3.4 and table 3.2). These antibiotics could be used as an agent to prevent contamination by bacteria in cell cultures. Other antibiotics as chloramphenicol, cycloheximide, neomycin G418, and tetracaine inhibit cell growth at lower concentrations making them a reasonable choice for selection of the antibiotic resistance cassette containing-transformants.

Comparison of cell sensitivity to *N. oceanica* and *N. gaditana*

Interestingly, a consistent pattern of cell growth could be observed for *N. gaditana* that seemed to tolerate higher concentrations of all nine antibiotics tested compared to *N. oceanica*, except cycloheximide where no growth of both species occurred (see figure 3.4). The observation could be explained by previously reported higher sensitivity of *N. oceanica* due to faster and efficient passage of the molecules through the cell walls (Vieler A. et al. 2012).

However, this pattern changed when one part of the growth assay with chloramphenicol concentrations of wider range (from 10–100 µg/mL) (experiment # 3) was conducted. *N. gaditana* has shown being more sensitive to the chloramphenicol as less intensity of the colonies was visualized (see figure 3.3). The figure 3.5 represents *N. oceanica* and *N. gaditana* cell growth at chloramphenicol concentration of 5 µg/mL determined by the customer built

Plate Imager (a part of experiment # 1). As predicted, *N. gaditana* had more intense colonies through all dilutions.

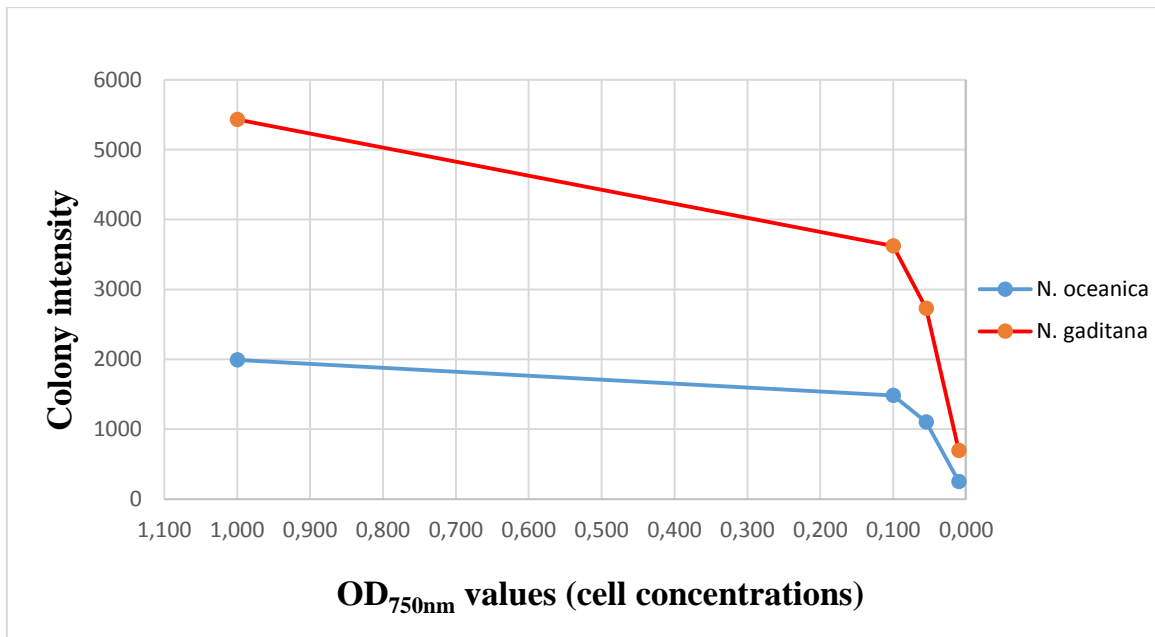


Figure 3.5: The correlation between intensity of the *N. oceanica* and *N. gaditana* cell colonies grown at 5 µg/mL chloramphenicol measured by Plate Imager and OD_{750nm} values as an indicator of cell concentrations (a part of the experiment # 1). Both *N. oceanica* and *N. gaditana* wild type were grown at 23°C and constant light intensity of 100 µE m⁻² s⁻¹ including continuous rotational shaking. The sensitivity of the cell growth to 5 µg/mL of chloramphenicol on the agar-solidified Cell-Hi CN medium was tested by spotting 3 µL of cell suspensions of different concentrations ranging from 4.98×10⁷ to 4.0×10⁴ cells/mL (indicated by OD_{750nm} values). After two weeks of incubation, the cell growth was analyzed by Plate Imager and relative colony intensities were calculated. Colonies of *N. oceanica* showed a lower density that may indicate higher sensitivity to chloramphenicol compared to *N. gaditana*.

The cell growth experiment # 3 included cells of *N. oceanica* and *N. gaditana* spotted 3 µL of the same concentrations as in the previous growth tests but now on the narrower range of chloramphenicol concentrations (10–100 µg/mL). Though the *N. gaditana* cells has been less sensitive to all antibiotics tested (experiment # 1), the growth pattern changed. *N. gaditana* became more sensitive to action of the antibiotics compared to *N. oceanica*. The new pattern of cell growth is shown in figure 3.6 (see also figure 3.3). The cell growth on the plates with chloramphenicol concentrations of 10 and 20 µg/mL were analyzed using Plate Imager.

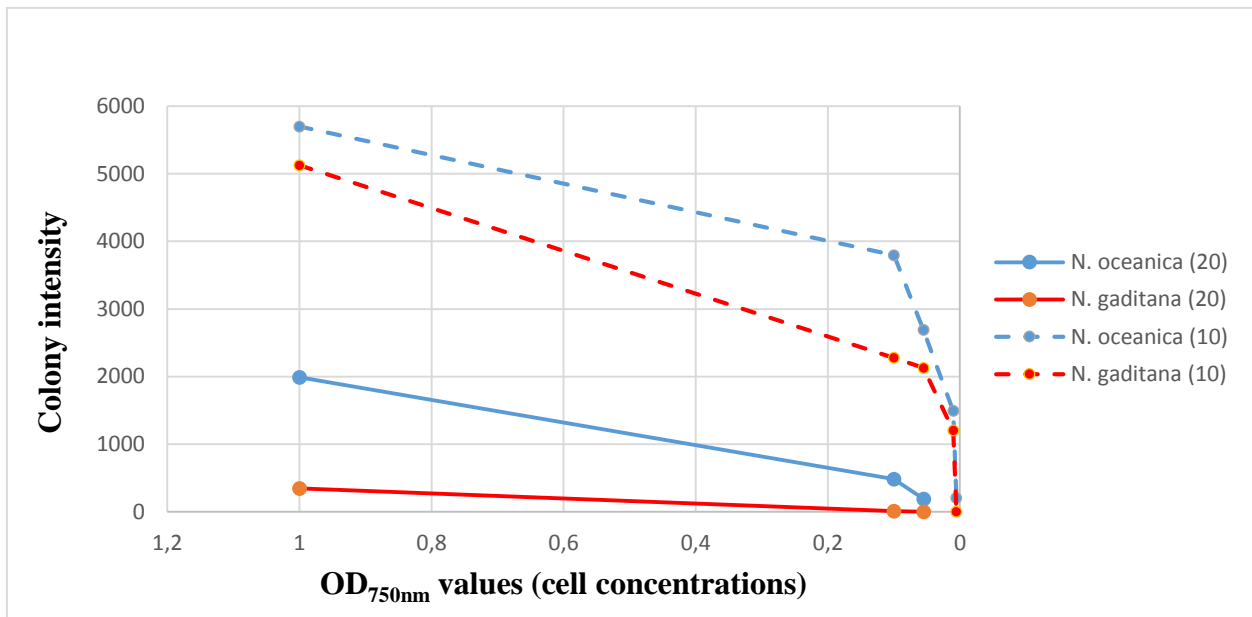


Figure 3.6: **The correlation between intensity of the *N. oceanica* (blue line) and *N. gaditana* (red line) cell colonies grown at 10 µg/mL (whole lines) and 20 µg/mL (dashed lines) of chloramphenicol measured by Plate Imager and OD_{750nm} values as an indicator of cell concentrations (experiment # 3).** *N. oceanica* and *N. gaditana* wild type were grown at 23°C and constant light intensity of 100 µE m⁻² s⁻¹ including continuous rotational shaking. The sensitivity of the cells to 10 and 20 µg/mL of chloramphenicol on the agar-solidified Cell-Hi CN medium was tested by spotting 3 µL of the cell suspension of different concentrations ranging from 4.98×10⁷ to 4.0×10⁴ cells/mL (indicated by OD_{750nm} values). After two weeks of incubation, the cell growth was analyzed by Plate Imager for determination of cell colonies intensity and therefore the cell growth. *N. gaditana* has shown becoming more sensitive to chloramphenicol compared to the experiment # 1, where *N. oceanica* was more sensitive to the chloramphenicol (see figure 3.5).

The fact that *N. gaditana* showed being less tolerable to the whole range of chloramphenicol concentrations at the cell growth experiment # 3, could be explained by one factor. The cell cultures of *N. oceanica* and *N. gaditana* taken for a more detailed growth assay with chloramphenicol (experiment # 3) were indeed grown at the same growth conditions. However, the cell culture of *N. gaditana* used for the cell growth assay was at a significantly higher density when used for the cell growth assay compared to *N. oceanica* culture. The negative effects of the cells being in a very dense cell culture include the induction of stress by nutrients and light deficiency. This could cause the cell wall changes at the plateau growth phase. Consequently, the *N. gaditana* cells used in the experiment # 3 (see figure 3.3) were more sensitive to the chloramphenicol present in the growth medium caused by cell stress resulting in a decreased cell growth compared to *N. oceanica* cells.

Conclusion

The main aim of the entire cell growth experiment was estimation of sensitivity of *N. oceanica* CCMP1779 cells to ten different antibiotics including hygromycin and chloramphenicol. This allowed selection of the transformants after successful nuclear and chloroplast transformations with pSELECT100 and pLit_chlL_chlor transformation plasmids containing the genes conferring resistance to antibiotics (hygromycin resistance gene and chloramphenicol resistance gene, respectively). For the selection of transformants containing hygromycin resistance gene, the selective agar-solidified medium should contain 50 µg/mL of hygromycin. For the selection of transformants containing chloramphenicol resistance gene, the selective agar-solidified medium should contain 40 µg/mL of chloramphenicol. As the cell growth assay was in parallel performed with *N. gaditana* cells, the results indicated *N. gaditana* species being less sensitive to the various range of antibiotics compared to *N. oceanica* species as long as the cells in the culture are not experiencing a growth stress.

Chapter IV

Transformation by Electroporation

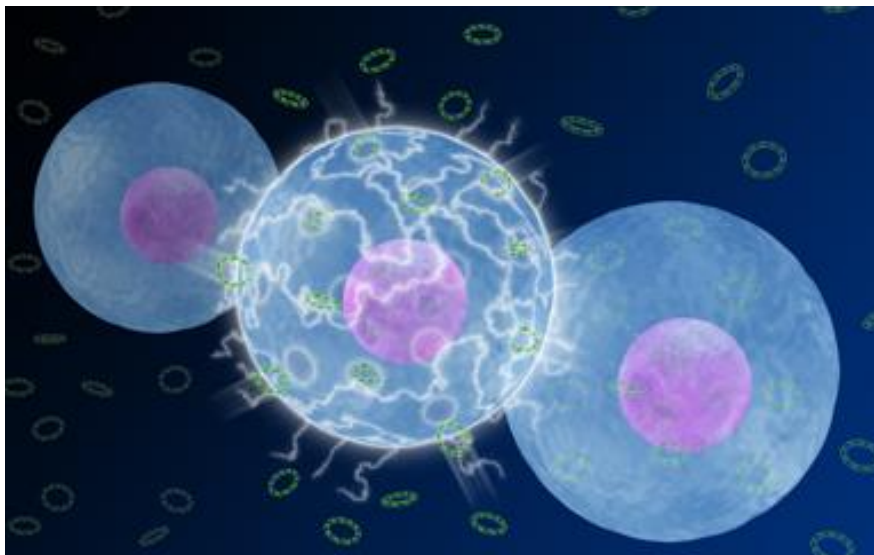


Photo: Punit Dhillon. <http://punitdhillon.com/2013/05/08/why-electroporation/>

Genetic transformation

For last decades, microalgae have become an attractive producer of renewable bioenergy. The ability to convert the solar energy into chemical compounds thereby storing potential energy (van deMeene A. M. et al. 2006, Chisti Y. 2008), led to a significant development of molecular and genetic tools that enable modification of the microalgae to benefit society. The creation of artificial life and redesign of natural organisms resulting in new features is the main goal of the synthetic biology (Benner S. A. 2003, Endy D. 2005). The idea of genetic transformation with new exogenous genetic material into a cell was first introduced in 1928 by British bacteriologist Frederick Griffith (Muller M. et al.). During the following decades, the transformation techniques were developed and adjusted for specific species in order to achieve high transformation efficiency.

The first successful transformation of green algae was conducted for more than two decades ago (Boynton J. E. et al. 1988, Debuchy R. et al. 1989) with still new approaches and methods being developed to this day. The methods employed for modifying microorganisms include particle bombardment (also called “gene gun“), glass beads agitation, microinjection, *Agrobacterium tumefaciens*-mediated transformation, and last but not least, electroporation (León-Bañares R. et al. 2004, León R. et al. 2007). A recent discovery demonstrated that the haploid genome of *Nannochloropsis* sp. (Kilian O. et al. 2011) can be highly efficiently transformed by electroporation. Furthermore, homologous recombination of the nuclear genome was observed in transformations with linearized plasmid. These findings and genome sequencing of different *Nannochloropsis* species make *Nannochloropsis* species an attractive species for further biotechnological improvement and development of functional genomics (Zhang C. et al. 2013).

Electroporation

At present, efficient transformation by electroporation has been reported for many marine species including species of red algae, green algae and diatoms. Gene transfer by electroporation has been in use for over 30 years, where animal, plant and bacterial cells were transformed efficiently without the need of large DNA quantities (Qin S. et al. 2012). The method has various advantages, as it is simple, low in cost, and producing transformants with high efficiency (Zhang C. et al. 2013). Gene deletion for several genes involved in nitrogen metabolism were performed successfully by homologous recombination (also called gene targeting) technique (Kilian O. et al. 2011). The technique includes insertion of the exogenous

genomic material (i.e. transformation plasmid) into the precise region of the host genome in order to delete the endogenous gene or insert some point mutations (Iizumi S. et al. 2006).

The electroporation method is based on the application of pulses of electric current through the cells, resulting in the disruption of cell walls and cell membranes. The exogenous genetic material (i.e. transformation plasmid) is then transferred inside the cells and becomes incorporated into the nuclear or plastid genome randomly as in most of the cases or by homologous recombination (in case of specifically constructed transformation plasmids). Various factors, such as electric voltage, resistance, amount of the inserted genetic material or cell amount resulting in different transformation efficiencies must be determined experimentally. For *Nannochloropsis* species, it has been shown that the insertion of linearized plasmid DNA by electroporation is more efficient than transformation with circular plasmid DNA, which did not result in formation of any transformants (Zhang C. et al. 2013). Generated transformants can be identified by the positive cell selection on the selective medium, followed by the colony PCR for confirmation of plasmid DNA-insertion into the host genome.

Recently, several research groups have reported the transformation of microalgae by electroporation (Kilian O. et al. 2011, Radakovits R. et al. 2012, Vieler A. et al. 2012, Zhang C. et al. 2013). These studies reported several crucial parameters influencing transformation efficiency, including the growth phase of cell culture, cell concentration and cell washing steps, amount of inserted plasmid, electroporation conditions including voltage and resistance, as well as subsequent incubation of transformed cells. The summary of all parameters and conditions is presented in table 4.1

Table 4.1: The summary of main parameters for efficient transformation by electroporation applied in recent studies of microalgae transformation resulting in rather high transformation efficiencies. The conditions include cell growth phase, cell washing with sorbitol solution, volume and amount of the transformed cells, amount of exogenous genetic material, voltage applied at electroporation, incubation conditions after the performed electroporation, and incubation time required for visible colonies to appear, as well as the determined transformation efficiencies.

Criteria	Zhang (2013)	Radakovits (2012)	Kilian (2011)	Vieler (2012)
Cells grown up to concentration (cells/mL)	4-5×10 ⁶	Mid-log phase	2×10 ⁶	Mid-log phase
Number of washing steps with sorbitol	3	2	4	2
Cell <u>concentration</u> per transformation (cells/mL)	2×10 ⁹	5×10 ⁹	1×10 ¹⁰	5×10 ⁸
Final <u>volume</u> of cell resuspension in sorbitol (µL)	100	100	100	200
Cell <u>amount</u> transformed (cells)	2×10 ⁸	5×10 ⁸	1×10 ⁹	1×10 ⁸
Plasmid amount (µg)	4 (add 40 µg salmon)	5	0,1-1	2-10 (add 20-100 µg salmon)
Electroporation parameters	2200 V 400 Ohm	900, 1050, 1200 V 500 Ohm 17-20 ms pulse	2200 V 500 Ohm	1100 V 600 Ohms 20-25 ms pulse
Resuspension in growth medium after transformation (mL), incubation	10 (12 h, low light, no shaking)	10 (12 h, low light, shaking)	10 (12 h, low light)	5 (48 h, shaking)
Antibiotic	Zeocin	Zeocin	Zeocin	Hygromycin B
Amount of the cells plated out (cells)	6,6×10 ⁷	5×10 ⁷	5×10 ⁸	1×10 ⁸
Transformation efficiency	2.8 × 10 ⁻⁵ colonies/cells/µg	12.5 × 10 ⁻⁶ colonies/cells/µg	2,500 transformants/µg	1.25 × 10 ⁻⁶ colonies/cells/µg

Difficulties

Despite the obvious progress in development of various genetic tools utilized by synthetic biology, there is always space for technology enhancement. In photosynthetic models, the synthetic biologists try to find ways of combatting intracellular oxidative stress, improvement of light harvesting and CO₂ fixation efficiency, utilization of metabolic modeling and network design for better understanding of cell processes. Fundamental to all these efforts is the ability to genetically manipulate the model organism efficiently. In order to further improve some aspects of transformation of marine algae, more studies targeting the mechanism behind genetic transformations are required (Wang B. et al. 2012).

Many factors influence transformation efficiency. Aforementioned transformation by electroporation has been in use for some decades already. Although a number of transformation protocols is established for specific species, there is always a space for improvement. Factors, such as the voltage applied at the electroporation system can be one of the decisive factors. A voltage that is too high, can cause complete cell wall disruption without any chance for recovery. A voltage that is too low, may be insufficient for cell wall breakage to occur, leaving many cells intact, thereby preventing the efficient entrance of exogenous genomic material. Another factor that might influence the transformation efficiency is cell density. Very dense cultures causes cells to experience stress due to nutrients and light deficiency. This causes the formation of rigid cell walls that prevent efficient electroporation. As the electroporation system applies electric pulses, the presence of salt from the growth medium, which is a good electrical conductor, can cause flow of electricity that destroys the cells. Therefore, it is essential to avoid any rests of growth medium by repetitive washing of the cells in the solution of sugar e.g. sorbitol solution. The amount of transformation plasmid inserted at electroporation is also one of the decisive factors. It has been reported that using the high amount of transforming DNA (1 µg or higher) can cause the multiple copies of selection marker DNA being integrated as concatamers.

Goal

The aim of the project was the establishment of the efficient transformation protocol by electroporation and investigation of various conditions influencing the transformation efficiency. Such factors included the cell concentration, the amount of exogenous genetic material, the voltage applied during electroporation, and addition of the salmon sperm DNA as a carrier DNA.

A number of different protocols are currently available for transformation of *Nannochloropsis* sp. by electroporation. Four of recently available transformation protocols (see table 4.1) were chosen for trial experiments in order to establish proper conditions for electroporation technique at our laboratory at Department of Biotechnology and Department of Biology. *Nannochloropsis oceanica* CCMP1779 was chosen as a competent model organism representing oleaginous microalgae and therefore a potentially attractive producer of biofuels. Transformations with hygromycin resistance cassette-containing plasmid pSELECT100 were performed.

Materials and Methods

Transformation plasmid pSELECT100

Transformation plasmid pSELECT100 was received from the Benning laboratory at Michigan State University. The plasmid contains a 497pLC-SfiI plasmid made by DNA Cloning Service (<http://www.dna-cloning.com>) that includes a 790 bp long native LDSP promoter (lipid droplet surface protein) that was amplified from *N. oceanica* CCMP1779 genomic DNA along with a 35S terminator region. The other features of the pSELECT100 include ampicillin resistance cassette (needed for bacterial resistance after cloning in *E.coli*), and open reading frame (ORF 1) containing hygromycin resistance gene and pBR2 origin. The hygromycin gene is under the control of the endogenous LDSP promoter (see figure 4.2).

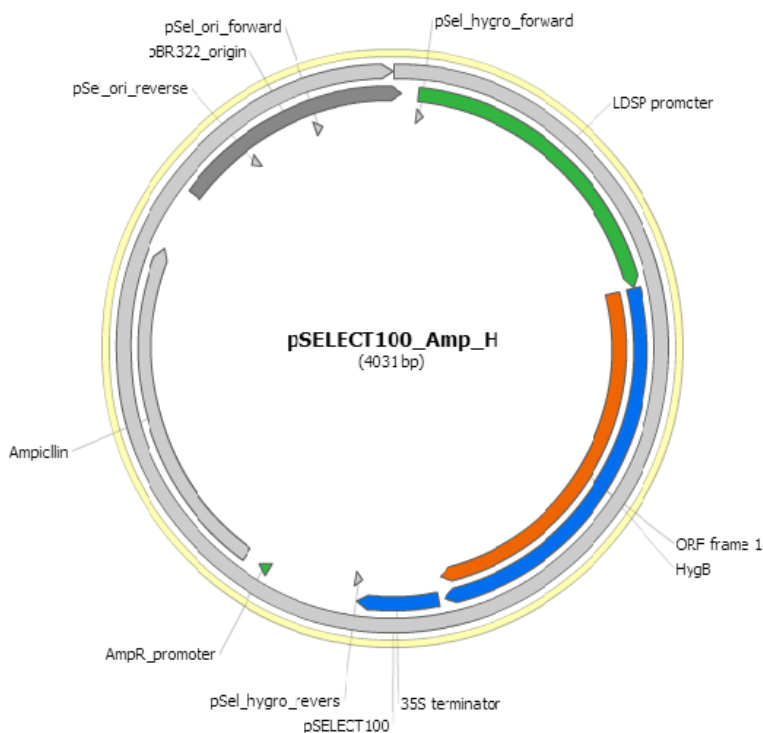


Figure 4.2: **The plasmid map of the pSELECT100.** The plasmid was used in the transformation of *N. oceanica* CCMP1779 cells by electroporation. The regions of the plasmid are annotated and include the hygromycin resistance cassette containing endogenous LDSP promoter and 35S terminator, ampicillin resistance cassette and pBR2 origin to mention the most important.

Hygromycin B is an antibiotic produced by the bacterium *Streptomyces hygroscopicus* (the mechanism of function is described in chapter III Cell Growth Assay - Introduction). The resistance gene for hygromycin is included in the pSELECT100 plasmid and codes for kinase protein called hygromycin phosphotransferase, which inactivates the antibiotic through its phosphorylation (Cabanas M. J. et al. 1978).

Plasmid verification

Cutting with SmaI

To identify the pSELECT100 plasmid quickly, it was cut with SmaI restriction enzyme. SmaI has its 100% activity with buffer # 4. 5 μ L pSELECT100 were added 1 μ L SmaI, 2 μ L buffer # 4 and diluted with water up to 20 μ L. The mixture was incubated at 25°C for 1.5 h. The cut plasmid parts were visualized by gel electrophoresis.

The gels for gel electrophoresis were made from 0.4 L of liquid agarose mixture containing 0.8% agarose and 30 μ L of GelGreen Nucleic Acid Gel Stain. The agarose mixture was stored at 70°C. For the verification of plasmid restriction patterns, 3 μ L water and 1 μ L 6X DNA loading dye (Thermo Scientific) were added to 1 μ L the pSELECT100 cut with SmaI. The same amounts of water and loading dye were added to 3 μ L GeneRuler 1kb DNA ladder (Thermo Scientific). The gel electrophoresis was performed at 100 volts for 1 h. Images of the gels were recorded using Molecular Imager ChemiDoc XRS+ (Bio-Rad).

DNA sequencing

The DNA sequencing was performed at GATC Biotech Company (www.gatc-biotech.com). For sequencing, ~5 μ L of 80-100 ng/ μ L plasmid DNA (400-500 ng total) were mixed with ~5 μ L 5 pmol of three primers. The total volume 10 μ L of the samples was reached by adding milliQ water. Primers used for the sequencing:

pSEL_ori_rev 5`- tctagttagccgtagttaggc-3`
pSEL_hygro_fwd 5`- aagatggagtggatggagga-3`
pSEL_hygro_rev 5`- tccagtgcctgcaggcatg-3`

Plasmid amplification methods

Different methods were applied to amplify the pSELECT100 plasmid (4031 bp long) for electroporation of *N. oceanica* CCMP1779. Heat-shock transformation of *E.coli* cells (Froger A. et al. 2007) was used to amplify the pSELECT100 plasmid. Extraction of the amplified

plasmid with Wizard *Plus* SV Minipreps DNA Purification Systems kit (Promega), however, resulted in very low yields of plasmid.

As an alternative to plasmid amplification in *E. coli* and plasmid extraction with Wizard *Plus* SV Minipreps DNA Purification Systems kit (Promega), amplification of the plasmid DNA by PCR was employed. Both standard PCR and touch-down (TD) PCR protocols were adjusted to the melting temperatures of the employed primers. This amplification resulted in linearization of the plasmid. The primers used for PCR amplification and their melting temperatures are shown below:

pSEL_ori_fwd	5`- cgacctacaccgaactgagata-3`	Tm° - 63.0
pSEL_ori_rev	5`- tctagtgtagccgtagtaggc-3`	Tm° - 59.2

The PCR mix included High Fidelity (HF) Phusion Polymerase known for its inherent proofreading capacity by removing noncomplementary sequences. 100 µL dNTP mix was prepared by mixing 10 µL of each nucleotide solution for adenosine, guanosine, thymidine and cytidine with 60 µL dH₂O. Circular pSELECT100 plasmid extracted from *E. coli* with Wizard *Plus* SV Minipreps DNA purification Systems kit (Promega) of concentration 40 ng/µL was used as a PCR template. The PCR mix was prepared according to the table 4.2.

Table 4.2: PCR mix used to amplify pSELECT100 plasmid (4031 bp) using both standard and touch-down PCR.

Reactant	Volume (µL)
dH ₂ O	32
MgCl ₂ free 10x buffer for HF Phusion Polymerase	10
dNTP	2.5
Forward primer	2.5
Reverse primer	2.5
HF Phusion Polymerase	0.5
Template DNA	1

For the amplification of the pSELECT100 plasmid, the TD PCR was used. In the TD PCR a gradient of successively lower annealing temperatures during each amplification cycle is applied. TD PCR was employed with the same settings as standard PCR with an additional step for primer annealing (see table 4.3). Afterwards, the plasmid was purified with QIAEX II Gel Extraction kit (QIAGEN).

Table 4.3 (a, b): The settings used for PCR amplification and therefore linearization of pSELECT100 transformation plasmid for both standard (a) and TD (b) PCR. TD PCR included a temperature gradient at annealing step for the initial 10 cycles, ranging from 56 – 65°C for a more efficient amplification and therefore higher product yield.

(a) Standard PCR				(b) Touch-down PCR			
Step	Temperature °C	Time (min.s)	Cycles (numbers)	Step	Temperature °C	Time (min.s)	Cycles (numbers)
Initial denaturation	98	3.00	1	Initial denaturation	98	3.00	1
Denaturation	98	0.30	25-30	Denaturation	98	0.30	10
Annealing	63	0.45		Annealing	56-65	0.45	
Extension	72	1.30		Extension	72	1.30	
Final extension	72	7.00		<i>Normal cycles</i>			
				Denaturation	98	0.30	15
				Annealing	63	0.45	
				Extension	72	1.30	
				Final extension	72	7.00	

Electroporation protocol

Previously published electroporation protocols were analyzed in order to derive transformation protocol parameters including the cell growth phase, the harvested cell amount, the amount of the transformation plasmid, the cell washing steps, electroporation conditions as well as the cell incubation followed the transformation.

Nannochloropsis oceanica CCMP1779 grew to a cell density of $3-8 \times 10^6$ cells/mL. A total of $1-5 \times 10^6$ cells were harvested by centrifugation ($3700 \times g$) for 10-15 min at 4°C. Collected cells were washed 2-3 times with 375 mM solution of sorbitol. The washed cells were distributed into aliquots in 2 mm electroporation cuvettes. An aliquot of 100 µL cells (5×10^7 - 10^8 cells) was incubated with plasmid amount ranging between 1.2–4.0 µg (see Results and Discussion Summarizing table 4.4 for more details for each transformation experiment). All the washing steps, concentrating and distribution of the cells were conducted on ice.

Electroporation was performed with Bio-Rad Gene Pulser II Electroporation System, which was adjusted to 500 Ohm shunt resistance, 25 µF capacitance and field strength of various

voltage ranging from 1100 to 2200 V. After electroporation, the cells were immediately collected from the electroporation cuvettes and transferred to 10 mL Cell-Hi CN medium. Subsequent incubation of the transformed cells was performed overnight at 23°C, constant light intensity of $100 \mu\text{E m}^{-2} \text{s}^{-1}$ and constant rotational shaking. Afterwards, the cells were collected by centrifugation ($3700 \times g$) for 10 min at room temperature and resuspended in 1 mL of the left Cell-Hi CN medium. 70 μL of the cell resuspension were plated out on the agar-solidified Cell-Hi CN medium containing 50 $\mu\text{g/mL}$ of hygromycin.

All calculation of appropriate cell concentrations for electroporation were performed based on $\text{OD}_{750\text{nm}}$ values as a cell count indicator (see chapter II – Correct Cell Count Estimation). The workflow for each of the transformation is described and summarized in the diagram (see figure 4.4).

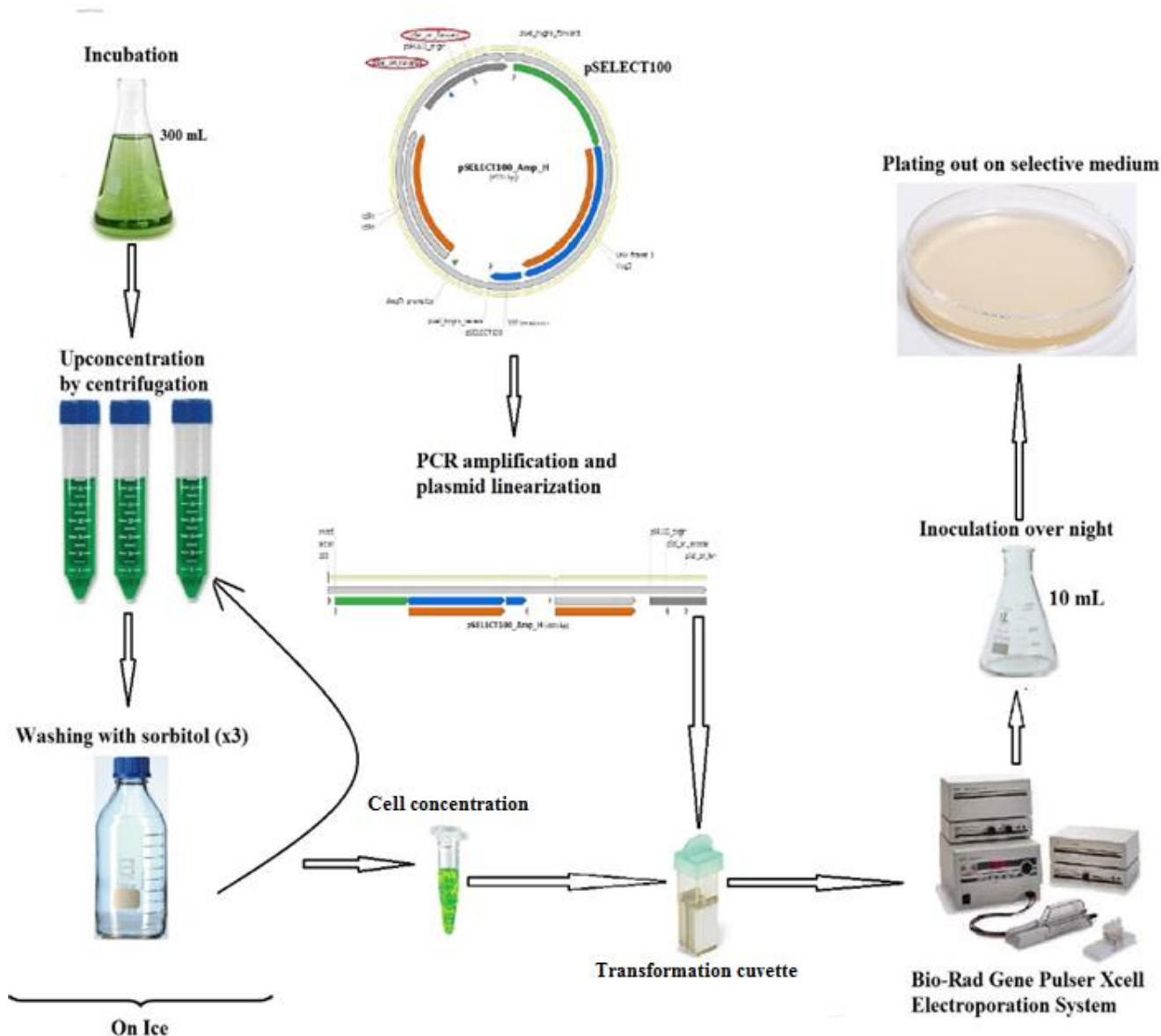


Figure 4.4: **The workflow for transformation by electroporation.** Harvesting of *N. oceanica* CCMP1779 cells, cell concentration and washing with sorbitol solution are initial steps of this transformation technique performed on ice. The washed and concentrated cells are transferred into the 2 mm electroporation cuvettes followed by PCR-amplified (linear) plasmid pSELECT100 containing hygromycin resistance. The cells are further exposed for electric pulses by Bio-Rad Gene Pulser Xcell Electroporation system under different voltages. The cells are then incubated overnight at 23°C, constant light intensity of 100 $\mu\text{E m}^{-2} \text{s}^{-1}$ and continuous rotational shaking. Afterwards, the collected cells are plated out on the selective medium containing 50 $\mu\text{g/mL}$ hygromycin.

Screening method

For detection of successful insertion of plasmid DNA into *N. oceanica* CCMP1779 genome, electroporation samples were plated out on the agar-solidified selective medium. The medium was prepared by adding 15 g of Microbiology Agar-agar (Merck Millipore), 1 mL of Cell-Hi CN medium (Varicon Aqua Solutions) and 1 mL of hygromycin (stock solution 50 mg/mL) to 1 L of sterile filtered and autoclaved seawater. The final concentration of hygromycin in selective medium was 50 $\mu\text{g/mL}$, which prevented growth of *N. oceanica* wild type (see

Chapter III – Cell Growth Assay - Results). “Master plates” containing 50 µg/mL of hygromycin were made for propagating colonies, which appeared on selective agar plates after electroporation. Colonies on these master plates were transferred to new master plates with selective medium every month. Transformation efficiencies were determined using a standard formula:

$$\text{Transformation efficiency} = \frac{(\text{Colonies})/(\text{Cells plated out})}{(\text{Amount of plasmid } (\mu\text{g}))}$$

To verify for positive transformants, the release of genome from the potentially transformed cells was performed by various methods. Amplification of the hygromycin resistance cassette by TD PCR (see table 4.3 b) was conducted in order to confirm the successful insertion of the pSELECT100 plasmid DNA into the *N. oceanica* CCMP1779 genome.

In first attempt to amplify genomic DNA, 32 random colonies from the master plate were directly transferred into PCR tubes for subsequent amplification of the hygromycin resistance cassette by TD PCR. The PCR setups were adjusted an initial denaturation step extra at 98°C for additional 10 min in order to break down the cell wall and liberate the DNA out of the cells. TD PCR was employed with *Taq* polymerase and Standard *Taq* polymerase buffer with the same setups described in table 4.3 b (TD PCR). The PCR mix for colony PCR included the 5 times less of quantities described in table 4.2. A positive control, pSELECT100 plasmid, was not included in the TD PCR amplifications. The primers applied for the amplification of the hygromycin resistance cassette were designed and included:

pSel_hygro_fwd 5`- aagatggagtggatggagga-3`
 pSel_hygro_rev 5`- tccagtgcactgcagcatg-3`

A second method to release of the genomic DNA included resuspension and incubation of colonies at temperature 96°C in 30 µL of milliQ water for either 6, 8, or 10 min. The availability of released genomic DNA was confirmed by NanoDrop 1000 spectrophotometer (Thermo Scientific).

A third method tested included boiling of *N. oceanica* colony pools picked from the master plate in 100 µL of milliQ water. Additionally, samples were frozen twice with liquid nitrogen to break the cells. The availability of liberated genomic DNA was assessed by NanoDrop 1000 spectrophotometer (Thermo Scientific).

A fourth method tested to release the genomic DNA was conducted by adding 20 µL of various lysis buffers, such as 10 mM Tris/1 mM EDTA (TE) buffer and SDS buffer (0.2 %) to the cell

colonies picked from the selective agar-solidified medium. In addition, other colonies were again dissolved in milliQ water for a second attempt to release the genomic DNA. Samples were vortexed vigorously, and incubated at 95°C for 7 min. Afterwards, the samples were centrifuged for 5 min at 4000 × g. An aliquot of 1 µL of supernatant was taken as PCR template for TD PCR with *Taq* polymerase and Standard *Taq* buffer. A positive control, pSELECT100 plasmid, was included in the TD PCR amplifications.

Finally, the Wizard Genomic DNA Purification kit (Promega) was used to extract DNA from *Nannochloropsis* cells. In advance, the colonies of *N. oceanica* cells obtained after the transformations at different conditions were cultivated in the liquid selective medium containing 50 µg/mL hygromycin. The cells were grown for 5-6 days in order to achieve a high cell concentration. The genomic DNA extracted with Wizard Genomic DNA Purification kit (Promega) was subsequently used as a template for TD PCR amplification of inserted hygromycin resistance cassette in order to confirm the integration of plasmid DNA into the *Nannochloropsis* genome.

Transformation added carrier DNA

The last transformation was performed with addition of carrier DNA, namely salmon sperm DNA. For this purpose, 7.65 µg of already extracted, dehydrated salmon sperm DNA were dissolved in 300 µL of sorbitol solution and resuspended by pipetting up and down ten times. Then, 1.5 mL of 96% ethanol was added and the sperm DNA suspension was cooled at -20°C for 2 h. Prior to centrifugation, the location of the pellet according to the placement of the tube and the rotation direction of the centrifuge, was marked due to transparency of the sperm DNA. It was hence centrifuged for 10 minutes, at 4000 × g and 4°C. The supernatant was vacuum pumped off with a sterile pipette tip. Then, 1 mL of 70% ethanol was added to the DNA pellet. The sperm DNA was centrifuged at the same position and the same conditions. The supernatant was vacuum pumped off for a second time and the rest of the ethanol was evaporated at the heatblock at 37°C for approximately 1 h.

The subsequent transformation of *N. oceanica* CCMP1779 included in total 10 samples, with 2 negative control samples, 4 samples containing high (4 µg) and 4 samples containing low amount (1.5 µg) of pSELECT100. A 10 fold of sperm DNA amount was added to two of each of the four samples, 40 and 15 µg respectively. The 10 samples were then transformed by electroporated at 1800 volts.

Results and Discussion

Plasmid verification

To confirm that the received plasmid is identical with the pSELECT100 plasmid reported in the corresponding publication, the plasmid was cut with restriction enzyme SmaI. The plasmid pSELECT100 has three cutting sites for SmaI enzyme and a complete digest should result in fragment sizes of 115 bp, 1333 bp, and 2601 bp. Gel electrophoresis of the partially digested plasmid revealed a fragment distribution that was consistent with the pSELECT100 cut with SmaI (see figure 4.5).

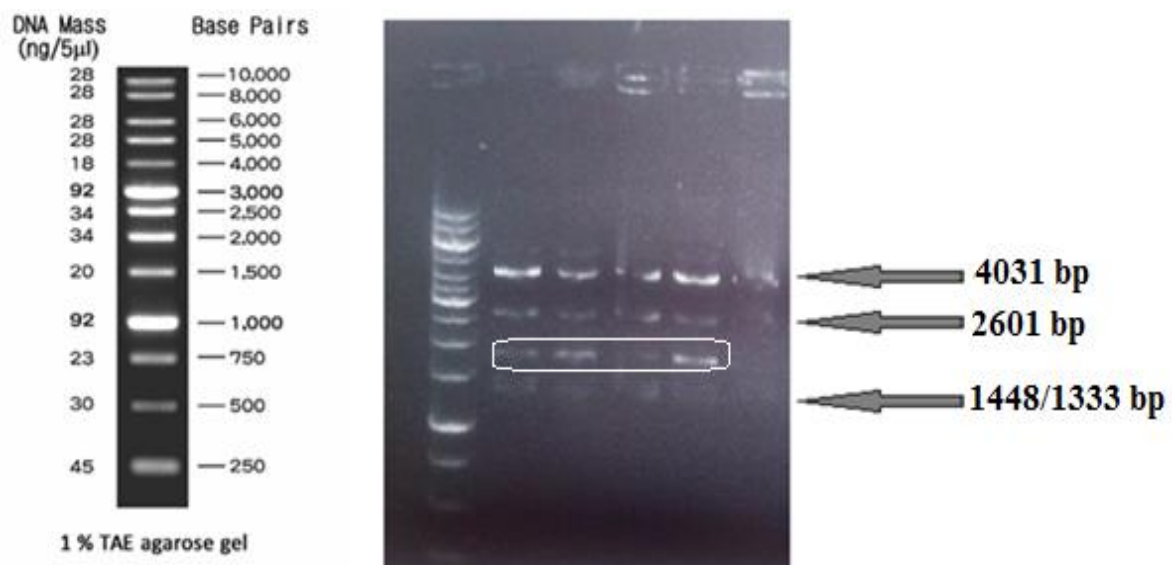


Figure 4.5: The gel image with a band pattern expected after cutting pSELECT100 plasmid with SmaI restriction enzyme. The top band indicates the pSELECT100 cut at one of the cutting sites resulting in a linearized plasmid (4031 bp). The next band represents a DNA piece of size 2601 bp indicating that the plasmid was cut twice. The two bands at the bottom close to each other indicates smaller parts of the plasmid with only 115 bp difference after being digested three times, namely 1448 and 1333 bp. The band representing the part of the plasmid of size ~1800 bp (circled white) has not been indicated, suggesting being a result of the SmaI digestion at an extra cutting site of pSELECT100.

All the fragments except the part of 115 bp, that might be further down on the gel, were visualized at the gel image, confirming the identity of pSELECT100. The band of 4031 bp indicates the linearized pSELECT100 (cut once), and bands 2601, 1448 and 1333 bp indicate pSELECT100 being cut twice or three times, respectively. However, the visualized on the gel image band of approximate size 1800 bp was not identified. A possible explanation for this would be an extra cutting site for SmaI, which is not annotated at the plasmid map of pSELECT100. However, after sequencing the pSELECT100 plasmid (see below), no more SmaI cutting sites (CCCGGG) were detected in the sequenced region, suggesting an additional cutting site outside the sequenced region. Though the digestion with SmaI restriction enzyme

gave good indication that the obtained plasmid was pSELECT100, albeit with an additional *Sma*I cutting site present, an additional verification step was performed.

pSELECT100 DNA sequencing

DNA sequencing of pSELECT100 transformation plasmid was performed in order to verify its identity, in particular, the presence of a functional hygromycin resistance cassette. Several regions of pSELECT100 plasmid were sequenced and analyzed by GATC Biotech Company. The resulted sequences were aligned with the available plasmid map of pSELECT100 provided by the Benning lab resulting in 100% match. The most essential part of pSELECT100 plasmid to be confirmed was the hygromycin resistance cassette, which confers resistance of transformants to hygromycin. The DNA sequences of hygromycin resistance cassette obtained by GATC Biotech Company were identical to the plasmid sequence provided by the Benning lab, with one exception. Extra nucleotides were detected on the pSELECT100 plasmid at the LDSP promoter region of hygromycin resistance cassette (68 – 855 bp), which are not present in the supplied DNA sequences of pSELECT100 (see figure 4.6).



Figure 4.6: **A sequenced DNA region of the pSELECT100 plasmid.** The DNA sequence of LDSP promoter (68-855 bp) is located upstream for hygromycin resistance gene (856-1881 bp) in the hygromycin resistance cassette of the pSELECT100 plasmid. The first DNA sequence (top) is available from the plasmid map of the pSELECT100 plasmid. The second DNA sequence (bottom) is the DNA sequence of the provided by the Benning lab pSELECT100 plasmid, sequenced at the GATC Biotech Company, revealing two extra nucleotides (position 831 and 832, marked red) in the region of LDSP promoter.

The presence of these extra nucleotides was considered being nonsignificant for successful formation of the transformants. The TC nucleotides were localized further upstream on the promoter region, which should not affect binding of RNA polymerase as it is not a part of the TATA box. Therefore, the decision to continue applying this plasmid for subsequent transformation of *N. oceanica* CCMP1779 was taken.

Sequence analysis of sequences obtained from the GATC Biotech Company and provided plasmid sequences revealed that the terminator 35S region was as well intact. Hence, the intactness of the whole hygromycin resistance cassette was confirmed.

Amplification of pSELECT100

After amplification of pSELECT100 transformation plasmid through its cloning into *E.coli* cells and subsequent purification with Wizard *Plus* SV Minipreps DNA purification Systems kit (Promega), the product yield was 40–60 ng/μL measured with NanoDrop1000 spectrophotometer (Thermo Scientific). This low yield was unsatisfactory for subsequent transformation of *N. oceanica* CCMP1779 cells that requires larger amounts of DNA.

This led choosing PCR methods (both standard and TD PCR protocols) for the amplification of plasmid DNA. Another advantage of the PCR amplification approach was linearization of the plasmid that was required for the efficient transformation of the *Nannochloropsis* as it was previously reported in one of the transformation studies (Kilian O. et al. 2011).

After the PCR amplification, the samples were run on the gel electrophoresis and the presence of the band of 4031 bp was confirmed. The product yield after purification of the plasmid was between 150-220 ng/μL, which is 3-5 times higher than amplifying the plasmid through cloning and plasmid miniprep in *E. coli* cells. TD PCR was able to successfully amplify the plasmid DNA, indicated by visible bands at the imaged gel, while standard PCR with a defined annealing temperature failed to provide visible amounts of PCR-product. This might be caused by true annealing temperatures values that are different from the values provided by various online T_m calculators.

In summary, the amplification of the plasmid by TD PCR is a very efficient method for amplifying plasmid DNA. An advantage of plasmid amplification by PCR over plasmid amplification in *E.coli* cells is based on that there is no requirement for subsequent cutting with restriction enzymes for plasmid linearization. Also transformation of *E.coli* cells and plasmid purification by miniprep is more time-consuming and gives a lower product yield of DNA compared to PCR amplification.

Electroporation

Electroporation of *N. oceanica* CCMP1779 cells was performed several times with Bio-Rad Gene Pulser II Electroporation System using different parameters. The conditions and comparison of all transformations performed are presented in table 4.4 where each performed electroporation abbreviated with EL_`number`. Electroporation performed with addition of salmon sperm DNA as the carrier DNA is abbreviated as EL_sperm.

Table 4.4: The summary of all transformation of *N. oceanica* CCMP1779 experiments performed by electroporation during the master project. Various conditions including the cell cultures concentrations, the cell washing steps with sorbitol, the transformed cell amount and volume, as well as parameters for the electroporation including voltage and used plasmid amount, as well as time required for the appearance of the colonies, are indicated for all of the transformation experiments. The transformations are given the names abbreviated EL_`number` for the better distinguishing of the performed experiments and their conditions.

Transformation criteria	EL1	EL2	EL3	EL4	EL5	EL_sperm
Cell grown to concentration (cells/mL)	7.78×10 ⁶	7.85×10 ⁶	1.77×10 ⁷	3.53×10 ⁶	4.51×10 ⁶	2.10×10 ⁶
Cell harvested (amount of cells in 300 mL)	2.33×10 ⁹	2.36×10 ⁹	5.31×10 ⁹	1.06×10 ⁹	1.35×10 ⁹	6.30×10 ⁸
Sorbitol concentration (mM)	375	375	375	375	375	375
Number of washing steps with sorbitol	2	2	3	3	3	3
Cell concentration per transformation (cells/mL)	9.36×10 ⁸	5.00×10 ⁸	5.57×10 ⁹	5.00×10 ⁸	5.00×10 ⁸	5.00×10 ⁸
Final volume of transformed cell (µL)	100	100	100	100	100	100
Cell amount transformed (cells)	9.36×10 ⁷	5.00×10 ⁷	5.57×10 ⁸	5.00×10 ⁷	5.00×10 ⁷	5.00×10 ⁷
Cell amount plated out (cells)	6.55×10 ⁶ (1.87×10 ⁷ in 200 uL)	3.50×10 ⁶	3.90×10 ⁷	3.50×10 ⁶	3.50×10 ⁶	1.75×10 ⁶
Voltage (V) + Plasmid amount (µg)	2200 + 3 2200 Neg.	2000 Neg. 1800 + 1.5 2000 + 1.5	1800 Neg. 2200 + 1.5 1800 + 4.1	2200 + 1.2 1800 + 1.2 1100 + 1.2 2200 + 4 1800 + 4 1100 + 4	2200 Neg. 1800 + 4.5 1400 + 4.5 2200 + 1 1800 + 1 1400 + 1	1800 + 4 1800 + 1.5 1800 + 4 + 40 µg sperm DNA 1800 + 1.5 + 15 µg sperm DNA
Visible colonies (weeks)	2-3	2-3	2-3	2-3	2-3	3-4

One of the most important criteria of successful transformation by electroporation was competence of the *N. oceanica* CCMP1779 cells. Previous studies (Kilian O. et al. 2011, Radakovits R. et al. 2012, Vieler A. et al. 2012, Zhang C. et al. 2013) indicated that the most competent cells are in their exponential phase of growth, presumably experiencing little stress. Cells experiencing stress would possess thickened cell walls, which would decrease the efficiency of DNA entering the cell during electroporation. The electric pulses of Bio-Rad Gene Pulser II Electroporation System would therefore not manage to disrupt the cell wall, and the supplied energy would disappear as heat, thereby damaging the cells. This effect was observed for some transformation samples, as their transformations produced sparkles during the transfer of electric pulses through the electroporation cuvette.

In general, it is essential to avoid any humidity while working with electroporation. As the electroporation cuvettes are stored on ice prior to the electroporation in order to keep the cells cooled, the metal plates of the electroporation cuvettes must be wiped with laboratory wipes to avoid the condensation problem.

For preparing the cells for transformation, a concentration step on ice is required. This concentration step is accomplished by centrifugation at 4°C keeping the cells cool. Washing steps with cold sorbitol solution are performed for the elimination of all salt and nutrient supplements that are part of the growth medium. Insufficient washing of cells can cause the sparkling or “explosion” of cell samples during electroporation, as salt is a good electricity conductor. The transformation trials, where concentrated cell samples were washed just twice caused cells to “explode” during transformation. The decision to perform the washing three times was thus taken.

As previously reported protocols (Kilian O. et al. 2011, Radakovits R. et al. 2012, Vieler A. et al. 2012, Zhang C. et al. 2013) of transformation microalgae by electroporation all used similar concentration of the cells (see table 4.1), the decision was taken to use cell concentration of $\sim 5 \times 10^8$ cells/mL. However, one transformation experiment included cell concentration ten times higher (EL_3), which caused difficulties in pipetting the cells and mixing them with pSELECT100 plasmid. Collecting the cells for the overnight incubation afterwards was also problematic as the cell sample became too dense and dry.

All the electroporation parameters are included in the table 4.4. Various combination of voltage and amounts of the pSELECT100 plasmid were tested out. A voltage that was too high would destroy the cell wall without any possibility for recovery, while a voltage that was too low could not accomplish the cell wall disruption resulting in an insufficient flow of exogenous genomic material into the cells. Therefore, the finding of proper voltage and plasmid amount was essential for establishing an efficient transformation. The subsequent determination of transformation efficiencies has revealed the best combination (see figure 4.14 below).

Table 4.5: Further description of the master plate # 5 (see figure 4.7) including all the *N. oceanica* cell colonies selected on the selective medium containing 50 µg/mL hygromycin. A tendency of the *N. oceanica* cells from the negative control transformation samples to form a colony on the selective medium was caused by the spontaneous mutation. The transformation parameters are presented for each colony from the master plate # 5. Though cell colonies transformed under the same conditions are spread all over the master plate, the results are collected and percentage of the formed colonies is determined.

2200 High	2200 Low	1800 High	1800 Low	1400 High	1400 Low	1100 High	1100 Low	Negative
13 green	1 green	6 green	16 green	23 green	34 nothing	10 green	8 green	4 green
14 green	2 green	7 green	29 green	24 green	35 green	11 green	9 green	5 green
15 green	3 green	20 yellow	30 green	25 green	36 green	71 green	67 green	17 green
52 green	12 green	21 yellow	31 green	26 green	37 yellow	72 green	68 nothing	18 green
62 -	27 green	22 green	32 green	53 green	38 green	73 green	69 green	19 yellow
63 -	28 green	41 green	33 green	54 green	39 green	%	100	47 green
64 -	56 green	65 green	44 green	55 green	40 green		%	48 green
80 -	57 green	66 green	45 green	97 green	42 green			74 green
81 -	58 green	87 green	46 green	98 yellow	43 green			75 green
82 -	59 green	88 green	49 -	99 green	109 green			76 -
83 -	60 green	89 green	50 green	100 green	110 yellow			90 -
136 green	61 green	122 -	51 green	%	91			91 green
137 green	77 green	123 green	84 green		112 green			92 yellow
138 green	78 green	124 -	85 green		%	77		93 yellow
139 yellow	79 green	125 -	86 green					94 green
140 -	101 green	126 green	104 green					95 yellow
141 green	102 green	127 green	105 green					96 yellow
142 green	103 green	128 green	106 green					113 green
%	50	%	72					114 little green
	116 green		107 green					115 -
	119 green		108 green					116 green
	120 green		134 green					130 -
	121 green		135 green					131 green
	%	100	%	95				132 green
								133 green
								%
								40

Some cells of the negative control samples, where no PCR-amplified pSELECT100 plasmid DNA was added, grew even on hygromycin-containing selection plates. However, the appearance of these colonies compared to colonies formed by cells transformed with the plasmid, and therefore likely to contain the resistance cassette, was less green and without a clearly marked colony shape. Therefore, these colonies were not included in determination of growth percentage (see table 4.5). The formation of the colonies gave insight in the transformation efficiencies and the nature of conditions most appropriate for the transformation. The insertion of the hygromycin resistance cassette was yet to be confirmed by releasing the genomic DNA out of the transformed cells and amplification of the cassette by TD PCR.

Many techniques have been applied in order to release the genomic DNA out of the transformed *N. oceanica* CCMP1779 cells. The first method included picking of 32 colonies from the master plate and their direct transfer into the PCR tubes for subsequent PCR amplification of the potentially inserted hygromycin resistance cassette with an extra denaturation step (see Materials and Methods). The lack of amplified DNA bands indicates that no successful release of the genomic DNA occurred using this method (see figure 4.8).

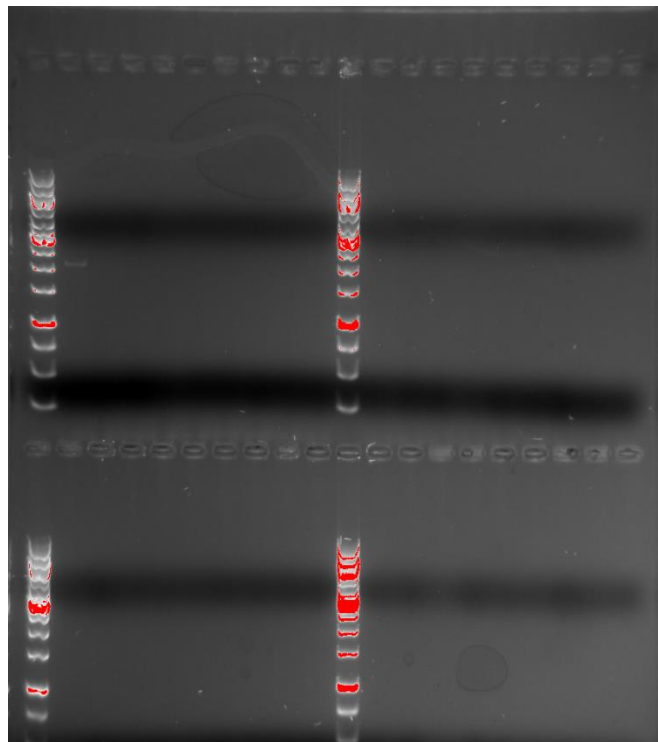


Figure 4.8: **Gel image of unsuccessful colony PCR after transformation of *N. oceanica* cells with PCR-amplified transformation plasmid pSELECT100.** 32 colonies of transformed by electroporation *N. oceanica* CCMP1779 cells selected on the selective medium with hygromycin, were picked and transferred into the PCR tubes for subsequent PCR amplification of the potentially inserted hygromycin resistance cassette. The gel picture shows no bands indicating that no insertion of the resistance cassette has occurred in the genome of *N. oceanica* cells. Unfortunately, a positive control was not included. The band observed on the first well did not indicate for any successful PCR-amplified hygromycin resistance cassette due to wrong size of the DNA sample.

It was concluded that the additional denaturation step at 98°C for 10 minutes did not cause the cell wall disruption and therefore release of the genomic DNA. The band visualized on the first well on the gel image did not indicate any successful PCR amplification due to incorrect size of the amplified DNA. As a positive control was not included, it may be argued that the PCR setups themselves were incorrect and caused the absence of the amplified hygromycin resistance cassette. However, the following methods will show that the problems with releasing

the genomic DNA were consistent indicating that *N. oceanica* cells could not be sufficiently disrupted at 98°C.

The second method for releasing DNA from *Nannochloropsis* cells included incubation of colonies picked from the master plate # 3 at 96°C for 6, 8, and 10 minutes. Concentrations of potentially liberated genomic DNA was measured with NanoDrop1000 spectrophotometer. The concentration of the released DNA determine was ranging between 1.9-8.7 ng/μL (see table C.3, appendix C). Clearly, these concentrations of potentially released genomic DNA was insufficient to serve as template for the subsequent PCR amplification. It can be argued that small concentrations of released DNA would be enough to serve as a template. Yet, concentration values, such as the ones measured, are in the range of noise recorded by NanoDrop of non-containing DNA samples. Therefore, no further attempt in amplification of the hygromycin resistance cassette was pursued, as it would likely be time-consuming and unsuccessful.

A further method for releasing *Nannochloropsis* genomic DNA, which included boiling and snap-freezing in liquid nitrogen of the cell colonies in milliQ water gave the DNA concentration values ranging from 3.4-7.7 ng/μL (see table C.4, appendix C). Neither boiling at 100°C nor rapid thawing of snap-frozen cells apparently was sufficient to release genomic DNA. Another potential reason for such low concentrations detected by NanoDrop could be the fact that genomic DNA remains associated with cell debris and sinking to the bottom of the eppendorf tubes during the centrifugation, leaving the supernatant free for genomic material. No PCR amplification with these samples was performed, as other methods were tested.

Another technique for releasing the genomic DNA from transformed *N. oceanica* cells included resuspension of several colonies picked from master plate # 3 in various lysis buffer. After incubation and running TD PCR with primers designed for hygromycin resistance cassette and subsequent analysis of the PCR outcome by gel electrophoresis, no bands were observed indicating that no genomic material was released using these various lysis buffers (see figure 4.9).

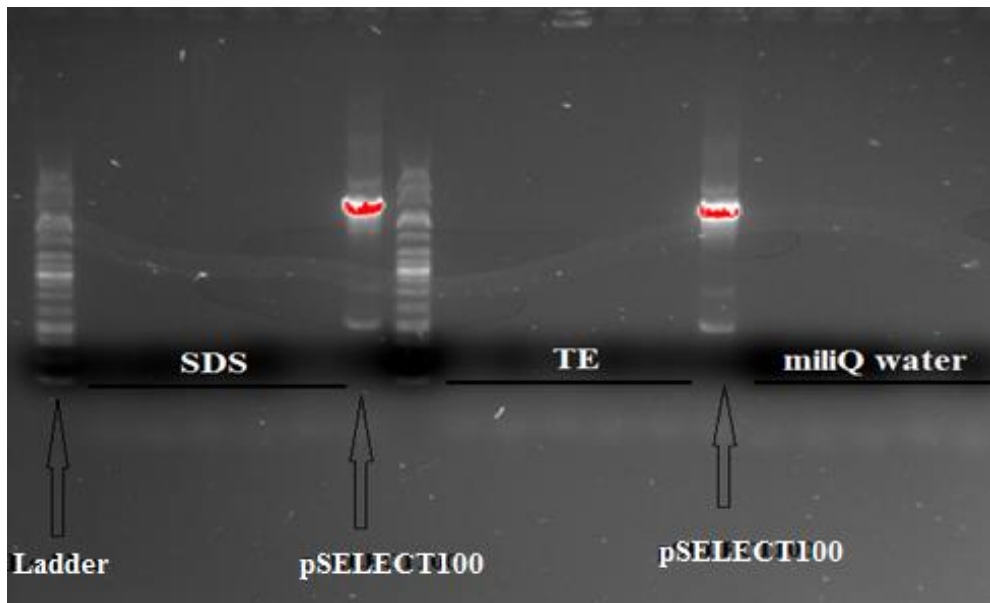


Figure 4.9: Gel image after releasing the genomic DNA of transformed *N. oceanica* cells using various lysis buffers for the subsequent PCR amplification of the hygromycin resistance cassette. Colonies of transformed *N. oceanica* CCMP1779 cells were incubated with different lysis buffers (SDS - 0.2% and 10 mM Tris/1 mM EDTA (TE)) and milliQ water. The cell samples were vortexed, incubated at 95°C for 7 min and centrifuged at $3000 \times g$. 1 μ L of the supernatant was used as a PCR-template for amplification of the hygromycin resistance cassette inserted into genome of *N. oceanica* after successful transformation. No visible bands were observed on the gel image indicating either low or no amounts of the released genomic DNA. The pSELECT100 plasmid DNA were added as a positive control (abbreviated as “pSELECT100” on the gel image).

A positive control, pSELECT100 plasmid, was included, and corresponding bands of ~2000 bp were visualized, indicating that PCR amplification conditions were adequate. However, no bands for transformed cell samples were observed, indicating yet another unsuccessful method for releasing the genomic DNA. The reason for this failure could be that the buffers were too weak, or having a wrong pH at which they were used. The other reason explaining the low concentration of the potentially released genomic DNA was adherence of the genomic material to the cell debris/cell walls and its subsequent vigorous centrifugation (see Materials and Methods) down to the bottom of the eppendorf tubes together with the cell debris.

As alternative, the last method of extracting the genomic DNA out of the transformed *N. oceanica* CCMP1779 cells utilized the Wizard Genomic DNA Purification kit (Promega). Prior to DNA extraction, the colonies of the cells transformed under different conditions including: 2200 V Negative, 2200 V 4 μ g, 1800 V 1.2 μ g, 1800 V 1 μ g, 2200 V 1.2 μ g, and 1800 V 4 μ g were incubated in a liquid medium containing hygromycin for achievement of higher cell density required by the protocol that came with the Wizard Genomic DNA Purification kit. Already at the incubation stage, the differences in cell growth were observed. The cells of negative control sample did not reach a high cell density compared to other samples (see figure 4.10).



Figure 4.10: **Cell cultures of *N. oceanica* CCMP1779 cells transformed at various conditions.** Cell colonies of *N. oceanica* CCMP1779 cells transformed under different conditions were incubated in liquid selective medium containing 50 µg/mL hygromycin for 10 days. The aim of incubation was to reach high cell concentrations to have sufficient cell material for extraction of the genomic DNA using the Wizard Genomic DNA Purification kit. Color of the negative control transformation sample indicates some (due to spontaneous mutation) yet small amount of the cells growing in hygromycin-containing medium compared to the transformed cells with pSELECT100 plasmid containing the hygromycin resistance gene.

The color of the negative control cell sample indicates that some cells were able to tolerate high concentrations of hygromycin. This cell growth might be due to spontaneous mutation, which occurs without presence of any factor inducing the mutagenesis, or possible operator mistakes under the process of electroporation in the form of contamination with plasmid DNA. However, as the cells of all negative samples from all transformations have possessed some growth, it is likely that spontaneous mutation and not the operator's inaccuracy that is behind the observed growth. To gain more insight into the growth of negative cell samples, a PCR amplification of hygromycin resistance cassette using the cells of both the negative control samples and the rest of the cell samples as templates was conducted (see figure 4.11).

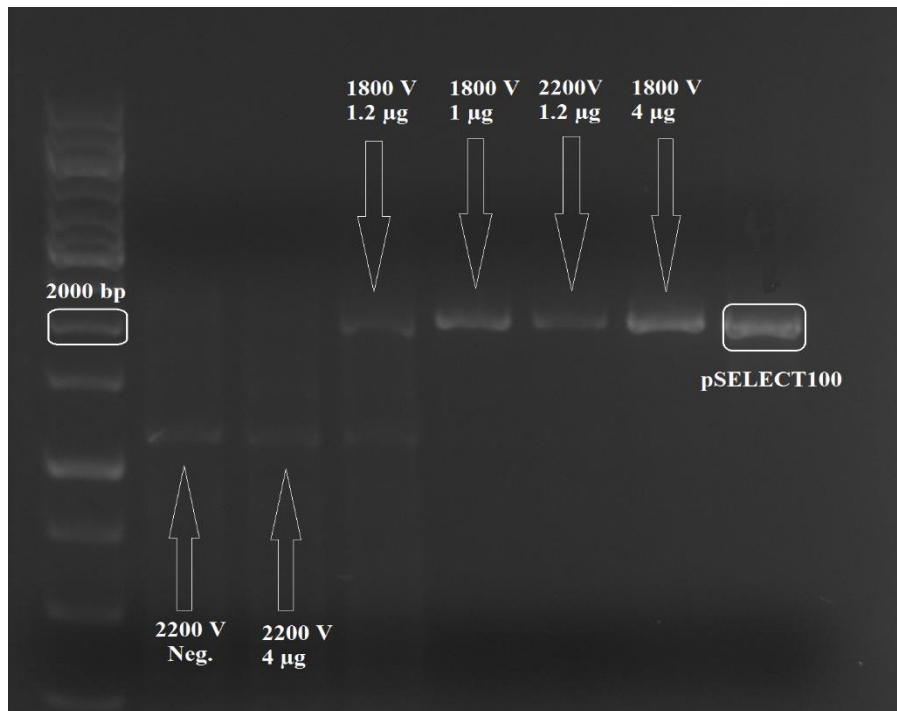


Figure 4.11: Gel image of the final PCR-amplified hygromycin resistance cassette from genomic DNA of *N. oceanica* CCMP1779 cells initially extracted using Wizard Genomic DNA Purification kit. The gel picture shows the visible bands for hygromycin resistance cassette of size ~2000 bp (see positive control pSELECT100) inserted in the genome of *N. oceanica* CCMP1779 cells after successful transformation by electroporation. The cells were transformed under different parameters including the voltage (V) applied at the electroporation and the amount of the transformation plasmid pSELECT100 (μg). Four of five transformed cell samples showed their genome being inserted with hygromycin resistance cassette. Neither the negative control sample (2200V Neg.) nor cell sample transformed at 2200 V added 4 μg of plasmid DNA contained the hygromycin resistance cassette.

The hygromycin resistance cassette, the PCR amplification target, is 2042 bp long. After running the gel electrophoresis of PCR reactions using the cells transformed under different conditions, bands could be observed for four of the samples. In these samples, the hygromycin resistance cassette was integrated into the genome of *Nannochloropsis*. The negative control sample, as expected, did not yield PCR-amplification products, and therefore the hygromycin cassette was not present in the genome of these negative control samples. The reason that these cells could grow in the presence of hygromycin (see figure 4.10) was therefore indeed likely spontaneously occurring mutations. The hygromycin tolerant cells either acquired features enabling them to produce an enzyme deactivating the antibiotic or a change in the target of the antibiotic.

The sample of the cells transformed with 2200 V and incubated with 4 μg of PCR-amplified pSELECT100 plasmid DNA, did not contain any hygromycin resistance insert, indicating that transformation protocol employed for generating these cells was not successful. The color of the sample (see figure 4.10) also indicates that a small number of cells acquired the antibiotic tolerance, likely indicating the occurrence of a spontaneous mutation event for these cells as

well. However, four of the five samples, which were transformed under various conditions, displayed the presence of hygromycin resistance cassette within their genomes. It is likely that the insertion occurred into the nuclear genome.

Transformation added carrier DNA

The last transformation performed (EL_sperm) included addition of carrier DNA. Transformation protocol of Zhang et al. (Zhang C. et al. 2013) included carrier DNA for achievement of high transformation efficiency. The reason for this choice was that non-relevant DNA could reduce the degradation of the PCR-amplified pSELECT100 plasmid DNA. Exo- and endonucleases can digest the carrier DNA while the pSELECT100 plasmid DNA remains intact and can therefore be inserted into the genome of *Nannochloropsis*. The used concentration of salmon sperm DNA was 7.569 µg/µL. A 10-fold large amount of salmon sperm DNA compared to the added pSELET100 plasmid DNA was added to each transformation sample (see table 4.7). Ten *N. oceanica* CCMP1779 cell samples including two negatives were electroporated. After overnight-incubation, samples had different appearance (see table 4.7 and figure 4.12).

Table 4.7: Ten *N. oceanica* CCMP1779 cell samples were transformed by electroporation at the voltage of 1800 volts. A high pSELECT100 DNA amount was added to 4 cell samples including 2 of these samples added 10-fold of the salmon sperm DNA amount. A low pSELECT100 DNA amount was added to 4 other cell samples including 2 of them added 10-fold of the salmon sperm DNA amount. Two negative control cell samples were included in the transformation experiment. After an overnight-incubation of transformed *N. oceanica* cells, prior to plating out on the hygromycin-containing selective medium, the cell suspensions had various appearance.

Sample	Voltage (V)	pSELECT100 amount (µg)	Salmon sperm DNA amount (µg)	Cell appearance after over-night incubation
1	1800	4	40	White suspension + clumps
2	1800	4	40	White suspension + clumps
3	1800	4	-	White suspension
4	1800	4	-	White suspension
5	1800	1.5	15	Green suspension
6	1800	1.5	15	Green suspension
7	1800	1.5	-	Green suspension
8	1800	1.1	-	Green suspension
Negative 1	1800	-	-	Green suspension
Negative 2	1800	-	-	Green suspension



Figure 4.12: **Appearance of the *N. oceanica* cell suspensions after performed transformation by electroporation with added carrier DNA of salmon sperm.** Ten *N. oceanica* CCMP1779 cell samples were transformed by electroporation at the same voltage of 1800 volts. To four of the samples a high amount of pSELECT100 DNA was added (# 1, 2, 3, and 4), and to two of these samples salmon sperm DNA was added (# 1 and 2). To four other cell samples a low amount of plasmid DNA were added (# 5, 6, 7, and 8), and to two of these samples salmon sperm DNA was added (# 5 and 6). After an overnight-incubation of transformed *N. oceanica* cells, prior to plating out on the hygromycin-containing selective medium, the cell suspensions had various appearance.

Four cell samples containing high amount of pSELECT100 were discolored during overnight-incubation. Two of them were added the carrier DNA. White clumps in these cell suspensions were visualized. The reason to such appearance could be a failure under the process of dissolution of dehydrated salmon sperm DNA. Apparently, under the process of dissolution the DNA fragmentation did not occur in a significant level. This caused big sperm DNA pieces being added to the transformation cell samples and therefore causing clumping of the cells. The cell samples added low amount of pSELECT100, and even those added sperm DNA, appeared green with no significant cell clumps. This indicates that electroporation performed with low amount of transformation plasmid added carrier DNA do not influence the appearance of the cells afterwards and is an optimal setup for transformation with carrier DNA.

Afterwards, the transformed cells were plated out on agar-solidified selective medium containing various hygromycin concentrations including 50, 62.5 and 75 $\mu\text{g}/\text{mL}$ in order to see if mutants tolerated even higher doses of the antibiotic. Following results were recorded after 4 weeks of incubation (see table 4.8).

Table 4.8: Transformed *N. oceanica* CCMP1779 cells added carrier DNA under the transformation were plated out on the selective medium containing various hygromycin concentrations, 50, 62.5 and 75 $\mu\text{g/mL}$. The colonies appearance were detected after four weeks of incubation at 23°C, constant light intensity of 100 $\mu\text{E m}^{-2} \text{s}^{-1}$ and continuous rotational shaking.

Transformation sample	Colonies grown on 50 $\mu\text{g/mL}$ hygromycin	Colonies grown on 62.5 $\mu\text{g/mL}$ hygromycin	Colonies grown on 75 $\mu\text{g/mL}$ hygromycin
1	-	-	-
2	-	-	-
3	-	-	-
4	-	-	-
5	11	13	15
6	10	15	15
7	63	27	19
8	44	18	17
Negative 1	11	No records	No records
Negative 2	20	No records	No records

The cell samples transformed with high amount of PCR-amplified pSELECT100 plasmid DNA (# 1, 2, 3 and 4) with two of the added the carrier DNA (# 1 and 2) did not result in any colonies indicating no cells being transformed under these conditions. For samples (# 1 and 2) difficulties occurred when plating out these samples, as cell clumps would not dissolve, even after several rounds of vortexing.

The cells transformed with low amounts of PCR-amplified pSELECT100 plasmid DNA (# 5, 6, 7 and 8) resulted in appearance of some colonies. However, the low PCR-amplified pSELECT100-containing samples that also contained carrier DNA only resulted in lowest number of colonies supporting the insignificance of the carrier DNA on the efficiency of transformations performed at our lab at the Department of Biotechnology.

In summary, the highest number of colonies appeared on the selective medium with 50 $\mu\text{g/mL}$ hygromycin from cells samples # 7 and 8. Small number of colonies occurred from negative cell samples, indicating that the spontaneous mutations occurred conferring resistance to hygromycin.

Transformation efficiency

Figure 4.13 presents the transformation efficiencies determined for all transformations, including the voltages applied and the amount of PCR-amplified transformation plasmid pSELCT100 added as they were identified as the most important transformation parameters (see table C.5 and C.6, appendix C for calculation of the transformation efficiencies).

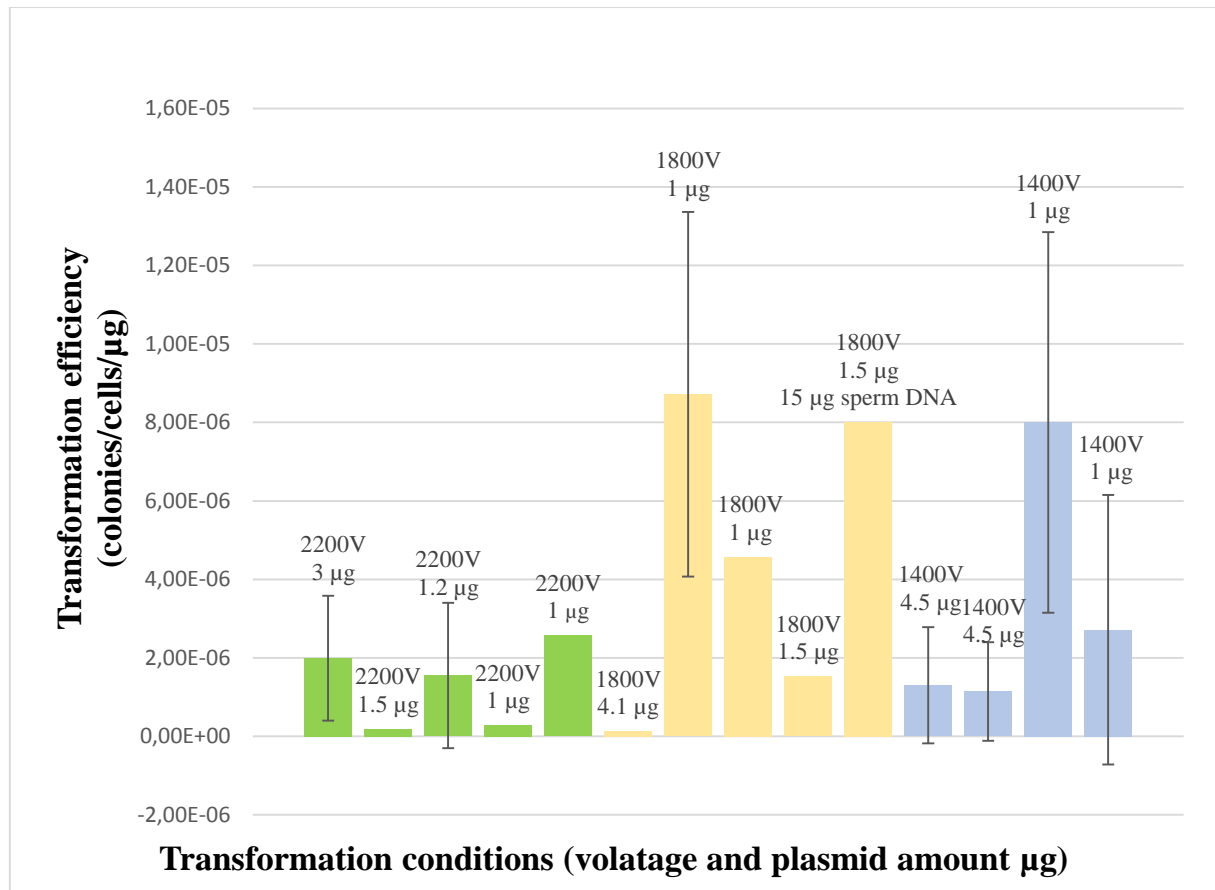


Figure 4.13: Transformation efficiencies based on various transformation parameters performed on *N. oceanica* CCMP1779 cells. *N. oceanica* cells were transformed by electroporation under different conditions (see table 4.4). The most important factors determining the transformation efficiency were the voltage applied at electroporation and the amount of PCR-amplified plasmid DNA added. The green bars presents transformation where the highest voltage of 2200 volts was applied, the yellow bars – 1800 volts, and blue bars - lowest voltage of 1400 volts. The standard deviations were calculated for some of the transformations as they were performed on cells at exactly the same conditions and both cell cultures growing in Cell-Hi CN medium and f/2 medium. As transformation performed on the *Nannochloropsis* cells growing in f/2 medium resulted in significantly low transformation efficiency compared to cells growing in Cell-Hi CN medium, the standard deviation values are very high.

The efficiencies of electroporation performed under 1800 volts are higher than the transformation when voltages over 2000 volts are applied, indicating the optimal range of the voltage for transformation of *N. oceanica* CCMP1779. High voltages could cause a serious cell damage causing low colony formation at the selective medium. A low voltage seemed to be

insufficient to disrupt the cell and allow the subsequent entrance of the exogenous genomic material.

The standard deviations given for some transformations have high values (see table C.6, appendix C). The reason for such big range in standard deviations is some transformations being performed on the cells also growing in f/2 medium, which was still used in initial phases of the experiments, while later the commercial Cell-Hi CN medium was employed. The transformation efficiencies for the cells grown in f/2 are an order of magnitude lower than for those grown in Cell-Hi CN medium. This again indicates the Cell-Hi CN medium being the most optimal for the *N. oceanica* growth. Therefore, the average and standard deviation reported for the transformation efficiencies are dependent on the type of growth medium used.

After establishing the voltage of 1800 V being efficient for achieving the successful formation of *N. oceanica* transformants, the optimal quantity of PCR-amplified pSELECT100 for the efficient transformation was established. The average of transformation efficiencies grouped after the used voltages and plasmid quantities (high and low amount) is presented in the figure 4.14 (see table C.7, appendix C).

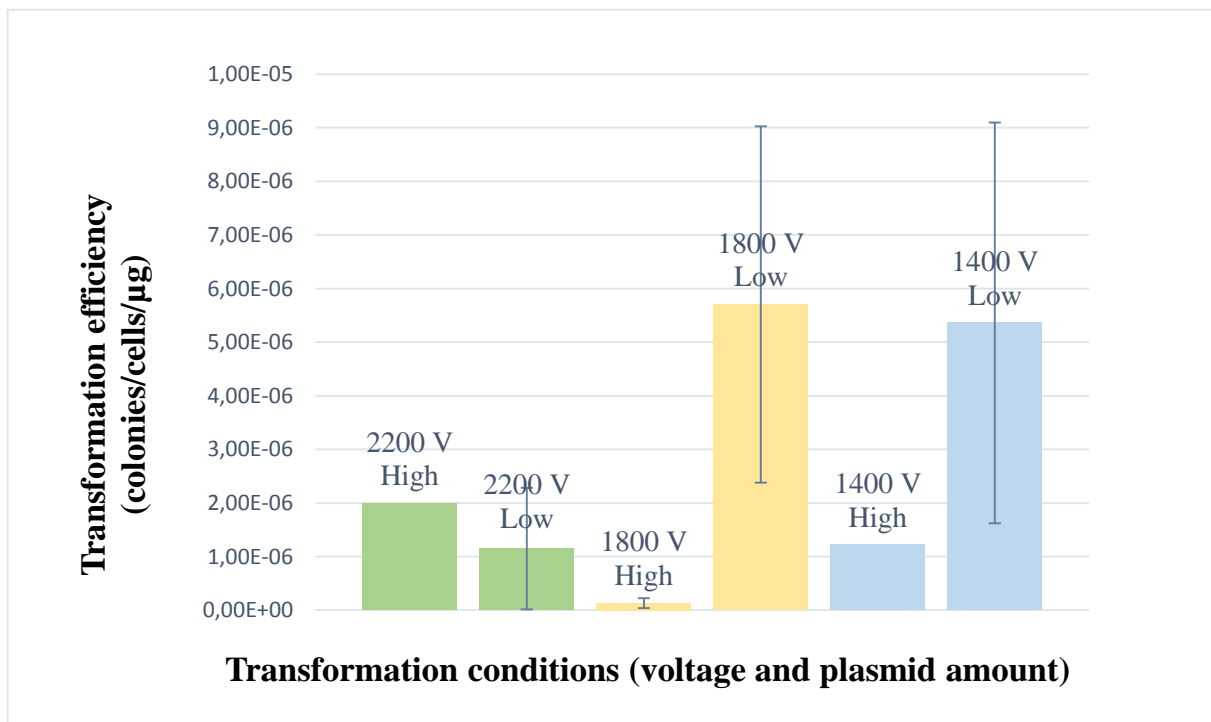


Figure 4.14: Average of the transformation efficiencies based on various transformation parameters performed on *N. oceanica* CCMP1779 cells. *N. oceanica* cells were transformed by electroporation using different parameters (see table 4.4). However, the most crucial factors determining transformation efficiency were the voltage applied at electroporation and the amount of PCR-amplified transformation plasmid pSELECT100 added. The average of transformations where the cells were added either high (3 – 4.5 µg) or low (1 – 1.5 µg) PCR-amplified plasmid amount is shown. Adding a low amount of the PCR- amplified transformation plasmid increased transformation efficiency compared to the high amount of the PCR-amplified plasmid.

The highest transformation efficiency for transformation of *N. oceanica* CCMP1779 cells by electroporation achieved during the master project was 4.08×10^{-5} colonies/cells/ μg (see table C.6, appendix C). However, this significantly higher value compared to the efficiencies of other transformations was not included in the determination of the average transformation efficiency value for the group “1800V High” presented in the figure 4.14 as it affected the average value to a large extent. To see how this high transformation efficiency value would affect the average see table C.8 and figure C.1, appendix C.

Conclusion

The main goal of the project performed and presented in this chapter was the establishment of the efficient transformation protocol by electroporation of *N. oceanica* CCMP1779 cells with PCR-amplified pSELECT100 plasmid DNA containing hygromycin resistance cassette. The important parameters reported by previous research groups were considered under the establishment of the transformation protocol. These parameters included the cell concentration, the cell washing steps, the incubation conditions, the quantities of transformation plasmid added, as well as the voltage applied, with the last two being the most decisive for an efficient transformation.

The highest transformation efficiency was obtained for the electroporation performed under 1800 volts and cells that were incubated with a low amount of the PCR-amplified pSELECT100 transformation plasmid. The highest transformation efficiency reached in this project was 4.08×10^{-5} colonies/cells/ μg (1800 V, low amount of the plasmid). The lowest transformation efficiency was also observed (1.27×10^{-7} colonies/cells/ μg) performed at 1800 V but the cells were incubated with high amounts of PCR-amplified plasmid. Overall however, the highest efficiencies reached in this project were of transformation performed with 1800 V and low amount of the transformation plasmid, having an average value of 5.70×10^{-6} colonies/cells/ μg (see figure 4.14 and table C.7, appendix C).

After succeeded establishment of the transformation protocol for *N. oceanica* CCMP1779 the next step would be insertion of GFP gene for its use as an expression tag of other genes, both endogenous and exogenous (for detailed description of future projects see Future Research).

Chapter V

Gibson Assembly

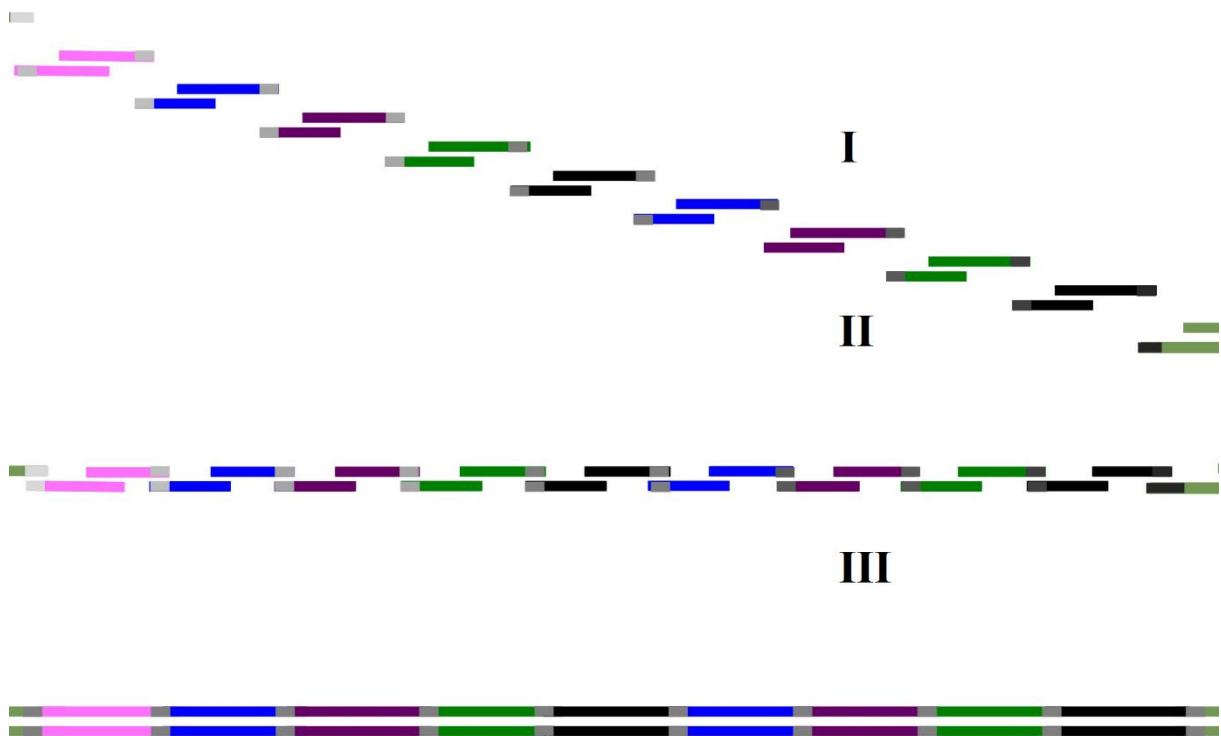


Photo: SynBio@TSL. Gibson Assembly. <http://synbio.tsl.ac.uk/?p=124>

Gibson Assembly

Gibson Assembly is a method for assembling of multiple overlapping DNA fragments into a linearized or circular DNA sequence. Short time requirement and high capacity for the assembling of DNA fragments of several kilo base pairs long in a single reaction make this technique preferable above other recombinant DNA technologies. It takes as little as 15 min of incubation for a proper reaction to occur and to achieve the desired product. The action of three enzymes in the Gibson Master Mix solution determines the process (see figure 5.1). The initially amplified DNA fragments with specifically designed primers with complementary overhanging regions for each of the fragments are mixed together and added Gibson Master Mix. The T5 exonuclease digests the DNA strands in the 5' → 3' direction resulting in single-stranded DNA overlapping regions on DNA fragments. The DNA polymerase fills up the gaps by incorporating single nucleotides. The last step is performed by the DNA ligase that covalently joins the DNA of adjacent fragments therefore eliminating the nicks in the DNA sequence (Gibson D. G. et al. 2009).

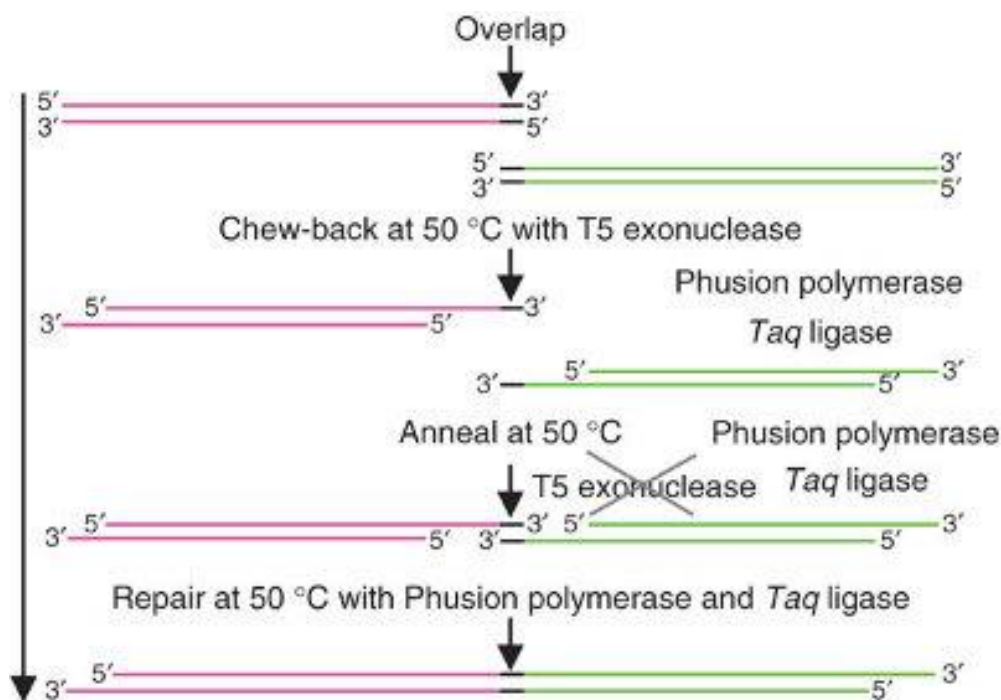


Figure 5.1: **Overview of the enzymes and their function in the Gibson Master Mix solution.** First, the DNA fragments are PCR-amplified with specially designed primers with overhanging regions to create elongated regions on the DNA fragments. Then, all the fragments are mixed together and added Gibson Master Mix. T5 exonuclease digests the DNA strands of all DNA fragments in 5' → 3' direction resulting in single stranded complementary overhanging regions that will anneal to each other. The polymerase adds the nucleotides. Ligase seals the nicks and repairs the DNA fragments of the resulting assembly product (BioLabs Inc. New England 2009).

The simplicity of the approach is based on all commercially available reagents and enzymes that do not compete with each other in a single-tube reaction. Both *Taq* polymerase and *Phusion High Fidelity* polymerase can be used in the assembly mix. *Phusion* polymerase is an enzyme of choice in most of the cases as it has inherent proofreading capacity for removing noncomplementary sequences from already assembled fragments. Gibson Assembly is a useful molecular tool for synthetic constructs, natural genes and entire genomes engineering. The method helps to clone multiple inserts into a whole vector without need for restriction sites and enzymes and subsequent ligation of the parts. The heat-shock transformation of *E.coli* cells with the assembly product is then performed. The *E. coli* cells are subsequently plated out on the agar-solidified selective medium for selection of the cells with the insert (see figure 5.2 for Gibson Assembly workflow) (BioLabs Inc. New England 2009, Gibson D. G. et al. 2009).

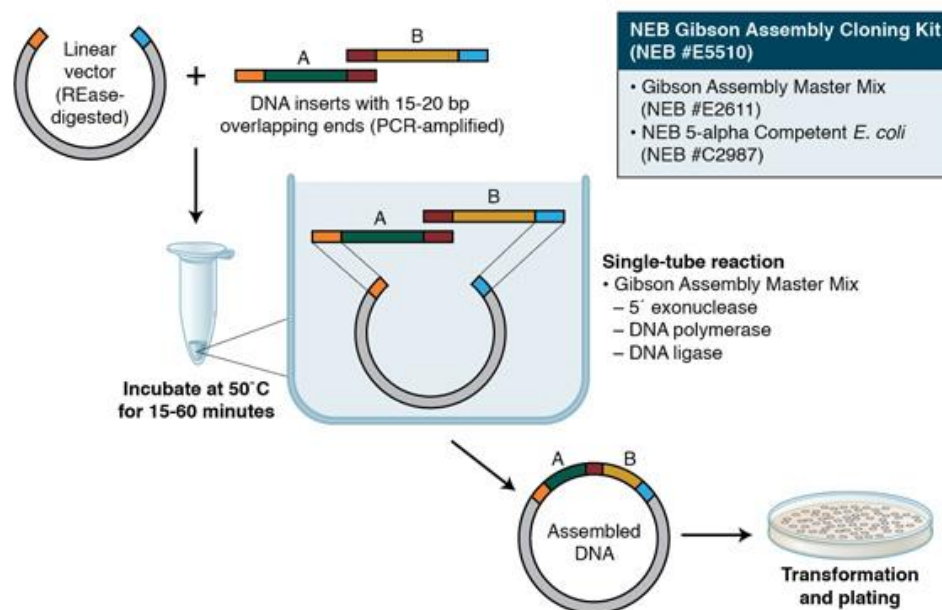


Figure 5.2: **Gibson Assembly workflow presenting the main steps in the assembling of DNA fragments** (BioLabs Inc. New England 2009). The incubation of the fragments with overlapping regions initially PCR-amplified using specially designed primers with overhanging sequences, is performed at 50°C for 15-60 min with addition of the Gibson Master Mix solution containing all required enzymes. The *E. coli* cells are then transformed with the assembly product by heat-shock for the plasmid cloning. The cells are subsequently plated out on the selective medium for positive selection of *E.coli* cells containing the assembly plasmid. The plasmid is extracted and purified afterwards.

In general, the first Gibson Assembly experiments included overlapping sequences of 450 base pairs (bp) of DNA fragments to be assembled. These experiments were successful and led to a new set of trials where shorter overlapping regions of (40 bp) were analyzed making the technique less complicated. The size limit of the possible DNA assembly fragments is not determined but products up to 990 kb can be achieved (Gibson D. G. et al. 2009).

Plasmid insertion by homologous recombination

Gene insertion by homologous recombination (also called gene targeting) is a technique applied to delete or change a specific endogenous gene. Introduction of point mutations or deletion of the exons are other goals achieved by the gene targeting. The creation of the plasmid containing a gene with the flanking homologous regions complementary to the regions of the native genome is essential in the process of gene targeting. The most advantageous method of making such a construct would be by the Gibson Assembly where several fragments are assembled together in single-tube reaction.

Three candidates for the gene targeting of chloroplast genome of *N. oceanica* CCMP1779 were chosen and analyzed for potential transformation by homologous recombination. Essentiality of two genes, *chlL* and *psbY* and a long DNA gap region on the chloroplast genome of *N. oceanica* CCMP1779 was discussed for potential insertion of the transformation plasmid.

chlL gene

Light energy trapping is an essential part of photosynthetic cell life. Therefore, the requirements of the most abundant organic molecule on Earth, chlorophyll, in the photosynthetic organisms is huge. The molecule is a subunit of photosynthetic machinery and drives light capturing (Reinbothe C. et al. 2011).

The chlorophyll biosynthesis occurring in chloroplasts of plants and algae, e.g. *Nannochloropsis* is an essential process for a successful photosynthesis leading to indispensable growth and development of the organism. Chlorophyll synthesis comprises an evolutionary diverse enzyme, protochlorophyllide oxidoreductase, catalyzing the reduction of protochlorophyllide to chlorophyllide (both are precursors of chlorophyll). The light-dependent protochlorophyllide oxidoreductase in eukaryotes consists of nucleus-encoded subunits and requires light to function. The light-independent protochlorophyllide oxidoreductase (LIPOR) comprises three diverse subunits encoded by chloroplast genome, ChlL, ChlB, and ChlN, and enables chlorophyll synthesis in the absence of light. *chlL* gene encodes protochlorophyllide reductase iron-sulfur ATP-binding subunit of the LIPOR (STRING 9.1, Fong A. et al. 2008, National Center for Biotechnology Information 2014).

As all cultures of *N. oceanica* used in our lab at Department of Biotechnology were cultivated at constant light intensity of $100 \mu\text{E m}^{-2} \text{s}^{-1}$, the importance of possessing LIPOR molecule was insignificant for these cell cultures. Therefore, the deletion of the *chlL* gene would not influence cell survival and life cycle of *N. oceanica* cells.

psbY gene

psbY gene encodes a small subunit of photosystem II protein Y (PsbY) on the chloroplasts of the *N. oceanica*. The protein functions as a manganese-binding polypeptide with L-arginine metabolizing enzyme activity earlier suspected to be essential for proper function of the manganese cluster in the O₂ evolution center of PSII (UniProt Knowledgebase, Wydrzynski T. J. et al. 2006). The gene encodes two diverse single-spanning chloroplast thylakoid membrane proteins (Gau A. E. et al.).

The experiments of deletion of the *psbY* gene on photosynthetic cyanobacterium *Synechocystis* sp. PCC 6803 have revealed the growth of wild type and the mutants being similar under the same conditions. It proved that *psbY* mutants have normal photosynthetic activities. Consequently, the protein Y is not crucial for oxygenic photosynthesis and does not provide any important binding site for manganese in photosynthesis II complex though the function of it remains to be determined (Meetam M. et al. 1999, Wydrzynski T. J. et al. 2006).

The gap region between *ycf54* and *secA* genes

One chloroplast genome region of *N. oceanica* is located between *ycf54* and *secA* genes and contains no annotated genes (see figure 5.3).

Nanochloropsis oceanica strain CCMP531 chloroplast, complete genome

NCBI Reference Sequence: NC_022263.1

[GenBank](#) [FASTA](#)

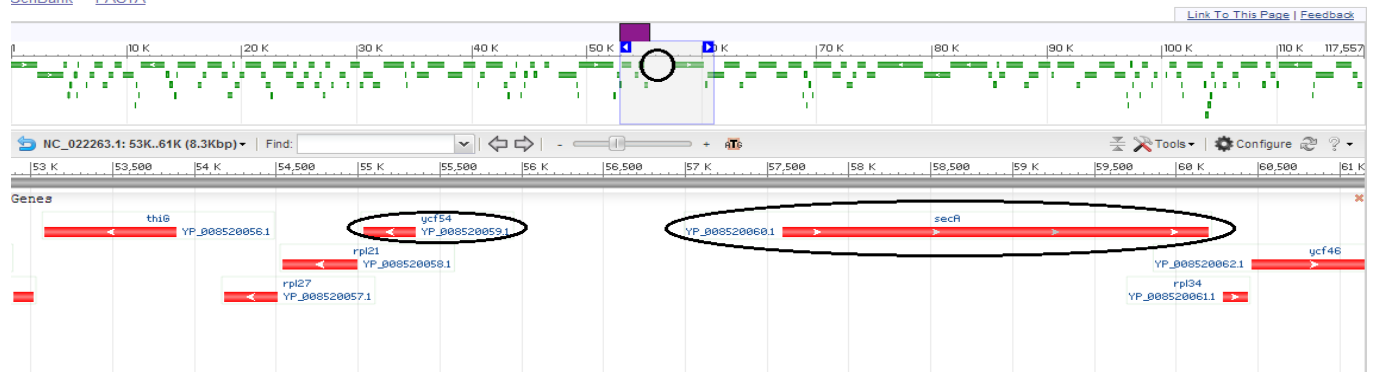


Figure 5.3: Screenshot of the chloroplast genome region of the *N. oceanica* CCMP531. The region includes *ycf54* and *secA* genes (circled black) and the gap between them with no annotated genes. The DNA gap is 2240 bp long and is an appropriate candidate for the gene targeting with the plasmid assembled using Gibson Assembly (National Center for Biotechnology Information).

Ycf54 protein encoded by *ycf54* gene is required for efficient activity of the magnesium protoporphyrin monomethylester oxidative cyclase structuring the isocyclic ring of the chlorophyll molecule (National Center for Biotechnology Information, Bollivar D. W. et al. 1996). The inactivation of *ycf54* gene leads to a significant reduction of chlorophyll levels.

Therefore, Ycf54 protein is crucial for the assembly of the cyclase complex (Hollingshead S. et al. 2012).

The *secA* gene encodes the translocase subunit SecA that enables the coupling of ATP hydrolysis to the transfer of proteins across the thylakoid membrane in chloroplasts of photosynthetic eukaryotes (Scaramuzzi C. D. et al. 1992, UniProt Knowledgebase 2013).

The gap between the aforementioned genes was analyzed by multiple sequence alignment program for proteins (Clustal Omega). The gap (see figure 5.3) is 2240 bp long and is located between 55355 – 57596 bp. At the position 56285 – 56311 bp the 26 bp long sequence (marked yellow) is shown to be least conserved after alignment of five *Nannochloropsis* species (see figure 5.4). That makes it a possible candidate for transformation of *Nannochloropsis* cells by homologous recombination (The European Bioinformatics Institute et al.).

However, the sequences some decades of base pairs upstream (marked brown) are shown to be sufficiently conserved throughout the five *Nannochloropsis* species which makes it an evolutionary significant and essential for organism`s growth and development (The European Bioinformatics Institute et al.). The attempt to design primers for the left flanking end upstream for the least conserved region did not result in any success as the most conserved region would be deleted by homologous recombination with pLit_chlL_chlor plasmid (see figure D.1, appendix D).

```

Salina  TTGAGTAATTTTATATAAAAAAACAAATATTTTTCAAAATTTCAATAAT----- 1248
Limnet.  TTAAGTAAATTTAAATAAAAAAATAAATATTTTTCAATTTTTAAAAATTTATTTAA---- 1253
Oceani.  TTAAATAAATCCAATAAAAAAATAAATTTTTTTCAATTTTTATAAATTTATTTAAATAA 1257
Granul.  TTAAATAAATTTAATAAAAAAATAAATCTTTTTCAATTTTTAAAAAATTTTATATTAA 1260
Ocult.  TTAAATAAATTTAATAAAAAAATAAATTTTTTTCAATTTTTAAAAATTTATTTAAATAA 1260
          ** * *** * * ***** ** ** ***** ** * **

Salina  -----ATTTGAAGATACGAGTTT 1266
Limnet.  -----ATACGTACTT 1263
Oceani.  -----GTAGCC 1263
Granul.  AATAAACTTAATAAAAAAGTTAATTCCTTTCCATTTTCAAACTTATTAACAGTAGCT 1320
Ocult.  CTAGCT-----A-----A 1268

Salina  GAAATGAAAGGTTTAAGTTCTAAAAATTTTACTTTTATATTCTCATTATGTAGCTCAGC 1326
Limnet.  GAAATAAATGGTTTCAATTTCTAAGAAATTTATTTTTATTTTTTCAATTAGAAATCTCAAT 1323
Oceani.  AAATAGATGGCTTTAAATTTCTAAAAAATCTACTTTTTATTTTTTGAACTAAAAATTTAAC 1323
Granul.  AAA--ATAAGATGTTTAATTCATAAAATTTACTTTTATTTTTTTCAATTAATAAATTTCAAT 1378
Ocult.  AGT--AAATGGTTTAAATTCATAAAATTTACTTTTATTTTTTTCAATTAATAAATTTAAT 1326
          * * * * * ** * ** * * ** * * *

```

Figure 5.4: The DNA sequence of the chloroplast genome to five species of genus *Nannochloropsis* between *ycf54* and *secA* gene. This DNA sequence contains the least conserved DNA region (marked yellow) at the position 56285 – 56311 bp, which was a potential site for insertion of the potential plasmid assembled by Gibson Assembly containing chloramphenicol resistance cassette. The DNA sequence marked brown is the most conserved region concluded after alignment of five *Nannochloropsis* species (*N. salina*, *N. limnetica*, *N. oceanica*, *N. granulata*, and *N. oculata*). Therefore the gene targeting may influence the cell development and cell cycle.

As both *ycf54* gene and *secA* gene were assessed coding for the proteins important for the cell viability, and the DNA gap between these genes having an evolutionary conserved region, the insertion of exogenous DNA in the gap region was considered as unsustainable with cell vitality.

Antibiotic resistance

Before year 1950, the knowledge about antibiotic resistance acquirement by bacteria was poor. Nowadays, there have been discovered four major mechanisms of antibiotic drug resistance. They are acquired due to chromosomal mutations or expression cassette insertion (Zhang Y.).

- Reduced drug accumulation: by increased efflux or decreased permeability of cell membrane
- Enzymatic inactivation or modification
- Drug-target alteration
- Metabolic pathway alteration

Chloramphenicol

Chloramphenicol is a bacteriostatic drug that inhibits protein synthesis in the organism. Protein chain elongation is prevented by inhibition of peptidyl transferase creating peptide bonds between adjacent amino acids. The drug influences the reproducing abilities of the organism but not necessarily harming the cells (TOKU-E The Evolution of BioPurity 2010). The chloramphenicol resistance is achieved by the action of the enzyme called chloramphenicol acetyltransferase coded by *cat*-gene. The enzyme inactivates the drug by covalently linking one or two acetyl groups derived from acetyl-CoA to chloramphenicol molecule by this preventing the drug binding to the ribosome and therefore affecting the protein synthesis (Shaw et al. 1979).

Goal

Creating a transformation plasmid with complementary sequences to the chloroplast genome of *N. oceanica* CCMP1779 was performed in order to incorporate a specific gene into the exact position of the genome using transformation technique. Another purpose of creating the plasmid was the organism's obtainment of a new feature and production of the new protein thereby achieving the deletion of an endogenous gene not essential for the cell's development and survival. The aim of the experiment was to construct a transformation plasmid containing a chloramphenicol resistance cassette and both flanking homologous regions amplified from the chloroplast genome of *N. oceanica* CCMP1779. The subsequent transformation by homologous recombination was one of the main aims of the project. As previous transformation experiments were based on random transformation (to either nuclear or chloroplastic genome – see chapter

IV – Transformation by Electroporation), this experiment would give better control and overview over transformants.

Materials and Methods

Primer design

DNA sequences of the chloroplast genome of *N. oceanica* for potential plasmid insertion, including *chlL*, *psbY* genes and a gap region between *ycf54* and *secA* genes were analyzed using National Center for Biotechnology Information (NCBI) web page. The alignment of chloroplast genome to five *Nannochloropsis* species including *N. salina*, *N. limnetica*, *N. oceanica*, *N. granulata*, and *N. oculata* was performed by Clustal Omega Bioinformatics Tool. The usage of the tool contributed to identification of both the evolutionary conserved and most unconserved regions at the gap region between *ycf54* and *secA* genes. OligoAnalyzer program version 3.1 by Integrated DNA Technologies was used to design the primers with complementary overhanging regions for subsequent Gibson Assembly of a plasmid containing chloramphenicol resistance cassette, right and left flanking regions, and plasmid backbone. The primers to create the plasmids used in potential transformations to obtain the deletion of *chlL* and *psbY* genes, was designed (see table 5.1). However, only plasmid for *chlL* gene deletion was selected for the actual construction using Gibson Assembly and was abbreviated pLit_chlL_chlor.

Table 5.1: Primers with complementary overlapping regions designed to assemble transformation plasmids by Gibson Assembly for subsequent insertion and deletion of the endogenous genes (*chlL* and *psbY*) at the chloroplast genome of *N. oceanica* CCMP1779. The abbreviations include left/right flanking end (LF/RF), extended meaning primer with overlapping DNA region (ext) and either sense (fw) or antisense (rev) primer.

Primers with overhanging regions	Knock-out genes	
	<i>chlL</i> gene	<i>psbY</i> gene
LF_ext_fw	5`-ggaacagctatgacctgacccgtcacgtaacctac- 3`	5`-ggaacagctatgacctgctggttaccgatgacgataa- 3`
LF_ext_rev	5`-aacgtctcatcgcggccgctgctcgatcacatccaatt- 3`	5`-aacgtctcatcgcggccgccgtccatgtagtggtt- 3`
RF_ext_fw	5`-acgcctgaatgcggccgcaaacctcgatacagaacaaa- 3`	5`-tggtgctacgcctgaatgcggccgccagccctgtgggtattat- 3`
RF_ext_rev	5`-ggttttccagtcacgactgctctagcaactatgattggaata- 3`	5`-ggttttccagtcacgacgggcaagattacgtgagtatt- 3`
Chlor_ext_fw	5`-gtgatccgaagcagcggccgcatgagacgttgatggcagc- 3`	5`-ctacatggacggcggccgcatgagacgttgatggcagc- 3`
Chlor_ext_rev	5`-tatccgagggttgcggccgattcaggcgtagcaccaggc- 3`	5`-ctaccacagggtgctggccgattcaggcgtagcaccaggc- 3`
Bb_ext_fw	5`-tattccaatcatagttgctagagcagctgtgactgggaaaacc- 3`	5`-aataactcacgtaaatctttgccctgtgactgggaaaacc- 3`
Bb_ext_rev	5`-gtagggtacgtgacgggtcatggtcatagctgtttcc- 3`	5`-cgtcatcgggtaaacagcatggtcatagctgtttcc- 3`

The schematic picture of designed primers with complementary overhanging regions for assembled fragments (left/right flanking ends, backbone and chloramphenicol resistance cassette) is presented in figure 5.5.

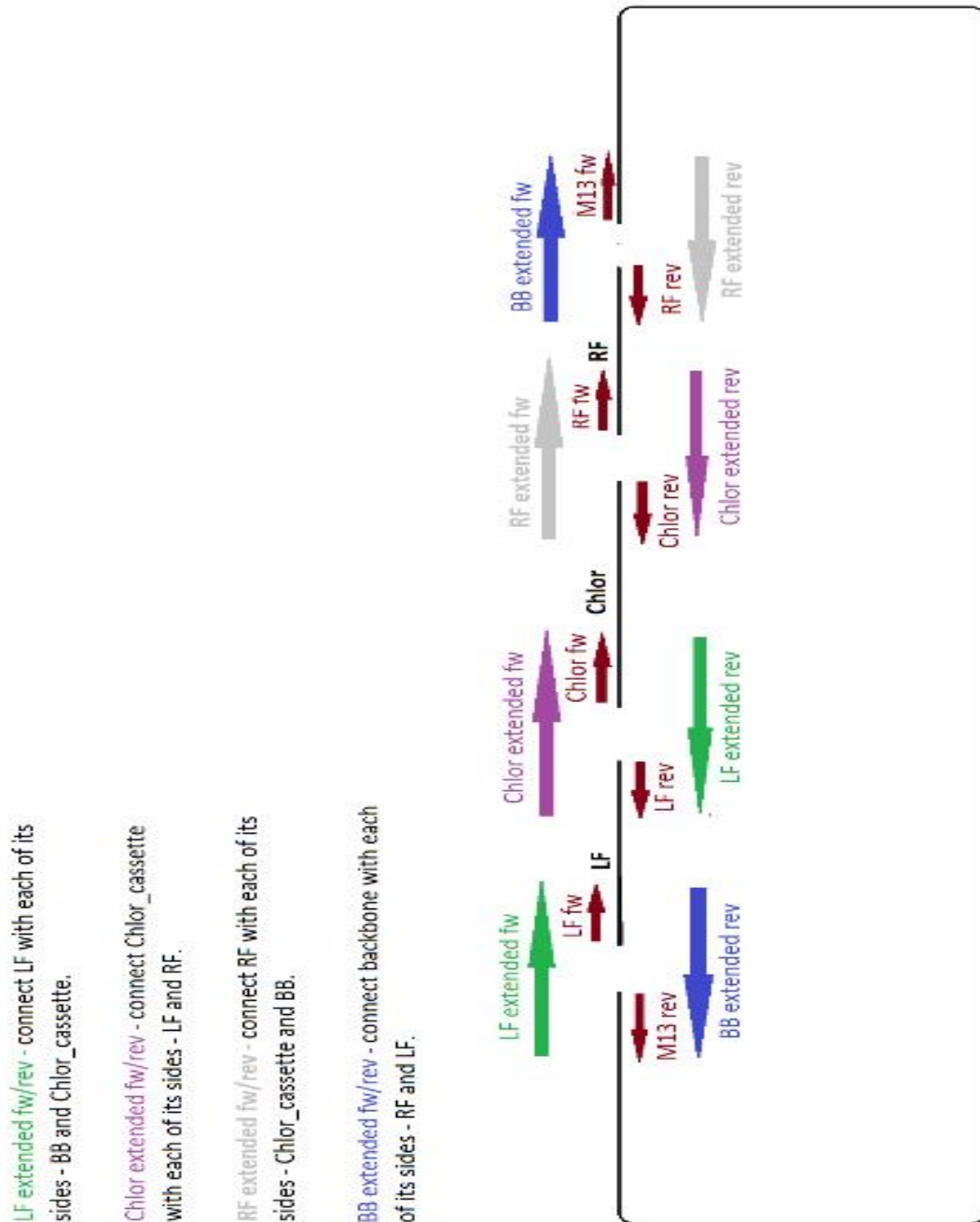


Figure 5.5: The schematic picture of the DNA fragments assembled by Gibson Assembly into the **pLit_chlL_chlor transformation plasmid**. The description of the primers with complementary overlapping DNA regions including the DNA fragments including both the left (LF) and the right homologous flanking region (RF) up- and downstream for *chlL* gene, which were PCR-amplified from the chloroplast genome of *N. oceanica* CCMP1779, the chloramphenicol resistance cassette PCR-amplified from pLit_Chlor plasmid, and the backbone PCR-amplified from pLit_Kan plasmid.

Amplification of the fragments

The extraction of *N. oceanica* genomic DNA was performed in order to amplify the 500 bp regions up- and downstream for *chlL* gene (complementary flanking ends). The DNA extraction was achieved using Wizard Genomic DNA Purification kit from (Promega). The further amplification of the regions was performed by touch-down PCR including extra primer annealing step for corresponding primer melting temperatures (see Chapter IV – Transformation by Electroporation Table 4.3 b). Chloramphenicol resistance cassette were amplified from pLitmus_Chlor (pLit_Chlor) plasmid, while backbone was amplified from pLitmus_Kanamycin (pLit_Kan) plasmid.

The Gibson Assembly protocol was used for calculation of fragments` quantities used for the assembly reaction. This calculation was based on fragments` length and weight measured in base pairs and nanograms, respectively (see tables 5.2 and 5.3). As backbone does not count as a fragment, it was used a defined amount of it, 1.2 µL. For assembly of 2-3 fragments, the recommended total amount of the fragments should be 0.02-0.5 pmoles. Therefore, three different Gibson Assembly reaction quantities, 0.1, 0.3, and 0.5 pmoles, were tested. The formula for calculation of pmoles given by the Gibson Assembly Protocol available online on BioLabs Inc. was used for determination of the volume needed for each Gibson Assembly sample (BioLabs Inc. New England).

$$\text{pmols} = (\text{weight in ng}) \times 1,000 / (\text{base pairs} \times 650 \text{ Daltons})$$

Table 5.2: The DNA fragments` weight measured in nanograms and length measured in base pairs were determined for creating the transformation plasmid pLit_chlL_chlor using Gibson Assembly technique. The data is important for calculation of the volumes required for the assembly reaction using Gibson Master Mix. Left and right flanking regions up- and downstream for the *chlL* gene are abbreviated LF (chlL) and RF (chlL). The chloramphenicol resistance cassette is abbreviated Chlor_cassette

Fragment	Weight (ng)	Length (bp)
LF (chlL)	120	596
RF (chlL)	157.5	477
Chlor_cassette	1050	2600

Table 5.3: Determination of DNA fragments` volumes required for three distinct Gibson Assembly reactions of different concentrations (0.1, 0.3 and 0.5 pmols) abbreviated pmols total. As only three DNA fragments (the volume of backbone was defined, 1.2 μ L) – left flanking region (LF chIL), right flanking region (RF chIL) and chloramphenicol resistance cassette (Chlor_cassette), were assembled, knowing the concentration of the PCR-amplified DNA fragments, which contributed to determination of the volumes.

pmoles total	pmoles fragment	LF (chIL) volume (μL)	RF (chIL) volume (μL)	Chlor_cassette volume (μL)
0.1	0.03	1.6	1.0	0.8
0.3	0.10	0.5	0.3	2.4
0.5	0.17	0.8	0.5	4.0

After the chloramphenicol resistance cassette were TD PCR-amplified from the pLit_Chlor plasmid, the resulted DNA fragment were incubated with DpnI endonuclease restriction enzyme for digestion of methylated fragments. 0.5 μ L of enzyme and 1.7 μ L Cut Smart buffer were added to 30 μ L of samples with chloramphenicol resistance cassette (70 ng/ μ L) and incubated at 37°C for 1 h.

Gibson Assembly

After the amplification of all DNA fragments, 7 μ L of Gibson Master Mix were added to their mixture of the DNA fragments and incubated at 50°C for 15 min. Afterwards, the heat-shock transformation of *E.coli* cells (the transformation protocol is given by the Transformation protocol of BioLabs Inc. (BioLabs Inc. New England)) was conducted for the cloning of the assembly product, pLit_chIL_chlor. Cells were plated out on the selective LB medium containing 100 μ g/mL ampicillin for the positive cell selection as the backbone of the construct contained the ampicillin resistance gene. Wizard® Plus SV Minipreps DNA Purification System protocol was employed for the extraction of the pLit_chIL_chlor plasmid DNA (BioLabs Inc. New England).

Efficient transformation of *N. oceanica* cells required the linearized pLit_chIL_chlor plasmid. Restriction enzyme PvuI was used for this purpose as it had cutting sites on both sides of the chloramphenicol restriction cassette assembled to right and left flanking regions. 10 μ L of the plasmid were added 2 μ L of PvuI enzyme and 4 μ L of Cut Smart buffer and incubated at 37°C for 2.5 h.

Results and Discussion

Three alternatives were proposed for deletion of the sequences of the chloroplastic genome of *N. oceanica* CCMP1779: either the *chlL* gene, the *psbY* gene or the large DNA gap between the *ycf54* and *secA* genes. The choice of the *chlL* gene for deletion from chloroplast genome of *N. oceanica* by insertion of chloramphenicol resistance cassette through transformation with pLit_chlL_chlor plasmid DNA was based on the unimportance of the gene for the cell survival. The alternative to insert the cassette into the DNA gap region between *ycf54* and *secA* genes was unsecure due to importance of the *ycf54* and *secA* genes and evolutionary conservation of one DNA sequence in the gap (see Introduction). The conserved DNA region suggested the obtainment of some important though not annotated genes or other essential parts of the genome.

The chloramphenicol resistance cassette with *cat*-gene encoding chloramphenicol acetyltransferase was used as a selection marker. The choice of this selection marker and corresponding antibiotic in selective medium was based on the results from cell growth test (see chapter III – Cell Growth Assay), where high cell sensitivity for chloramphenicol was detected.

The gel images of the TD PCR-amplified fragments for pLit_chlL_chlor construct including the left/right flanking regions, the plasmid backbone, and the chloramphenicol resistance cassette, are presented on the figure 5.6. The sizes of the fragments given detected on the gel image corresponded to sizes of the pLit_chlL_chlor fragments, which are 595, 476, 823, and 2631 bp respectively.

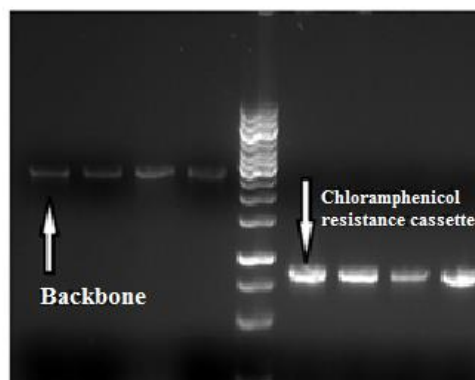
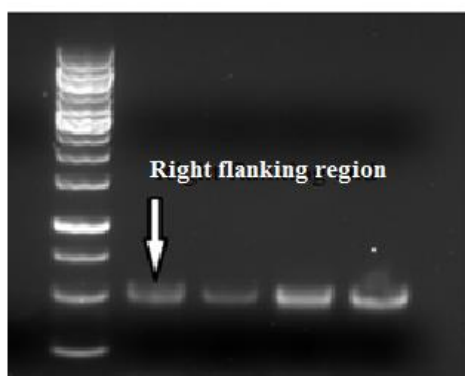
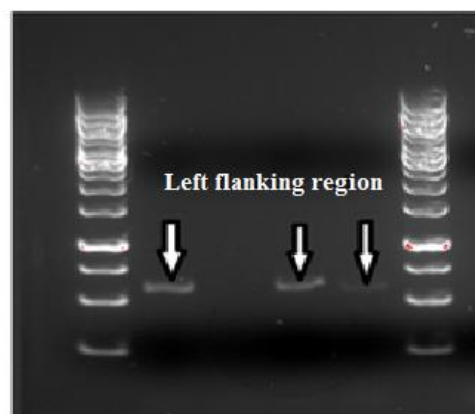
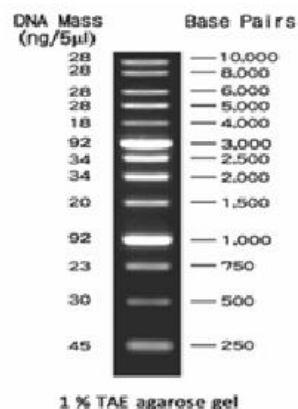


Figure 5.6: **The TD PCR-amplified fragments of the pLit_chlL_chlor plasmid constructed by Gibson Assembly.** The left and right flanking homologous regions were PCR-amplified from the extracted genomic DNA of *N. oceanica* CCMP1779. The backbone and the chloramphenicol resistance cassette were PCR-amplified from the pLit_Kan and the pLit_Chlor plasmids, respectively. The sizes of the bands on the gel picture correspond to DNA fragments` sizes 595, 476, 823, and 2631 bp for the left/right flanking regions, the chloramphenicol resistance cassette and the backbone respectively. The DNA fragments were assembled into the transformation plasmid pLit_chlL_chlor using Gibson Master Mix solution containing the enzymes necessary for the successful assembly.

The plasmid map of pLit_chlL_chlor plasmid (see figure 5.7) describes location of the designed primers with overhanging regions for each fragment (see table 5.1). Both the ampicillin resistance cassette (Amp r) at the backbone PCR-amplified from the pLit_Kan plasmid, left (LF) and right (RF) homologous flanking regions PCR-amplified from the host chloroplast genome, and chloramphenicol resistance cassette (Chl r) PCR-amplified from pLit_Chlor plasmid are annotated on the plasmid map.

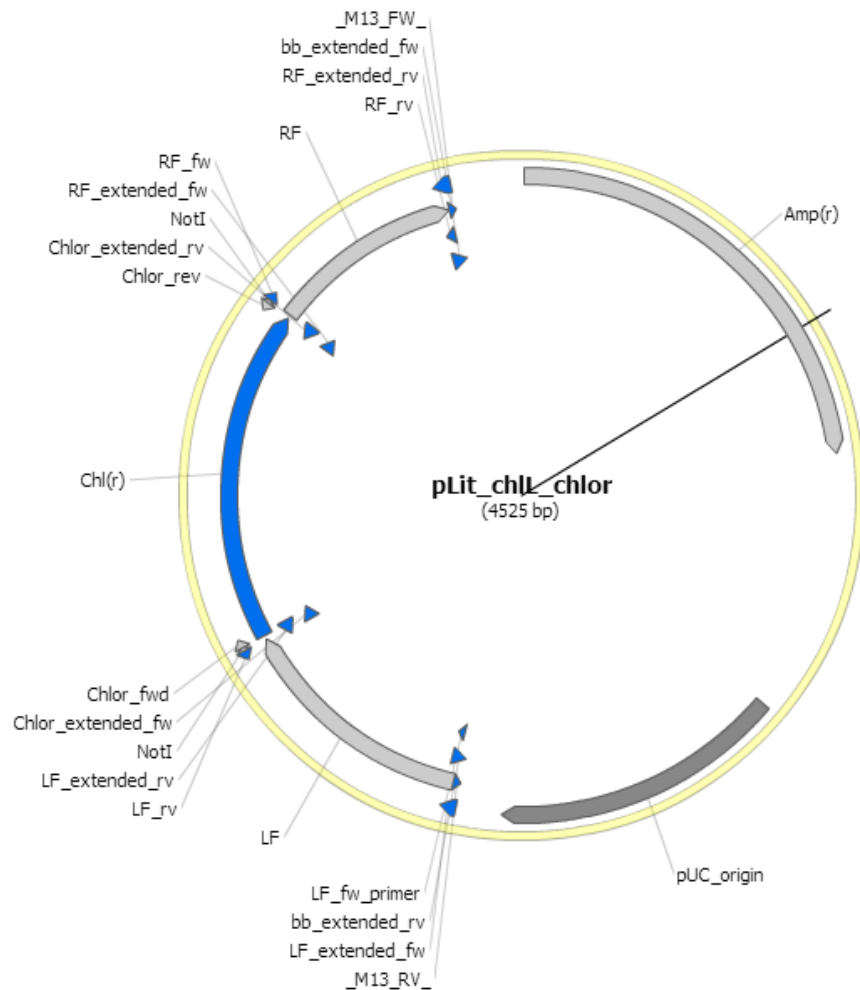


Figure 5.7: **Plasmid map of the pLit_chlL_chlor transformation plasmid.** The plasmid contains the backbone region PCR-amplified from the pLit_Kan plasmid, the chloramphenicol resistance cassette PCR-amplified from the pLit_Chlor plasmid (dark blue), the left and right flanking regions PCR-amplified from the chloroplast genome of *N. oceanica* CCMP1779 (light grey). The map describes the designed primers with overhanging regions contributing to the assembly of all fragments into one plasmid. In addition, the pLit_chlL_chlor plasmid contains the ampicillin resistance cassette necessary for positive selection of the *E. coli* cells growing on the selective medium added ampicillin after heat-shock transformation with pLit_chlL_chlor plasmid.

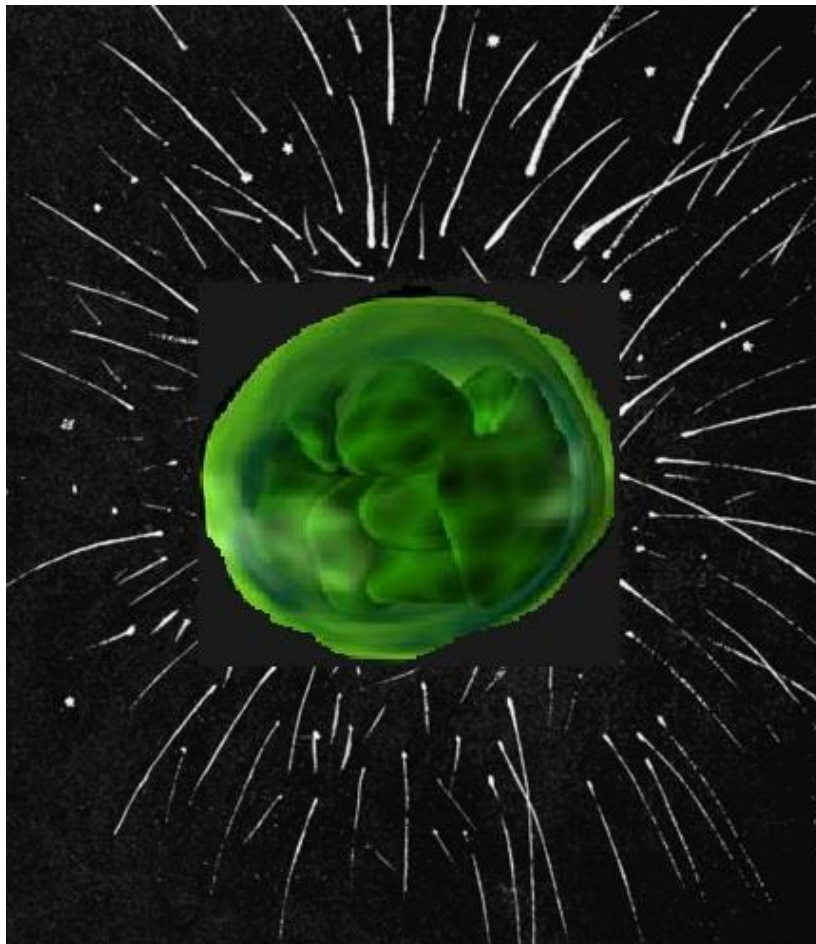
For the subsequent efficient transformation of *N. oceanica* CCMP1779 cells, the plasmid had to be linearized, as insertion of a circular plasmid is not efficient in the eukaryotes (Kilian O. et al. 2011). The only restriction enzyme that did not cut inside the antibiotic resistance cassette or flanking regions was PvuI restriction enzyme (see figure 5.8).

Conclusion

The assembly product, plasmid pLit_chlL_chlor containing the chloramphenicol resistance cassette and the homologous regions up- and downstream for the *chlL* gene on the chloroplast genome of *N. oceanica* CCPM1779, was constructed using modern DNA recombination technique - Gibson Assembly. The plasmid was created for the subsequent transformation of the *N. oceanica* cells by homologous recombination to obtain the deletion of the *chlL* gene coding for the protein unimportant for the cell growth and survival at the constant light.

Chapter VI

Biolistic Transformation



Chapter VI – Biolistic Transformation: Introduction

An important aspect in research work with transgenic microalgae is the establishment of the efficient transformation protocols. Microalgae are potential producers of biofuels, and have been successfully transformed over the past decades (Falciatore A. et al. 1999, León R. et al. 2007, Kilian O. et al. 2011). In general, the ability of microalgae to survive a temporary destabilization of the cell walls caused by various outside factors, allows the entrance of exogenous genomic material therefore resulting in transformation of these cells.

The existence of various transformation techniques (see chapter IV – Transformation by Electroporation - Introduction) has made the field of transgenic microalgae to develop extensively in the past decades (León R. et al. 2007). After successful rounds of random transformation by electroporation of the *N. oceanica* CCMP1779 genome with PCR-amplified transformation plasmid pSELECT100 (see chapter IV – Transformation by Electroporation), the attempt to transform the *Nannochloropsis* cells by homologous recombination was performed. Transformation by homologous recombination (also called gene targeting) is based on the endogenous gene deletion by insertion of the exogenous genomic material containing two specific homologous regions of the host genome flanking a selection marker. Therefore, the insertion of the plasmid DNA occurs in the specific location of the host genome disrupting the endogenous gene.

For the experiment presented in this chapter, the transformation plasmid pLit_chlL_chlor for homologous recombination was constructed using Gibson Assembly technology (see chapter V – Gibson Assembly). The transformation plasmid pLit_chlL_chlor contained the chloramphenicol resistance cassette for deletion of the endogenous *chlL* gene on the chloroplast genome of *N. oceanica* CCMP1779 by homologous recombination. However, the trial experiment of the transformation of the *N. oceanica* CCMP1779 cells by electroporation with the pLit_chlL_chlor under the most efficient conditions determined in chapter IV – Transformation by Electroporation (voltage of 1800 volts with low amount of the transformation plasmid added) resulted in no colony appearance (not described in the chapter IV due to result deficiency).

The idea of performing biolistic transformation with pLit_chlL_chlor plasmid instead of transformation by electroporation appeared after considering all the successful biolistic transformation reported in last decades (Ying C. et al. 1998, Falciatore A. et al. 1999, Lapidot M. et al. 2002, Kroth P. G. 2007). This technique allows the transformation of chloroplast and mitochondria genomes by homologous recombination supporting targeted insertion of the exogenous genes (Doetsch N.A. et al. 2001, Lapidot M. et al. 2002). Numerous stable transformations of diatoms were achieved and developed in 1990s (Dunahay T. G. et al. 1995,

Falciatore A. et al. 1999). After further development of new transformation techniques, more attention was paid for the improvement of these new transformation systems, However, the biolistic transformation remained being the most efficient.

Biolistic transformation

The biolistic transformation (also called particle bombardment or “gene gun”) system is considered as the most useful tool for transformation of the algae independent of their cell wall composition and life cycle. In addition, various cell tissues (animals, bacteria, fungi and plant tissues) can be transformed with exogenous DNA using this technique. The biolistic transformation was revealed as the only efficient technique for transformation of the plastid genome (Niu Y. F. et al. 2014). Due to the complicated structures of algal genes and their functions, the construction of proper exogenous plasmids may be at some degree complicated. Despite this, it was assumed not being a problem as the biolistic transformation allows application of a diversity of vectors.

Particle bombardment is considered as a controllable transformation system, where all physical and chemical factors can be determined and manipulated for various species (Purton S. 2007). The parameters include the pressure and vacuum degree applied at the bombardment, determining the force the particles are applied to the target cells. The concentration of the plasmid DNA is also a decisive factor and had a significant effect on transformation of *N. oceanica* CCMP1779 by electroporation (see chapter – Transformation by Electroporation). The distance between DNA-coated microcarriers and target cells determines the distribution area of the microparticles (Qin S. et al. 2012).

The biolistic transformation is based on the delivery of DNA-coated microparticles (microcarriers) into the target cells gaining their force from pressurized helium. The technique does not include any complicated pre- or post-bombardment manipulations. Despite the instruments` price, biolistic transformation is a convenient and less time-consuming technology compared to the electroporation (Bio Rad Laboratories). The helium applied in the particle delivery system has an advantage of being a clean and adjustable propellant. Due to helium`s low atomic weight, the maximum gas expansion is achieved inside the bombardment chamber resulting in a sufficient acceleration of the microcarriers. The system involves the insertion of the plate with the target cells into the chamber, where the vacuum is built up and causes the acceleration of the microparticles to about 500 m s⁻¹.

Both gold and tungsten particles (0.-1.5 µm) are utilized for the cell shooting. Though gold particles are more expensive, they are preferable due to their uniform size, and natural inertness in contrast to tungsten, which in turn can cause cell mutagenesis in addition to slow DNA degradation due to tungsten`s toxicity (Leon R. et al. 2007). The rupture disk included in the

modern devices bursts at the defined pressure. The stopping screen beneath the macrocarrier applied with microcarriers (DNA-coated particles), stops and thus protects the target cells from detritus of the rupture disk, still letting the microcarriers to pass and reach them (Bio Rad Laboratories). Since the microparticles become accelerated due to gunpowder explosion, their achieved kinetic energy becomes sufficient for penetration of both the cell wall, the plasma membrane and two membranes surrounding chloroplast. Multiple copies of transformation DNA is thus delivered into the organelles (see figure 6.1) (Leon R. et al. 2007). The cells are supposed to be only partially damaged during biolistic transformation, allowing the opportunity to perform the cell membrane repair and complete cell recovery (Kroth P. G. 2007).

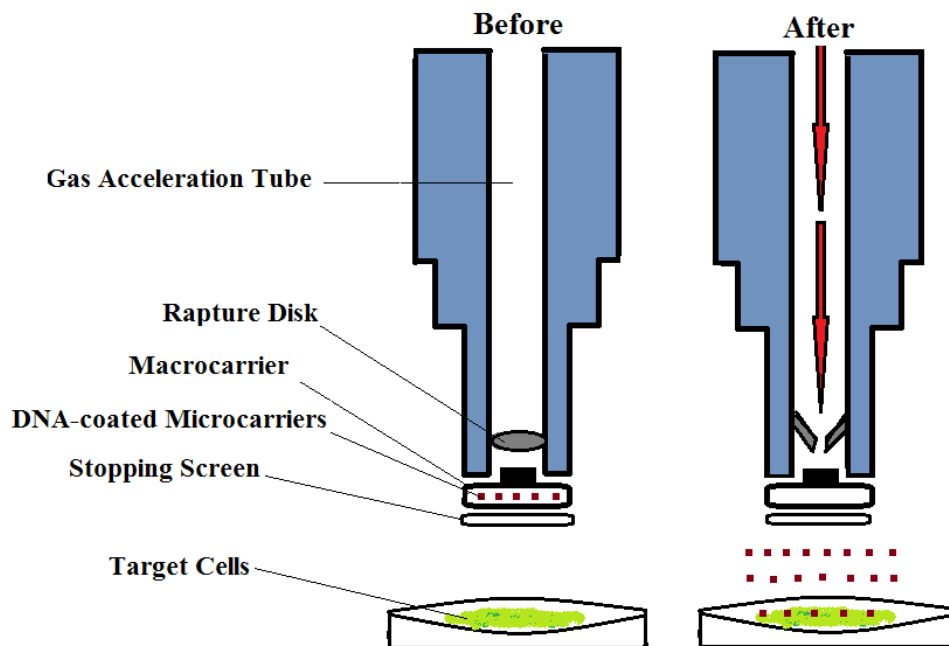


Figure 6.1: **The biolistic transformation technique.** The plate with applied target cells is inserted into the chamber. The high helium pressure is built up and is released by the rupture of the rupture disk at a specific pressure. This causes the acceleration of the plasmid DNA-coated microparticles (microcarriers) towards the target cells. After the gunpowder is applied and rupture disk is disrupted, the microcarriers reach a high kinetic energy, thus becoming applied onto the target cells. The stopping screen protects the target cells from the debris of disrupted rupture disk.

Previous biolistic transformations of microalgae have reported important parameters, which were evaluated prior to perform the biolistic bombardment of the *N. oceanica* CCMP1779 cells with the PvuI digested (linearized) pLit_chlL_chlor plasmid DNA (see table 6.1). The parameters include the cell concentration, amount of plasmid DNA added, the type of microcarriers (and their size), the pressure applied under the bombardment, the distance between the microcarriers and target cells, as well as the period of incubation of the target cells after the performed microparticle bombardment.

Table 6.1: The important parameters reported by the previous biolistic transformation studies on microalgae, which were evaluated for the establishment of the efficient biolistic transformation of *N. oceanica* CCMP1779 by homologous recombination using PvuI digested (linearized) transformation plasmid pLit_chlL_chlor. The parameters include the cell concentration, the amount of the transformation plasmid, the type of the microcarriers, the pressure applied at the bombardment, the travel distance of the microparticles and therefore their distribution area on the target cells, as well as incubation of the target cells after performed microparticles bombardment.

Conditions	Remacle (Remacle C. et al. 2006)	Falciatore (Falciatore A. et al. 1999)	Kroth (Kroth P. G. 2007)	Lapidot (Lapidot M. et al. 2002)
Cell amount transformed (cells)	1×10^8	5×10^7	1×10^8	1×10^8
Plasmid DNA amount (μg)	1-2	1	1	0.8
Microcarriers	Tungsten	Tungsten (0.4/0.7/ 1.1 mm)	Tungsten	Tungsten (0.7 mm)
Pressure (psi)	1100	650/1100/1550	1550	1300
Distance between microcarriers and target cells (cm)	7	6	-	9
Incubation of target cells (h)	-	48	24	24
Cell amount plated out on selective medium	Assuming all cells (1×10^8)	1×10^7	2.5×10^7	Assuming all cells (1×10^8)
Transformation efficiency	100-250 transformants/ μg	1×10^{-6} colonies/cells/ μg	-	2.5×10^{-4} colonies/cells/ μg

Goal

The aim of the experiment presented in this chapter was the establishment of an efficient chloroplast transformation protocol for *N. oceanica* CCMP1779 by homologous recombination with the transformation plasmid pLit_chlL_chlor. In this experiment, the deletion of the *chlL* gene on the chloroplast genome of the *N. oceanica* CCMP1779 was performed based on the *chlL* gene unimportance for cell survival and life cycle (see chapter V - Gibson Assembly for the description of *chlL* gene). Due to unsuccessful transformation of *N. oceanica* CCMP1179 with pLit_chlL_chlor transformation plasmid by electroporation conducted previously (not described), the biolistic transformation became a technique of choice in this experiment.

Materials and Methods

Cell culture

The cells of *N. oceanica* CCMP1779 were cultivated in the Cell-Hi CN medium (Varicon Aqua Solutions) at 23°C at constant light intensity of 100 $\mu\text{E m}^{-2} \text{s}^{-1}$ and continuous rotational shaking (see chapter II – Correct Cell Count Estimation, Cell growth). After reaching the exponential growth phase concentration ($2\text{-}4 \times 10^6$ cells/mL), the *Nannochloropsis* cells were harvested using centrifugation at $3000 \times g$ for 10 min at 22°C. Various cell concentrations were spread in a circle with a ~5 cm diameter on agar-solidified Cell-Hi CN medium 24 h prior to the biolistic transformation. Two plates contained 5×10^7 cells, while two other plates contained 1×10^8 cells. All four plates were incubated under the same growth conditions.

Preparation of microcarriers

100 mg of tungsten M-10 Microcarriers (0.7 μm) (Bio Rad, Norway) were weighed out and placed into a sterile 1.5 mL eppendorf tube and washed with 1 mL of 96% ethanol. Three times of vortexing for 2 min were included in between the washing steps. The microcarriers were centrifuged at maximum speed for 1 min. The supernatant was discarded, and the microparticles were resuspended in 1 mL of sterile water. Aliquots of 50 μL were prepared in sterile eppendorf tubes. During the preparation of the aliquots, the sedimentation of the tungsten microparticles was avoided by frequent vortexing. The aliquots were stored at -20°C for subsequent use.

Preparation of microcarriers for biolistic transformation

The aliquots of the tungsten microparticles were thawed and resuspended by vortexing. 50 μL of the transformation plasmid pLit_chlL_chlor (120 ng/ μL), 50 μL of 2.5 M CaCl_2 , and 20 μL of 1 M sperimidine were added to a 50 μL aliquot of tungsten microparticles under constant low-speed vortexing. The microparticles were centrifuged at $2000 \times g$ for 5 s. The supernatant was discarded. The microparticles were resuspended in 140 μL of 70% ethanol and vortexed at lower speed for washing. The microparticles were centrifugation at $2000 \times g$ for 2 min, and the supernatant was discarded. The microparticles were resuspended in 140 μL of 96% ethanol, vortexed, and centrifuged at $2000 \times g$ for 2 min. After the supernatant was discarded, the microparticles were finally resuspended in 50 μL of 96% ethanol. The DNA-coated tungsten microcarriers were subsequently used during 1 h after preparation.

Preparation of Particle Delivery System

The Bio Rad® PSD-1000/He Particle Delivery System (Bio Rad, Munchen, Germany) (see figure 6.2) was used for the biolistic transformation of the *N. oceanica* CCMP1779 cells with PvuI digested pLit_chlL_chlor transformation plasmid. The helium was supplied with a pressure of 1700 psi. Both the rupture disks (1550 psi rupture pressure; Bio Rad), the metallic stopping screens (Bio Rad) and the macrocarriers (Bio Rad) were sterilized with 70% ethanol and left to allow complete evaporation of the ethanol. The biolistic transformation was performed in a laminar floor hood, with constant sterilization of the Delivery System and its components with 70% ethanol in between the DNA-coated microparticle shots onto the target cells of *N. oceanica* CCMP1779.

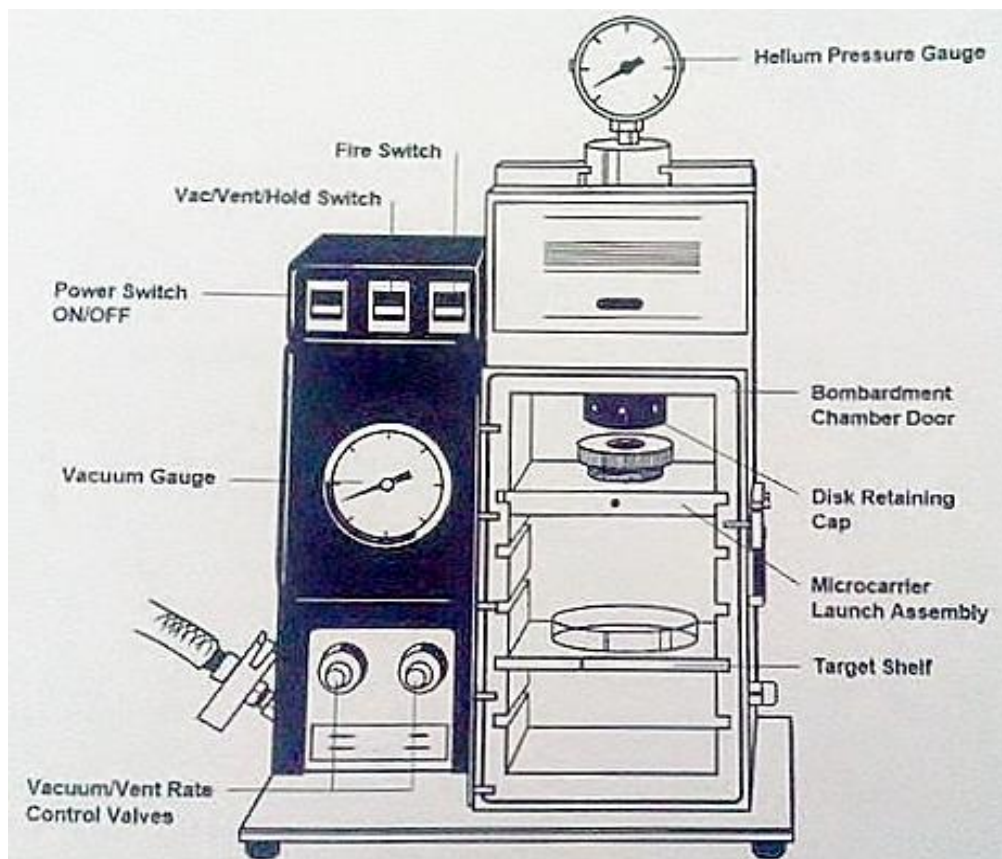


Figure 6.2: Schematic picture of the Bio Rad® PSD-1000/He Particle Delivery System main unit (Bio Rad, Munchen, Germany).

Microparticles bombardment

The sterile metallic stopping screen was placed in the microcarrier launch assembly (see figure 6.2). The microcarriers were vortexed thoroughly, and 10 μ L of the particles containing 1 μ g of the PvuI digested transformation plasmid pLit_chlL_chlor was applied on the sterile

macrocarrier and left to allow complete evaporation of the ethanol. The macrocarrier was installed on top of the stopping screen, while a rapture disk was installed in the disk retaining cap (see figure 6.2). The agar plate with the *N. oceanica* CCMP1779 cells was placed at the second level from the bottom creating a travel distance for DNA-coated microcarriers of 6 cm. The air was deflated by opening the control valve for building a vacuum of 25 psi as measured using the vacuum gauge (see figure 6.2). The helium button (fire switch), was held until the pressure reached a value of 1700 psi and the rapture disk burst, causing the DNA-coated microparticles to accelerate into the target *N. oceanica* cells. The vacuum was released by opening another control valve (see figure 6.2). Each of the plates containing 5×10^7 and 1×10^8 cells were shot 2 and 3 times, respectively.

Results and Discussion

After three weeks of incubation of the *N. oceanica* CCMP1779 cells transformed by biolistic particle bombardment with pLit_chlL_chlor plasmid containing the chloramphenicol resistance cassette, a number of colonies has formed on the selective medium containing 40 $\mu\text{g}/\text{mL}$ chloramphenicol. Cells of two different concentrations were transformed with two different amount of plasmid, including 2 and 3 μg (see Materials and Methods – Microparticles bombardment). The difficulty occurred under counting the colonies due to their unusually small size creating a need for usage of the magnifier. Although distinguishing the colonies of size as small as $\frac{1}{4}$ of the 0.5-10 μL pipette tip was problematic, some estimation of their approximate number for each transformation sample was made. The transformation efficiency was determined for each transformation sample, and resulted in very low values (see table 6.2).

Table 6.2: *N. oceanica* CCMP1779 cells were transformed by biolistic transformation using the assembled transformation plasmid pLit_chlL_chlor containing the chloramphenicol resistance gene. Cells of two different concentrations were transformed with different plasmid amounts. After three weeks of incubation on the agar-solidified selective medium containing 40 $\mu\text{g}/\text{mL}$ chloramphenicol, the colonies have appeared resulting in a low transformation efficiency.

Cell amount exposed to particle bombardment (cells)	Plasmid amount (μg)	Amount of cells plated out (cells)	Colonies formed	Transformation efficiency (colonies/cells/ μg)
5×10^7	2	3.33×10^7	5-10	3.75×10^{-8} - 7.50×10^{-8}
5×10^7	3	3.33×10^7	~23	1.15×10^{-7}
1×10^8	2	6.67×10^7	~4	6.00×10^{-8}
1×10^8	3	6.67×10^7	~5	5.00×10^{-8}

The reason to imprecise number of the colonies observed on the selective medium was due to high amount of the cells plated out for transformant-screening. This resulted in a very dense

layer of the cells on the selective medium, making it difficult to distinguish the distinctly formed colonies. Though the achieved transformation efficiencies were significantly lower than previously reported in other studies, chloroplast genome of *Nannochloropsis* has yet not been transformed by biolistic transformation, suggesting this experiment being an initial study. In addition, other factors could influence the transformation efficiency, arguing against the fact that biolistic transformation is not a transformation technique of choice for *Nannochloropsis* cells.

The aforementioned high density of the cells plated out on the selective medium causing the deficiency in growth medium, could affect the formation of the colonies. It has been previously reported that the incubation of the cells transformed by biolistic bombardment on the agar plates without antibiotics should not exceed 24 h (Kroth P. G. 2007). In case of the experiment described in this chapter, the cells were incubated for more than 48 h. This could result in an inefficient induction of the potentially inserted chloramphenicol resistance gene, resulting in lower selection of the positive transformants.

As the chloramphenicol resistance cassette in the pLit_chlL_chlor plasmid did not possess an endogenous *Nannochloropsis* promoter, the transcription of the resistance gene could be inefficient affecting the transformation efficiency. Therefore, one of the factors resulting in an increased transformation efficiency could be the use of an endogenous promoter (the possibilities of improving the biolistic transformation of *Nannochloropsis* are discussed in chapter Future Research).

The further attempt to induce the cell resistance to the chloramphenicol of potentially transformed cells, was the transfer of the newly formed cell colonies to the liquid medium containing the same chloramphenicol concentration of 40 µg/mL. However, the incubation carried out at the same growth conditions for 7 days resulted in a deficient growth of the transformants. There are several reasons causing a decreased cell growth in the liquid selective medium. The cell colonies picked from the agar-solidified selective medium for their subsequent inoculation in the liquid selective medium, were of very small size precluding the colony transfer using the 0.5-10 µL pipette tip under the magnifier. A level of sensitivity of the *Nannochloropsis* cells to the antibiotic in the liquid selective medium compared to agar-solidified selective medium containing the same antibiotic concentration could be different. That could cause the cell death of even transformed cells. A possibility of a decreased to some extent cell growth rate could require more time for achieving a higher cell density. Due to time limits for the master thesis, this study is suggested for future research, where more experiments are required to either confirm or refute the successful formation of the transformants after biolistic transformation of *N. oceanica* cells.

Conclusion

The goal of this experiment was the establishment of a protocol for an efficient biolistic transformation of *N. oceanica* CCMP1779 cells with chloramphenicol resistance cassette-containing pLit_chlL_chlor plasmid via homologous recombination. The result of the transformation was the deletion of the *chlL* gene at the chloroplast genome of the *Nannochloropsis* cells and subsequent formation of the transformants resistant to the high concentration of chloramphenicol. The transformation efficiency achieved at this experiment after screening the cells on the selective medium, was significantly low, compared to other biolistic transformation studies of other microalgae and to efficiencies achieved after transformation of the *N. oceanica* CCMP1779 cells by electroporation (see chapter IV – Transformation by Electroporation). The selection of the transformants in the liquid medium containing the same chloramphenicol concentration did not result in any cell growth suggesting either the cells not being transformed at all, or different sensitivity of the transformed cells to the liquid selective medium compared to agar-solidified selective medium. Due to time shortage of this project, the biolistic transformation of *N. oceanica* CCMP1779 is suggested for future research.

Future Research

The main goal of the master project was the establishment of an efficient protocol for transformation of *Nannochloropsis oceanica* CCMP1779 cells with the hygromycin resistance cassette-containing plasmid pSELECT100 by electroporation. The transformation proved to be successful and resulted in a random insertion of the hygromycin resistance cassette into the *Nannochloropsis* genome. However, the attempt to achieve the insertion of the plasmid pLit_chlL_chlor constructed using Gibson Assembly into the chloroplast genome of *N. oceanica* CCMP1779 by the same transformation technique was ineffective and led to consideration of another technique as an alternative. After evaluation of the recent available protocols, the biolistic transformation became a technique of choice for a target transformation of the *N. oceanica* CCMP1779 cells by homologous recombination and hence deletion of the endogenous *chlL* gene. The detection of the positive transformants on the selective medium containing chloramphenicol indicated a successfully performed biolistic transformation of the *N. oceanica* cells.

Electroporation and biolistic transformation techniques are considered the two most popular modern transformation techniques for microalgae (Niu Y.F. et al. 2014). Although both of these techniques have been successfully applied during the master project, more experiments are still required in order to improve both techniques.

Cell growth

Regarding the competence of the *Nannochloropsis* cells to achieve a successful transformation, more evaluation is necessary. Conditions such as light, temperature, and composition of the growth medium can be adjusted to achieve a more efficient cell growth, eliminating stress factors (Rocha J. M. S. et al. 2003). Variations in light intensity and wavelength could be one of the factors influencing the cell growth, and therefore also the cell's stability, which would influence the result of a subsequent transformation. Exploitation of different light/dark cycles might also result in changed cell viability, thus causing differences in cell health and fluctuations in the transformation efficiencies.

The temperature is another factor influencing cell growth. Determining at what extend the fluctuation in temperatures might affect the cell growth and therefore the transformation efficiencies, would be an informative experiment.

Nannochloropsis cells are sensitive to pH changes in the growth medium. pH control could be obtained using various buffers (e.g. Tris-HCl) or inorganic acids. As no control of pH was

carried out during the cultivation of *N. oceanica* cells in this master project, the effect of induced pH differences could be considered in future transformation experiments.

The Varicon Aqua Solutions Company producing the Cell-Hi CN growth medium used for cultivation of the *N. oceanica* cells in this master project keeps the medium components and their concentration a trade secret, making manipulation of this medium difficult. However, f/2 medium used for the initial growth of *Nannochloropsis* cells consists of known concentrations of known nutrients and can therefore be manipulated to investigate how the differences in cell growth caused by the growth medium can affect the transformation efficiency. Addition of glucose and ammonium sulphate increases the cell growth, although the risk of contamination also becomes higher (Rocha J. M. S. et al. 2003). The effect of urea as a nitrogen source on the cell growth reported in the previous study could also be studied in detail in regard to transformation efficiency (Rocha J. M. S. et al. 2003). Manipulations of the growth medium and its influence on the transformation efficiencies would be an informative experiment to perform.

Another factor affecting cell growth is the shear forces introduced to the cells through the air-supplying bubbling system used for initial cultivation of the *Nannochloropsis* cells. The cells were hence transferred to another type of rotational shaking. The effect of the new shaker type, which might also expose the cells to shear forces and thus cause stress, was not investigated in this project. Therefore, the determination of efficient growth conditions, and their effect on transformation efficiency is the aim of future experiments.

Colony PCR

Some difficulties occurred during the post-transformational colony PCR procedure. Numerous methods were employed to release the genomic DNA, which ranged between snap-freezing to cell incubation at 100°C, as well as the addition of various lysis buffers to break down the cell walls. The only method resulting in genomic DNA release was the use of Wizard Genomic DNA Purification kit. The preliminary cultivation of the colonies and the utilization of the kit made the method time-consuming and expensive. The establishment of an efficient protocol for the colony PCR for *Nannochloropsis* cell would therefore be a part of future research work.

GFP

Another advantageous experiment would be the heterologous expression of the gene coding for the green fluorescence protein (GFP) by recombinant DNA technology (Kilian O. et al. 2005, Tanaka Y. et al. 2005). The DNA sequence of the GFP gene can be inserted into a plasmid containing the gene of interest, either between the promoter and the gene of interest, or downstream to the gene of interest. Not only will the insertion of the GFP gene serve as an

efficient extension of the screening method for the positive transformants, it would also make it possible to see the location of the fusion protein inside the cells using the proper microscopy equipment. Due to the GFP protein's small size not affecting the function of the resulting fusion protein; its possibility to fluoresce without any additional compounds inducing the fluorescence; the opportunity to control and observe the gene expression induced by different environmental factors, as well as its non-toxicity, makes the co-expression of GFP significant tool in the field of transgenic microalgae (Zimmer M.).

The need for an appropriate promoter

For the construction of the pLit_chlL_chlor plasmid, the chloramphenicol resistance cassette was amplified from the pLitmus_Chlor plasmid available at the Department of Biotechnology, NTNU. Unfortunately, the information about the promoter upstream to the chloramphenicol resistance gene was missing suggesting it being a bacterial promoter, which might be inefficient compared to an endogenous promoter. Therefore, an appropriate promoter is required in order to achieve efficient transformations. The use of endogenous promoters such as promoters of lipid droplet surface protein (LDSP) or violaxanthin/chlorophyll a-binding protein (VCP) genes would be a better choice for successful transcription and expression of the genes of interest. Undoubtedly, the heterologous expression would also be improved due to the continued development of DNA sequencing technologies and genome annotation.

Biolistic transformation

Concerning the potentially successful biolistic transformation performed in this master project, some additional research is required. The appearance of colonies after transformation of the *N. oceanica* cells with pLit_chlL_chlor plasmid indicated successfully formed transformants, where the chloramphenicol resistance cassette has been inserted into the chloroplast genome. However, employment of a selective medium as the only screening method is inadequate for complete confirmation of the formation of positive transformants. The current screening method might at some point yield incorrect results if spontaneous mutation of the cells takes place. As already stated, an improved protocol for efficient colony PCR is required, where an additional genomic DNA extraction procedure is unnecessary. In case no other method besides using the Wizard Genomic DNA Purification kit is established and approved, the kit should be used for the genomic DNA extraction and PCR amplification of the chloramphenicol resistance cassette to confirm the formation of the transformants.

The application of GFP is also relevant in this study. The Gibson Assembly technique can be employed to assemble an expression construct consisting of a selection marker, the GFP and two specific homologous regions of the host genome flanking a selection marker.

The protocol for biolistic transformation of the *Nannochloropsis* cells also requires modifications. The long-term study assessing variation of the transformation parameters was not performed in this master project due to time deficiency. The influence of different parameters, such as various pressure values, travel distance for the microparticles, pre- and post-incubation of the target cells, concentration of the transformation plasmid, as well as the effect of different types of microcarriers should be determined for the *N. oceanica*, involving a series of experiments.

Bacterial Magnetic Particles

The inclusion of a new type of microparticles and the determination of their effects on the biolistic transformation efficiency could be an experiment of future research. Bacterial Magnetic Particles (BMPs) are purified from one species of the magnetotactic bacteria called *Magnetospirillum* sp. AMB-1 (Niu Y.F. et al. 2014). These bacteria have their natural habitat on the geomagnetic field of Earth, and possess organelles called magnetosomes containing 15-20 magnetic crystals of magnetite or greigite (35–120 nm) (Yoshino T. et al. 2010, Yana L. et al. 2012). A thin phospholipid layer covers the particles and enables them to bind large quantities of DNA compared to gold and tungsten particles. The advantages of gold over tungsten particles and therefore their preference in the biolistic transformation were described in the chapter VI – Biolistic Transformation. However, the biolistic transformation performed with BMPs is considered more efficient than with gold particles, demonstrating its superiority in the range of DNA microcarriers used in microparticle bombardment (Niu Y.F. et al. 2014). One study has reported successful transformation of marine cyanobacterium *Synechococcus* sp. NKBG15041c using BMPs during biolistic transformation (Matsunaga T. et al. 1991). Therefore, transformation of marine *Nannochloropsis* cells using BMPs would be an informative and significant study.

Gene knock-out

Future research on *Nannochloropsis* may include deletion of genes significant for the cell viability, as it was previously reported in the study of Kilian O. (Kilian O. et al. 2011). A new plasmid containing the PCR-amplified hygromycin resistance cassette originating from the pSELECT100 plasmid, embedded between two homologous flanking regions of e.g. nitrate reductase or nitrite reductase genes of *Nannochloropsis*, could be constructed using Gibson Assembly. The deletion either of the genes would select the transformants growing only on a medium having ammonium as the only nitrogen source, and the antibiotic corresponding to the selection marker.

Beyond doubt, the field of transgenic microalgae and bioenergy is one of the most extensively developed fields of the biotechnology. As the future demand on biofuels will increase

continuously, more resources will be spent on the establishment of species-adjusted transformation protocols and detection of the shortcomings of these protocols. Determination of efficient and stable cell growth conditions, as well as development of DNA sequencing technology and genome annotation for a better understanding of the metabolic pathways in the cells would result in successful genetic manipulation of the microalgae. The essence of the research on microalgae and bioenergy is the bright future of clean, sustainable, and renewable bioenergy.

References

- Antimicrobial Resistance Learning Site. (2011). "Pharmacology: Chloramphenicol." from <http://amrls.cvm.msu.edu/pharmacology/antimicrobials/antibiotics-of-veterinary-importance/chloramphenicol>.
- Austin A. Open Ponds Versus Closed Bioreactors. Biomass Magazine.
- BD Biosciences. "BD Accuri™ C6 Flow Cytometer Optical Filter Guide." from http://www.bdbiosciences.com/documents/BD_Accuri_Optical_Filter_Guide.pdf.
- Benner S. A. (2003). "Synthetic biology: Act natural." Nature Communications **421**: 118.
- Berkow R. (1999). "The Merck Manual of Medical Information - Home Edition." Pocket.
- Bio Rad Laboratories Biolistic (R) PDS-1000/He Particle Delivery System. B. Rad.
- BioLabs Inc. New England "Gibson Assembly® Master Mix – Transformation."
- BioLabs Inc. New England. "Gibson Assembly® Protocol (E5510)." from <https://www.neb.com/protocols/2012/12/11/gibson-assembly-protocol-e5510>.
- BioLabs Inc. New England. (2009). "Gibson Assembly® Cloning (Application Overview)." Retrieved February, 2014, from <https://www.neb.com/applications/cloning-and-synthetic-biology/gibson-assembly-cloning>.
- Bollivar D. W. and Beale S. I. (1996). "The Chlorophyll Biosynthetic Enzyme Mg-Protoporphyrin IX Monomethyl Ester (Oxidative) Cyclase." Plant Physiology **112**: 105-114.
- Bondioli P., Della Bella L., Rivolta G., Chini Zittelli G., Bassi N., Rodolfic L., Casini D., Prussi M. and Chiaramonti D. (2012). "Oil production by the marine microalgae *Nannochloropsis* sp. F&M-M24 and *Tetraselmis suecica* F&M-M33." Bioresource Technology **114**: 567-572.
- Boynton J. E., Gillham N. W., Harris E. H., Hosler J. P., Johnson A. M., Jones A. R., Randolph-Anderson B. L., Robertson D., Klein T. M., Shark K. B. and S. J. C. (1988). "Chloroplast transformation in *Chlamydomonas* with high velocity microprojectiles." Science **240**: 1534-1538.
- Cabanas M. J., Vazquez D. and Modolell J. (1978). "Dual interference of hygromycin B with ribosomal translocation and with aminoacyl-tRNA recognition. ." European Journal of Biochemistry **87**(1): 21-27.
- Campbell C. J. (1997). "The coming oil crisis. ." Multi-science Publishing Company and petroconsultants S.A.
- Chisti Y. (2007). "Biodiesel from microalgae." Biotechnology Advances **25**: 294–306.
- Chisti Y. (2008). "Biodiesel from microalgae beats bioethanol." Trends in Biotechnology **26**: 126–131.

- Converti A., Casazza A. A., Ortiz E. Y., Perego P. and Del Borghi M. (2009). "Effect of temperature and nitrogen concentration on the growth and lipid content of *Nannochloropsis oculata* and *Chlorella vulgaris* for biodiesel production " **48**(6): 1146-1151.
- Cruz A., Coburn C. M. and Beverley S. M. (1991). "Double targeted gene replacement for creating null mutants." PNAS, Proceedings of the National Academy of Sciences **88**: 7170-7174.
- Debuchy R., Purton S. and R. J. D. (1989). "The argininosuccinatelyase gene of *Chlamydomonas reinhardtii*: an important tool for nuclear transformation and for correlating the genetic and molecular maps of the ARG7 locus." The EMBO Journal **8**: 2803-2809.
- Dismukes, G. C., Carrieri D., Bennette N., Ananyev G. M. and Posewitz M. C. (2008). "Aquatic phototrophs: efficient alternatives to land-based crops for biofuels." Current Opinion in Biotechnology **19**: 235-240.
- Doetsch N.A., Favreau M.R., Kuscuoglu N., Thompson M.D. and Hallick R.B. (2001). "Chloroplast transformation in *Euglena gracilis*: splicing of a group III twintron transcribed from a transgenic psbK operon. ." Current Genetics **39**: 49-60.
- Dunahay T. G., Jarvis E. E. and Roessler P. G. (1995). "Genetic transformation of the diatoms *Cyclotella cryptica* and *Navicula saprophila*." Journal of Phycology **31**(6).
- Dunn R. O. (2011). Improving the Cold Flow Properties of Biodiesel by Fractionation. Soybean: Applications and Technology. Rijeka, Croatia.
- Endy D. (2005). "Foundations for engineering biology." Nature Communications **438**(7067): 449-453.
- Falciatore A., Casotti R., Leblanc C., Abrescia C. and Bowler C. (1999). "Transformation of Nonselectable Reporter Genes in Marine Diatoms." Marine Biotechnology **1**: 239-251.
- Fawley K. P. and Fawley M. W. (2007). "Observations on the diversity and ecology of freshwater *Nannochloropsis* (Eustigmatophyceae), with descriptions of new taxa. ." Protist **158**: 325-336.
- Fong A. and Archibald J. M. (2008). "Evolutionary Dynamics of Light-Independent Protochlorophyllide Oxidoreductase Genes in the Secondary Plastids of Cryptophyte Algae." Eukaryot Cell **7**.
- Froger A. and Hall J. E. (2007). "Transformation of Plasmid DNA into *E. coli* Using the Heat Shock Method." Journal of Visualized Experiments : JoVE **6**: 253.
- Galloway R. E. (1990). "Selective conditions and isolation of mutants in salt-tolerant, lipid-producing microalgae." Journal of Phycology **26**(4): 752-760.
- Gau A. E., Mant A. and Thompson S. J. "PSBY - photosystem II protein psbY-2." Retrieved February, 2014, from <http://www.wikigenes.org/e/gene/e/843099.html>.
- Gibson D. G., Young L., Chuang R. Y., Venter J. C. and Hutchison C. A. (2009). "Enzymatic assembly of DNA molecules up to several hundred kilobases." Nature Methods **VOL.6**

- Gouveia L. and Oliveira A.C. (2008). "Microalgae as a raw material for biofuels production." Journal of Industrial Microbiology and Biotechnology **36**: 269-274.
- Grigoryev Y. (2013). "Cell Counting with a Hemocytometer." from <http://bitesizebio.com/13687/cell-counting-with-a-hemocytometer-easy-as-1-2-3/>.
- Hibberd D. J. (1981). "Notes on the taxonomy and nomenclature of the algal classes Eustigmatophyceae and Tribophyceae (synonym Xanthophyceae)." Botanical journal of the Linnean society **82**(2): 93-119.
- Hoek C., Mann D. G. and Jahns H. M. (1998). "Igae. An Introduction to Phycology." Photosynthetica **35**(4): 506-506.
- Hollingshead S., Kopečná J., Jackson P. J., Canniffe D. P., Davison P. A., Dickman M. J., Sobotka R. and Hunter C. N. (2012). "Conserved Chloroplast Open-reading Frame ycf54 Is Required for Activity of the Magnesium Protoporphyrin Monomethylester Oxidative Cyclase in *Synechocystis* PCC 6803." The Journal of Biological Chemistry.
- Hu Q., Sommerfeld M., Jarvis E., Ghirardi M., Posewitz M., Seibert M. and Darzins A. (2008). "Microalgal triacylglycerols as feedstocks for biofuel production: perspectives and advances. ." The Plant Journal **54**(4): 621–639.
- Iizumi S., Nomura Y., So S., Uegaki K., Aoki K., Shibahara K., Adachi N. and Koyama H. (2006). "Simple one-week method to construct gene-targeting vectors: application to production of human knockout cell lines." BioTechniques **41**: 311-316.
- Janouskovec J., Horák A., Oborník M., Lukes J. and Keeling P.J. (2010). "A common red algal origin of the apicomplexan, dinoflagellate, and heterokont plastids." Proceedings of the National Academy of Sciences of the United States of America **107**: 10949-10954.
- Kilian O., Benemann C. S. E., Niyogi K. K. and Vick B. (2011). "High-efficiency homologous recombination in the oil-producing alga *Nannochloropsis* sp." Proceedings of the National Academy of Sciences of the United States of America.
- Kilian O. and Kroth P.G. (2005). "Identification and characterization of a new conserved motif within the presequence of proteins targeted into complex diatom plastids." Plant Journal **41**: 175–183.
- Kroth P. G. (2007). Genetic Transformation: A Tool to Study Protein Targeting in Diatoms. Methods in Molecular Biology. M. v. d. Giezen. **390**.
- Lapidot M., Raveh D., Sivan A., Arad S. and Shapira M. (2002). "Stable Chloroplast Transformation of the Unicellular Red Alga *Porphyridium* Species." Plant Physiology **129**.
- León-Bañares R., González-Ballester D., Galván A. and Fernández E. (2004). "Transgenic microalgae as green cell-factories." Trends in Biotechnology **22**(1): 45-52.
- Leon R. and Fernandez E. (2007). Nuclear Transformation of Eukaryotic Microalgae: historical overview, achievements and problems. Transgenic Microalgae as Green Cell Factories. Leon R., Galvan A. and Fernandez E. **616**: 34-43.

- León R. and Fernández E. (2007). "Nuclear transformation of eukaryotic microalgae: ." Advances in Experimental Medicine and Biology **6**(16): 1-11.
- León R. and Fernández E. (2007). "Nuclear transformation of eukaryotic microalgae: historical overview, achievements and problems." Advances in Experimental Medicine and Biology **6**(16): 1-11.
- Li J., Han D., Wang D., Ning K., Jia J., Wei L., Jing X., Huang S., Chen J., Li Y., Hu Q. and Xu J. (2014). "Choreography of Transcriptomes and Lipidomes of *Nannochloropsis* Reveals the Mechanisms of Oil Synthesis in Microalgae." American Society of Plant Biologists.
- Marie D., Simon N. and Vaultot D. (2005). Chapter 17: Phytoplankton Cell Counting by Flow Cytometry. Algal Culturing Techniques. R. Andersen. Provasoli-Guillard National Center for Culture of Marine Phytoplankton, West Boothbay Harbor, ME USA.
- Matsunaga T., Sakaguchi T. and Tadakoro . (1991). "Magnetite formation by a magnetic bacterium capable of growing aerobically." Applied Microbiology and Biotechnology **35**: 651-655.
- Meenakshi A. (2013). "Cell Culture Media: A Review." from <http://www.labome.com/method/Cell-Culture-Media-A-Review.html>.
- Meetam M., Keren N., Ohad I. and Pakrasi H. B. (1999). "The PsbY Protein Is Not Essential for Oxygenic Photosynthesis in the Cyanobacterium *Synechocystis* sp. PCC 68031." Plant Physiology **Vol. 121**: 1267–1272.
- Muller M. and UIC University of Illinois at Chicago. "The First demonstration of bacterial transformation.", from <http://www.uic.edu/classes/bios/bios100/summer2003/freddy.htm>.
- Murakami R. and Hashimoto H. (2009). "Unusual Nuclear Division in *Nannochloropsis oculata* (Eustigmatophyceae, Heterokonta) which May Ensure Faithful Transmission of Secondary Plastids." Protist **160**: 41-49.
- National Center for Biotechnology Information. "Nannochloropsis oceanica strain CCMP531 chloroplast, complete genome." Retrieved March, 2014, from <http://www.ncbi.nlm.nih.gov/nuccore/542687962?report=graph>.
- National Center for Biotechnology Information. (2014, 6, April, 2014). "chlL ATP-binding subunit of protochlorophyllide reductase subunit [*Nannochloropsis oculata*]." from <http://www.ncbi.nlm.nih.gov/gene/16791721>.
- Niu Y. F., Huang T., Yang W. D., Liu J.S. and Li H. E. (2014). Genetic Engineering of Microalgae. Recent Advances in Microalgal Biotechnology. Dr. Jin Liu, Dr. Zheng Sun and Dr. Henri Gerken. 731 Gull Ave, Foster City. CA 94404, USA, OMICS Group eBooks.
- Niu Y.F., Huang T., Yang W.D., Liu J.S. and Li H.Y. (2014). Genetic Engineering of Microalgae. Recent Advances in Microalgal Biotechnology. L. J.S., Sun Z. and Gerken H., OMICS eBooks.
- Pan K., Qin J. J., Li S., Dai W. K. and Zhu B. H. (2011). "Nuclear monoploidy and asexual propagation of *Nannochloropsis oceanica* (Eustigmatophyceae) as revealed by its genome sequence." Journal of Phycology **47**: 1425–1432.

- Picot J., Guerin C. L., Le Van Kim C. and Boulanger C. M. (2012). "Flow cytometry: retrospective, fundamentals and recent instrumentation." Cytotechnology **VOL. 64**.
- Pulz O. and Gross W. (2004). "Valuable products from biotechnology of microalgae." Applied Microbiology and Biotechnology **65**: 635–648.
- Purton S. (2007). Tools and Techniques for Chloroplast transformation of Chlamydomonas. Transgenic Microalgae as Green Cell Factories. Leon R., Galvan A. and Fernandez E., Landes Bioscience. **616**.
- Qin S., Lin H. and Jiang P. (2012). "Advances in genetic engineering of marine algae." Biotechnology Advances **30**: 1602-1613.
- Qin S., Lin H. and Jiang P. (2012). "Advances in genetic engineering of marine algae." Biotechnology Advances **30**: 1602–1613.
- Radakovits R., Jinkerson R. E., Darzins A. and Posewitz M.C. (2010). "Genetic Engineering of Algae for Enhanced Biofuel Production." Eukaryotic Cell **9**.
- Radakovits R., Jinkerson R. E., Fuerstenberg S. I., Tae H., Settlage R. E., Boore J. L. and Posewitz M. C. (2012). "Draft genome sequence and genetic transformation of the oleaginous alga *Nannochloropsis gaditana*." Nature Communications **3**.
- Ras M., Steyer J.-P. and Bernard O. (2013). "Temperature effect on microalgae: a crucial factor for outdoor production " Reviews in Environmental Science and Bio/Technology.
- Reinbothe C., El Bakkouri M., Buhr F., Muraki N., Nomata J., Kurisu G., Fujita H. and Reinbothe S. (2011). "Chlorophyll biosynthesis: spotlight on protochlorophyllide reduction." Trends in Plant Science **15**(11).
- Remacle C., Cardol P., Coosemans N., Gaisne M. and Bonnefoy N. (2006). "High-efficiency biolistic transformation of *Chlamydomonas* mitochondria can be used to insert mutations in complex I genes." Proceedings of the National Academy of Sciences **103**(12): 4771-4776.
- Rocha J. M. S., Garcia J. E. C. and Henriques M. H. F. (2003). "Growth aspects of the marine microalga *Nannochloropsis gaditana*." Biomolecular Engineering **20**: 237-242.
- Rodolfi L., Chini Zittelli G., Bassi N., Padovani G., Biondi N., Bonini G. and Tredici M. R. (2009). "Microalgae for oil: strain selection, induction of lipid synthesis and outdoor mass cultivation in a low-cost photobioreactor." Biotechnology and Bioengineering **102**(1): 100-112.
- Sandnes J. M. , Källqvist T., Wenner D. and Gislerød H R. (2005). "Combined influence of light and temperature on growth rates of *Nannochloropsis oceanica*: linking cellular responses to large-scale biomass production " Journal of Applied Phycology **17**: 515-525.
- Scaramuzzi C. D., Hiller R. G. and Stokes H. W. (1992). "Identification of a chloroplast-encoded *secA* gene homologue in a chromophytic alga: possible role in chloroplast protein translocation." Current Genetics **22**(5): 421-427.

Shaw, W. V., L. C. Packman, B. D. Burleigh, A. Dell, H. R. Morris and B. S. Hartley (1979). "Primary structure of a chloramphenicol acetyltransferase specified by R plasmids." Nature **282**(5741): 870-872.

Sheehan J., Dunahay T., Benemann J. and Roessler P. (1998). "A look back at the US Department of Energy's Aquatic Species Program—biodiesel from algae." National Renewable Energy Laboratory.

Simionato D., Block M. A., La Rocca N., Jouhet J., Maréchal E., Finazzi G. and Morosinotto T. (2013). "The response of *Nannochloropsis gaditana* to nitrogen starvation includes de novo biosynthesis of triacylglycerols, a decrease of chloroplast galactolipids, and reorganisation of the photosynthetic apparatus." Eukaryotic Cell **12**: 665-676.

STRING 9.1. "Search Tool for the Retrieval of Interacting Genes/Proteins." from http://string-db.org/newstring.cgi/show_network_section.pl?identifier=1140.Synpcc7942_1419.

Tanaka Y., Nakatsuma D., Harada H., Ishida M. and Matsuda Y. (2005). "Localization of soluble beta-carbonic anhydrase in the marine diatom *Phaeodactylum tricornutum*. Sorting to the chloroplast and cluster formation on the girdle lamellae." Plant Physiology **138**: 207-217.

The European Bioinformatics Institute and Clustal Omega. "CLUSTAL O(1.2.1) multiple sequence alignment,

Results for job clustalo-I20140318-131949-0249-76715769-oy." from <https://www.ebi.ac.uk/Tools/services/web/toolresult.ebi?jobId=clustalo-I20140318-131949-0249-76715769-oy&analysis=alignments>.

Tickell J., Tickell K. and Roman K. (2000). From the fryer to the fuel tank. The complete guide to using vegetable oil as an alternative fuel. Tallahassee, USA.

TOKU-E The Evolution of BioPurity. (2010). "Chloramphenicol, USP - PRODUCT DATA SHEET ", from <http://www.toku-e.com/Upload/Products/PDS/20120618001452.pdf>.

UniProt Knowledgebase. (February 19, 2014). "Q4G385 (PSBY_EMIHU) - Photosystem II protein Y." Retrieved February, 2014, from <http://www.uniprot.org/uniprot/Q4G385>.

UniProt Knowledgebase. (2013, April 16, 2014). "K9ZV01 (K9ZV01_9STRA) Protein translocase subunit SecA." from <http://www.uniprot.org/uniprot/K9ZV01>.

van deMeene A. M., Hohmann-Marriott M. F., Vermaas W. F. and Roberson R. W. (2006). "The three-dimensional structure of the cyanobacterium *Synechocystis* sp. PCC6803." Archives of Microbiology **184**: 259-270.

Vieler A., Wu G., Tsai C. H., Bullard B. and Cornish A. J. (2012). "Genome, Functional Gene Annotation, and Nuclear Transformation of the Heterokont Oleaginous Alga *Nannochloropsis oceanica* CCMP1779." PLoS Genet **8**(11).

Wang B., Wang J., Zhang W. and Meldrum D. R. (2012). "Application of synthetic biology in cyanobacteria and algae." Frontiers in Microbiology.

Wydrzynski T. J. and Satoh K. (2006). "Photosystem II: The Light-Driven Water: Plastoquinone Oxidoreductase." Advances in Photosynthesis and Respiration **87**(3): 331-335.

Yana L., Zhanga S., Chenb P., Liud H., Yinb H. and Lib H. (2012). "Magnetotactic bacteria, magnetosomes and their application." Microbiological Research **167**(9).

Ying C., Wen-bin L., Qin-hua B. and Yong-ru S. (1998). "Study on transient expression of gus gene in *Chlorella ellipsoidea* (Chlorophyta) by using biolistic particle delivery system." Chinese Journal of Oceanology and Limnology **16**(1): 47-49.

Yoshino T., Maeda Y. and Matsunaga T. (2010). "Bioengineering of Bacterial Magnetic Particles and their Applications in Biotechnology." Recent Patents on Biotechnology **4**(3): 214-225.

Zhang C. and Hua H. (2013). "High-efficiency nuclear transformation of the diatom *Phaeodactylum tricornutum* by electroporation." Marine Genomics.

Zhang Y. "Mechanisms of Antibiotic Resistance in the Microbial World."

Zimmer M. (May 2013). "GFP - Green Fluorescent Protein." from <http://www.conncoll.edu/ccacad/zimmer/GFP-ww/prasher.html#DNA>.

Appendix

Appendix A – Chapter II: Correct Cell Concentration Estimation

Table A.1: *N. oceanica* CCMP1779 cell concentrations measured by hemocytometer (HC) and flow cytometer (FC). *N. oceanica* cells grew until they reached the exponential phase concentration ($\sim 2 \times 10^6$ cells/mL). The dilution series in triplicate were prepared, and cell counting was performed via hemocytometer and flow cytometer. Setups of flow cytometer included excitation at 488 nm, detection of fluorescence of the sample cells with FL3 filter (670 nm), threshold 30000 FSC, medium velocity (69 $\mu\text{L}/\text{min}$) for 2 min run. The data were used for establishment of the correlation between manual, time-consuming hemocytometer and automatized flow cytometer as two different cell counting methods. The standard deviations (STD) are assessed, having low values, with flow cytometry standard deviation being lowest, confirming higher precision of this cell counting method.

Dilution series	Cell concentration by hemocytometer (cells/mL)	STD HC	STD HC %	Cell concentration by flow cytometer (cells/mL)	STD FC	STD FC %
High	$5,69 \times 10^6$	-	-	$5,85 \times 10^6$	-	-
1:0.5	$4,13 \times 10^6$	$6,36 \times 10^4$	1,5	$3,60 \times 10^6$	$5,38 \times 10^4$	1,5
1:1	$3,12 \times 10^6$	$2,55 \times 10^5$	8,2	$2,53 \times 10^6$	$1,32 \times 10^5$	5,2
1:2	$1,89 \times 10^6$	$1,41 \times 10^4$	0,8	$1,68 \times 10^6$	$5,98 \times 10^3$	0,4
1:5	$9,56 \times 10^5$	-	-	$8,04 \times 10^5$	$1,22 \times 10^4$	1,5
1:9	$5,37 \times 10^5$	$1,98 \times 10^4$	3,7	$5,41 \times 10^5$	$5,44 \times 10^3$	1,0
1:11	$4,50 \times 10^5$	$3,61 \times 10^4$	8,0	$4,41 \times 10^5$	$1,96 \times 10^3$	0,4
1:15	$3,57 \times 10^5$	$4,24 \times 10^3$	1,2	$3,27 \times 10^5$	$7,26 \times 10^3$	2,2
1:19	$2,62 \times 10^5$	$5,66 \times 10^3$	2,2	$2,52 \times 10^5$	$7,89 \times 10^3$	3,1
	Average			Average		
		$5,69 \times 10^4$	3,6		$2,83 \times 10^4$	1,9

Table A.2: New dilution series of *N. oceanica* cell culture growing up to exponential growth phase ($\sim 2 \times 10^6$ cells/mL). The cell concentration values were determined using flow cytometer (using same settings), hemocytometer, and OD_{750nm}. The data were used for establishment of the correlation between flow cytometry and OD_{750nm}, and hemocytometer and OD_{750nm}, for an eventual usage of OD_{750nm} as an indicator of cell growth.

Dilution series	Cell concentration by flow cytometer (cell/mL)	Cell concentration by hemocytometry (cell/mL)	OD_{750nm} measured using Tecan Infinite 200 Pro
High	$5,85 \times 10^6$	$5,69 \times 10^6$	0,1169
1:0.5	$3,60 \times 10^6$	$4,13 \times 10^6$	0,0868
1:1	$2,53 \times 10^6$	$3,12 \times 10^6$	0,0646
1:2	$1,68 \times 10^6$	$1,89 \times 10^6$	0,0433
1:5	$8,04 \times 10^5$	$9,56 \times 10^5$	0,0212
1:9	$5,41 \times 10^5$	$5,37 \times 10^5$	0,0119
1:11	$4,41 \times 10^5$	$4,50 \times 10^5$	0,0117
1:15	$3,27 \times 10^5$	$3,57 \times 10^5$	0,0104
1:19	$2,52 \times 10^5$	$2,62 \times 10^5$	0,0062

Table A.3: Standard deviation of *N. oceanica* cell concentrations measured by flow cytometer for determination of correlation between flow cytometry and OD_{750nm} (addition to the table A.2).

Cell concentration by flow cytometer (cell/mL)	STD flow cytometry	STD %
$5,85 \times 10^6$	-	-
$3,60 \times 10^6$	$5,38 \times 10^4$	1,5
$2,53 \times 10^6$	$1,32 \times 10^5$	5,2
$1,68 \times 10^6$	$5,98 \times 10^3$	0,4
$8,04 \times 10^5$	$1,22 \times 10^4$	1,5
$5,41 \times 10^5$	$5,44 \times 10^3$	1,0
$4,41 \times 10^5$	$1,96 \times 10^3$	0,4
$3,27 \times 10^5$	$7,26 \times 10^3$	2,2
$2,52 \times 10^5$	$7,89 \times 10^3$	3,1
Average		
	$2,83 \times 10^4$	1,9

Table A.4: Standard deviation of *N. oceanica* cell concentrations measured by hemocytometer for determination of correlation between hemocytometer and OD_{750nm} (addition to the table A.2).

OD_{750nm} measured using Tecan Infinite 200 Pro	STD OD_{750nm}	STD %
5,69×10 ⁶	-	-
4,13×10 ⁶	6,36×10 ⁴	1,5
3,12×10 ⁶	2,55×10 ⁵	8,2
1,89×10 ⁶	1,41×10 ⁴	0,7
9,56×10 ⁵	-	-
5,37×10 ⁵	1,98×10 ⁴	3,7
4,50×10 ⁵	3,61×10 ⁴	8,0
3,57×10 ⁵	4,24×10 ³	1,2
2,62×10 ⁵	5,66×10 ³	2,2
Average		
	5,69×10 ⁴	3,6

Table A.5: Standard deviation of OD_{750nm} of *N. oceanica* cell dilution series measured by Tecan Infinite® 200 Pro Multimode Reader. The data were used for determination of correlation between flow cytometer and OD_{750nm}, and hemocytometer and OD_{750nm} (addition to the table A.2).

Cell concentration by hemocytometer (cell/mL)	STD hemocytometry	STD %
0,1169	-	-
0,0868	0,0041	4,7
0,0646	0,0017	2,6
0,0433	0,0006	1,4
0,0212	0,0018	8,7
0,0119	0,0012	10,2
0,0117	0,0006	4,8
0,0104	0,0015	13,3
0,0062	0,0002	3,4
Average		
	0,0015	6,1

Table A.6: The *N. oceanica* cell count loss after the treatment with glutaraldehyde (0.1-1%) as a potential storage method measured by flow cytometer using the same settings as for count determination of untreated cell sample (table A.2). The standard deviation of the cell concentrations and average cell count loss for both each dilution sample and for all samples are given.

Dilution series	Cell concentration by flow cytometer (cell/mL)	STD	STD %	Average cell loss %
1:0.5	$3,38 \times 10^6$	$6,38 \times 10^4$	1,9	6,8
1:1	$2,47 \times 10^6$	$3,55 \times 10^3$	0,1	2,4
1:2	$1,65 \times 10^6$	$1,06 \times 10^4$	0,6	1,4
1:5	$7,90 \times 10^5$	$3,05 \times 10^4$	3,9	1,4
Average				
			1,6	3,0

Table A.7: The *N. oceanica* cell count loss after the snap-freeze with liquid nitrogen as a potential storage method measured by flow cytometer using the same settings as for count determination of untreated cell sample (table A.2). The standard deviation of the cell concentrations and average cell count loss for both each dilution sample and for all samples are given.

Dilution series	Cell concentration by flow cytometer (cell/mL)	STD	STD %	Average cell loss %
1:0.5	$3,29 \times 10^6$	$3,80 \times 10^4$	1,2	9,2
1:1	$2,31 \times 10^6$	$1,20 \times 10^5$	5,2	8,7
1:2	$1,73 \times 10^6$	$4,32 \times 10^4$	2,5	-3,3
1:5	$8,38 \times 10^5$	$2,96 \times 10^4$	3,5	-4,5
1:9	$5,32 \times 10^5$	$2,84 \times 10^3$	0,5	1,4
1:11	$4,25 \times 10^5$	$3,10 \times 10^3$	0,7	3,1
1:15	$3,17 \times 10^5$	$3,69 \times 10^3$	1,2	2,9
1:19	$2,49 \times 10^5$	$2,23 \times 10^3$	0,9	1,1
Average				
			2,0	2,3

Table A.8: The *N. oceanica* cell count loss after the second snap-freeze in liquid nitrogen as a potential storage method measured by flow cytometer using the same settings as for count determination of untreated cell sample (table A.2). The standard deviation of the cell concentrations and average cell count loss for both each dilution sample and for all samples are given.

Dilution series	Cell concentration by flow cytometer (cell/mL)	STD	STD %	Average cell loss %
1:0.5	$3,25 \times 10^6$	$1,39 \times 10^5$	4,3	10,3
1:1	$2,53 \times 10^6$	$1,65 \times 10^5$	6,5	0,1
1:2	$1,71 \times 10^6$	$2,87 \times 10^4$	1,7	-2,4
1:5	$7,48 \times 10^5$	$5,70 \times 10^3$	0,8	6,6
1:9	$5,23 \times 10^5$	$8,35 \times 10^3$	1,6	3,0
1:11	$4,29 \times 10^5$	$4,28 \times 10^2$	0,1	2,1
1:15	$3,18 \times 10^5$	$8,20 \times 10^2$	0,3	2,8
1:19	$2,49 \times 10^5$	$5,27 \times 10^3$	2,1	1,1
Average				
			2,2	2,9

Table A.9: Dilution series of a very dense *N. oceanica* cell culture and their concentrations measured with flow cytometer with corresponding OD_{750nm} values are presented. The cell concentration of the samples were additionally calculated using the theoretical dilution factors. The data were used in order to continue the previously established correlation line between flow cytometry and OD_{750nm}. The attempt was to determinate at what cell concentration and OD_{750nm} value the correlation would not be reliable as an indicator of cell growth. The cell concentration value marked bold indicates the breaking point, after which the cell concentration decreases drastically with continuously increasing OD_{750nm} values. The theoretical cell concentrations indicate the significant difference between the real cell concentration values compared to the values determined by flow cytometer.

Dilution series	Cell concentration by flow cytometer (cell/mL)	Cell concentration calculated with dilution factors (cell/mL)	OD_{750nm} measured by Tecan Infinite 200 Pro
High	6,69×10 ⁶	3,95×10 ⁷	0,6232
1:0.5	1,67×10 ⁷	2,63×10 ⁷	0,4493
1:1	1,91×10 ⁷	1,98×10 ⁷	0,3572
1:1.5	2,09×10 ⁷	1,58×10 ⁷	0,2873
1:2	2,19×10⁷	1,32×10 ⁷	0,2508
1:2.5	2,06×10 ⁷	1,13×10 ⁷	0,2250
1:3	1,88×10 ⁷	9,88×10 ⁶	0,1979
1:5	1,28×10 ⁷	6,58×10 ⁶	0,1389
1:7	9,75×10 ⁶	4,94×10 ⁶	0,1055

Table A.10: The standard deviations of the cell concentration values measured by flow cytometer and corresponding OD_{750nm} values presented in table A.9.

Dilution series	STD flow cytometer	STD %	STD OD_{750nm}	STD %
High	6,09×10 ⁵	9,9	0,0118	1,8
1:0.5	5,08×10 ⁴	0,8	0,0002	0,0
1:1	5,10×10 ⁴	0,7	0,0062	1,6
1:1.5	1,88×10 ⁵	1,1	0,0045	1,4
1:2	3,44×10 ⁵	2,1	0,0053	1,9
1:2.5	3,31×10 ⁵	2,0	0,0156	6,2
1:3	2,20×10 ⁵	1,3	0,0064	2,8
1:5	1,26×10 ⁵	0,7	0,0027	1,6
1:7	1,43×10 ⁵	0,7	0,0040	3,0
Average				
	2,29×10 ⁵		2,1	0,0063
				2,3

Appendix B – Chapter III: Cell Growth Assay (Antibiotic Susceptibility)

Table B.1: *N. oceanica* and *N. gaditana* wild type cells were growing at 23°C and constant light intensity of 100 $\mu\text{E m}^{-2} \text{s}^{-1}$ including continuous rotational shaking. The cell cultures of *N. oceanica* and *N. gaditana* were prepared dilution series of having certain values of OD_{750nm} corresponding to certain cell concentration. *N. oceanica* and *N. gaditana* cell samples of different concentrations were spotted 3 μL onto agar-solidified Cell-Hi CN medium containing different antibiotic type at various concentration. The subsequent incubation was performed under the same growth conditions as for wild type cell cultures, namely 23°C, constant light intensity of 100 $\mu\text{E m}^{-2} \text{s}^{-1}$, and continuous rotational shaking.

OD of cells spotted on agar plates	1.0	0.1	0.055	0.010	0.0055
Cell concentration (cells/mL) according to OD value	$4,98 \times 10^7$	$4,77 \times 10^6$	$2,52 \times 10^6$	$2,65 \times 10^5$	$4,00 \times 10^4$
Cell amount spotted on agar plates in 3.0 μL (cells)	$1,49 \times 10^5$	$1,43 \times 10^4$	$7,56 \times 10^3$	$7,95 \times 10^2$	$1,20 \times 10^2$

Appendix C – Chapter IV: Transformation by Electroporation

Table C.1: The colonies of selected *N. oceanica* cells after the transformation by electroporation at different parameters appeared on the selective medium (master plates) containing 50 µg/mL hygromycin. In order to confirm the formation of the transformants caused by successful insertion of the hygromycin resistance cassette and not by spontaneous mutation or growth on a potential antibiotic-free media, the cell colonies were transferred onto the new master plates with selective medium (# 3). These contained hygromycin concentration of 50 and 75 µg/mL in order to observe the transformants' higher tolerance to the antibiotic. The table gives the number of the colonies from the master plate # 1 transferred onto two new master plates # 3 with different antibiotic concentration. The appearance of the new colonies is described as either "Green", "Little green", "Yellow", and "Little yellow".

Electroporation conditions	Master plate # 1 (colony number)	Master plate # 3 (50 and 75 µg/uL) (colony/location number)	Cell growth (50 µg/uL)	Cell growth (75 µg/uL)
EL_4 Cell-Hi CN				
2200V 1.2µg	2	1	Green	Green
2200V 1.2µg	3	2	Green	Green
2200V 1.2µg	4	3	Green	Green
Neg. 2200V	10	4	Little green	No colonies
Neg. 2200V	11	5	Little green	No colonies
1800V 4µg	26	6	Green	Green
1800V 4µg	28	7	Green	Green
1100V 1.2µg	32	8	No colonies	No colonies
1100V 1.2µg	34	9	No colonies	No colonies
1100V 4µg	39	10	No colonies	No colonies
1100V 4µg	40	11	No colonies	No colonies
EL_4 f/2				
2200V 1.2µg	41	12	Green	Green
2200V 4µg	44	13	Green	Green
2200V 4µg	45	14	Green	Green
2200V 4µg	46	15	Green	Green
1800V 1.2µg	49	16	Green	Green
EL_5 Cell-Hi CN				
Neg. 2200V	68	17	Little yellow	Little yellow
Neg. 2200V	70	18	Little yellow	Little yellow
Neg. 2200V	73	19	Little yellow	Little yellow
1800V 4.5µg	77	20	Yellow	Little yellow
1800V 4.5µg	78	21	Yellow	Little yellow
1800V 4.5µg	80	22	No colonies	Little yellow
1400V 4.5µg	83	23	No colonies	Little yellow
1400V 4.5µg	85	24	Yellow	Little yellow
1400V 4.5µg	86	25	Yellow	Little yellow

1400V 4.5µg	88	26	Yellow	Little yellow
2200V 1µg	90	27	Little yellow	Little yellow
2200V 1µg	91	28	Little yellow	Little yellow
1800V 1µg	96	29	Yellow	Little yellow
1800V 1µg	98	30	Yellow	Little yellow
1800V 1µg	99	31	Yellow	Little yellow
1800V 1µg	100	32	Yellow	Little yellow
1800V 1µg	101	33	Yellow	Little yellow
1400V 1µg	102	34	No colonies	Little yellow
1400V 1µg	103	35	Little yellow	Little yellow
1400V 1µg	104	36	Little yellow	Little yellow
1400V 1µg	105	37	Little yellow	Little yellow
1400V 1µg	106	38	Little yellow	Little yellow
1400V 1µg	107	39	Little yellow	Little yellow
1400V 1µg	108	40	Little yellow	Little yellow
EL_5 f/2				
1800V 4.5µg	110	41	Yellow	Little yellow
1400V 1µg	112	42	Yellow	Little yellow
1400V 1µg	115	43	Green	Green
1800V 1µg	118	44	Green	Green
1800V 1µg	119	45	Yellow	Yellow
1800V 1µg	120	46	Yellow	Yellow
EL_2 Cell-Hi CN				
Neg. 2200V	149	47	No colonies	No colonies
Neg. 2200V	151	48	No colonies	No colonies
1800V 1.5µg	153	49	No colonies	No colonies
1800V 1.5µg	157	50	Green	Green
1800V 1.5µg	158	51	Little green	Little green
EL_1 Cell-Hi CN				
2200V 3µg	168	52	No colonies	Little green
EL_5 Cell-Hi CN				
1400V 4.5µg	179	53	Yellow	Yellow
1400V 4.5µg	180	54	Yellow	Yellow
1400V 4.5µg	183	55	Yellow	Yellow

Table C.2: The colonies of selected *N. oceanica* cells after the transformation by electroporation at different parameters appeared on the selective medium (master plates) containing 50 µg/mL hygromycin. In order to confirm the formation of the transformants caused by successful insertion of the hygromycin resistance cassette and not by spontaneous mutation or growth on a potential antibiotic-free media, the cell colonies were transferred on the new master plates with selective medium (# 3). These contained hygromycin concentration of 50 and 75 µg/mL in order to observe the transformants' higher tolerance to the antibiotic. The table gives the number of the colonies from the master plate # 2 transferred onto two new master plates # 3 with different antibiotic concentration. The appearance of the new colonies is described as either "Green", "Little green", "Yellow", and "Little yellow".

Conditions	Master plate # 2 (colony number)	Master plate # 3 (50 and 75 µg/uL) (colony/location number)	Growth (50 µg/uL)	Growth (75 µg/uL)
EL_4 Cell-Hi CN				
2200V 1.2µg	1	56	Little green	Little green
2200V 1.2µg	2	57	Little green	Little green
2200V 1.2µg	3	58	Little green	Little green
2200V 1.2µg	4	59	Green	Green
2200V 1.2µg	5	60	Little green	Little green
2200V 1.2µg	6	61	Green	Little green
2200V 4µg	7	62	Little green	Little green
2200V 4µg	8	63	Little green	No colonies
2200V 4µg	9	64	Little green	Little green
1800V 4µg	10	65	Green	Little green
1800V 4µg	11	66	Little green	Little green
1100V 1.2µg	12	67	Green	Little green
1100V 1.2µg	13	68	Little green	Little green
1100V 1.2µg	14	69	Little green	Little green
1100V 1.2µg	15	70	Little green	Little green
1100V 4µg	16	71	Little green	Little green
1100V 4µg	17	72	Little green	Little green
1100V 4µg	18	73	Little green	Little green
Neg. 2200V	19	74	Green	Little green
Neg. 2200V	20	75	Green	Little green
Neg. 2200V	21	76	Green	Little green
EL_4 f/2				
2200V 1.2µg	22	77	Green	Little green
2200V 1.2µg	23	78	Green	Little green
2200V 1.2µg	24	79	Green	No colonies
2200V 4µg	25	80	Green	Green
2200V 4µg	26	81	Green	Green
2200V 4µg	27	82	Green	Green
2200V 4µg	28	83	Green	Green
1800V 1.2µg	29	84	Green	Green

1800V 1.2µg	30	85	Green	Green
1800V 1.2µg	31	86	Green	Little green
1800V 4µg	32	87	Green	Little green
1800V 4µg	33	88	Green	Little green
1800V 4µg	34	89	Green	Green
EL_5 Cell-Hi CN				
Neg. 2200V	35	90	Little green	Little green
Neg. 2200V	36	91	Little green	Little green
Neg. 2200V	37	92	Green, little yellow	Little green
Neg. 2200V	38	93	Green, little yellow	Little green
Neg. 2200V	39	94	Green, little yellow	Little green
Neg. 2200V	40	95	Yellow	Yellow
Neg. 2200V	41	96	Yellow	Yellow
1400V 4.5µg	42	97	Green, little yellow	Green, little yellow
1400V 4.5µg	43	98	Green, little yellow	Green, little yellow
1400V 4.5µg	44	99	Green, little yellow	Green, little yellow
1400V 4.5µg	45	100	Green, little yellow	Green, little yellow
2200V 1µg	46	101	Green, little yellow	Green, little yellow
2200V 1µg	47	102	Green, little yellow	Green, little yellow
2200V 1µg	48	103	Green, little yellow	Green, little yellow
1800V 1µg	49	104	Green, little yellow	Green, little yellow
1800V 1µg	50	105	Green, little yellow	Green, little yellow
1800V 1µg	51	106	Green, little yellow	Green, little yellow
1800V 1µg	52	107	Green, little yellow	Green, little yellow
1800V 1µg	53	108	Green, little yellow	Green, little yellow
1400V 1µg	54	109	Green, little yellow	Green, little yellow
1400V 1µg	55	110	Green, little yellow	Green, little yellow
1400V 1µg	56	111	Green, little yellow	Green, little yellow
1400V 1µg	57	112	Green, little yellow	Green, little yellow
EL_3 Cell-Hi CN				
Neg. 1800V	58	113	Green, little yellow	Little green
Neg. 1800V	59	114	Green, little yellow	Little green
Neg. 1800V	60	115	Little green	Little green
Neg. 1800V	61	116	Little green	Little green
Neg. 1800V	62	117	Little green	Little green
2200V 1.5µg	63	118	Little green	Little green
2200V 1.5µg	64	119	Little green	Little green
2200V 1.5µg	65	120	Little green	Little green
2200V 1.5µg	66	121	Little green	Little green
1800V 4.1µg	67	122	Little green	Little green
1800V 4.1µg	68	123	Little green	Little green
1800V 4.1µg	69	124	Little green	Little green
1800V 4.1µg	70	125	Little green	Little green
1800V 4.1µg	71	126	Little green	Little green

1800V 4.1µg	72	127	Little green	Little green
1800V 4.1µg	73	128	Little green	Little green
EL_2 Cell-Hi CN				
Neg. 2200V	75	130	Little green	Little green
Neg. 2200V	76	131	Little green	Little green
Neg. 2200V	77	132	Little green	Little green
Neg. 2200V	78	133	Little green	Little green
1800V 1.5µg	79	134	Little green	Little green
1800V 1.5µg	80	135	Little green	Little green
EL_1 Cell-Hi CN				
2200V 3µg	82	136	Little green	Green
2200V 3µg	83	137	Little green	Green
2200V 3µg	84	138	Little green	Green
2200V 3µg	85	139	Little green	Green, little yellow
200V 3µg	86	140	Green, little yellow	Little green
2200V 3µg	87	141	No colonies	No colonies
Neg. 2200V	89	142	Green	Green

Table C.3: *N. oceanica* CCMP1779 cells transformed under different transformation parameters were incubated for different periods at 96°C in order to release the genomic DNA, for subsequent PCR-amplification of potentially inserted hygromycin resistance cassette by random incorporation into the genome. The concentration of the released genomic DNA was too low to proceed with PCR-amplification, as the concentration values indicated the noise detected by the NanoDrop 100 spectrophotometer and not a significant DNA amount.

Incubation time	Colony number from master plate # 3	Transformation conditions	Genomic DNA concentration (ng/µL)
6 min	3	2200 V 1.2 µg	7.0
	4	2200 V 1.2 µg	1.9
	93	2200 V 1.0 µg	6.7
8 min	46	2200 V 4.0 µg	5.9
	70	2200 V Negative	7.1
	91	2200 V 1.0 µg	8.7
10 min	10	2200 V Negative	3.6
	44	2200 V 4.0 µg	5.2
	88	1400 V 4.5 µg	7.7

Table C.4: The cell colonies (picked from the master plate # 3 see table B.1 and B.2) of *N. oceanica* CCMP1779 transformed with pSELET100 plasmid were incubated at 100°C and snap-frozen in the liquid nitrogen twice in order to disrupt the cell wall and release the genomic DNA. The procedure was conducted for the subsequent PCR-amplification of the potentially inserted hygromycin resistance cassette by random incorporation into the cell genome. The concentration of released genomic DNA was too low to proceed with PCR-amplification, as the concentration values indicated the noise detected by the NanoDrop 100 spectrophotometer and not a significant DNA amount.

Colony number from master plate # 3	Transformation conditions (voltage, plasmid amount)	Genomic DNA concentration after boiling at 100°C (ng/μL)	Genomic DNA concentration after snap-freezing x2 (ng/μL)
3, 4, 5	2200V 1.2 μg	3.4	4.5
77, 78, 79	1800V 4.5 μg	5.2	4.6
94, 95, 96	1800V 1.0 μg	4.6	6.5
102, 103, 104	1400V 1.0 μg	7.7	4.9

Table C.5: A series of tables showing the calculation of transformation efficiencies for each transformation performed on *N. oceanica* cells by electroporation (abbreviated EL_`number`) including the growth medium (Cell-Hi CN or f/2 medium). The parameters of parallel transformation samples including voltage (V) and pSELECT100 amount (μg) are given, following the amount of the cells plated out on the selective medium containing 50 μg/mL hygromycin. The number of colonies formed after 2-4 weeks of incubation at 23°C, constant light intensity of 100 μE m⁻² s⁻¹ and continuous rotational shaking is presented. The transformation efficiency is the relation between the cells plated out, the formed colonies and the transformation plasmid amount. The units for transformation efficiency is colonies/cells/μg.

	EL_5 Cell-Hi CN					
Conditions	2200 V	1800 V	1400 V	2200 V	1800 V	1400 V
Plasmid amount (μg)	Neg.	4,5	4,5	1	1	1
Cells plated out	3,50×10 ⁶	3,50×10 ⁶	3,50×10 ⁶	3,50×10 ⁶	3,50×10 ⁶	3,50×10 ⁶
Colonies grown	21	0	37	0	19	16
Colonies/cells plated out	6,00×10 ⁻⁶	-	1,06×10 ⁻⁵	-	5,43×10 ⁻⁶	4,57×10 ⁻⁶
Transf. efficiency	-	-	2,35×10 ⁻⁶	-	5,43×10 ⁻⁶	4,57×10 ⁻⁶

EL_5 F/2						
Conditions	2200 V	1800 V	1400 V	2200 V	1800 V	1400 V
Plasmid amount (µg)	Neg.	4,5	4,5	1	1	1
Cells plated out	$3,50 \times 10^6$	$3,50 \times 10^6$	$3,50 \times 10^6$	$3,50 \times 10^6$	$3,50 \times 10^6$	$3,50 \times 10^6$
Colonies grown	15	0	4	1	42	40
Colonies/cells plated out	$4,29 \times 10^{-6}$	-	$1,14 \times 10^{-6}$	$2,86 \times 10^{-7}$	$1,20 \times 10^{-5}$	$1,14 \times 10^{-5}$
Transf. efficiency	-	-	$2,54 \times 10^{-7}$	$2,86 \times 10^{-7}$	$1,20 \times 10^{-5}$	$1,14 \times 10^{-5}$

EL_4 Cell-Hi CN						
Conditions	2200 V	1800 V	1400 V	2200 V	1800 V	1400 V
Plasmid amount (µg)	1,2	4,5	4,5	1	1	1
Cells plated out	$3,50 \times 10^6$	$3,50 \times 10^6$	$3,50 \times 10^6$	$3,50 \times 10^6$	$3,50 \times 10^6$	$3,50 \times 10^6$
Colonies grown	12	0	37	0	19	16
Colonies/cells plated out	$3,43 \times 10^{-6}$	-	$1,06 \times 10^{-5}$	-	$5,43 \times 10^{-6}$	$4,57 \times 10^{-6}$
Transf. efficiency	$2,86 \times 10^{-6}$	-	$2,35 \times 10^{-6}$	-	$5,43 \times 10^{-6}$	$4,57 \times 10^{-6}$

EL_4 F/2						
Conditions	2200 V	1800 V	1400 V	2200 V	1800 V	1400 V
Plasmid amount (µg)	1,2	4,5	4,5	1	1	1
Cells plated out	$3,50 \times 10^6$	$3,50 \times 10^6$	$3,50 \times 10^6$	$3,50 \times 10^6$	$3,50 \times 10^6$	$3,50 \times 10^6$
Colonies grown	1	2	4	9	0	1
Colonies/cells plated out	$2,86 \times 10^{-7}$	$5,71 \times 10^{-7}$	$1,14 \times 10^{-6}$	$2,57 \times 10^{-6}$	-	$2,86 \times 10^{-7}$
Transf. efficiency	$2,38 \times 10^{-7}$	$1,27 \times 10^{-7}$	$2,54 \times 10^{-7}$	$2,57 \times 10^{-6}$	-	$2,86 \times 10^{-7}$

EL_3 Cell-Hi CN			
Conditions	1800 V	2200 V	1800 V
Plasmid amount (µg)	Neg.	1,5	4,1
Cells plated out	$3,90 \times 10^7$	$3,90 \times 10^7$	$3,90 \times 10^7$
Colonies grown	33	11	21
Colonies/cells plated out	$8,46 \times 10^{-7}$	$2,82 \times 10^{-7}$	$5,39 \times 10^{-7}$
Transf. efficiency	-	$1,88 \times 10^{-7}$	$1,31 \times 10^{-7}$

EL_2 Cell-Hi CN			
Conditions	2000 V	1800 V	2000 V
Plasmid amount (µg)	Neg.	1,5	1,5
Cells plated out	$3,50 \times 10^6$	$3,50 \times 10^6$	$3,50 \times 10^6$
Colonies grown	27	8	0
Colonies/cells plated out	$7,71 \times 10^{-6}$	$2,29 \times 10^{-6}$	-
Transf. efficiency	-	$1,52 \times 10^{-6}$	-

EL_1 Cell-Hi CN			
Conditions	2200 V	2200 V	2200 V
Plasmid amount (µg)	Neg.	3	3
Cells plated out	$6,55 \times 10^6$	$6,55 \times 10^6$	$6,55 \times 10^6$
Colonies grown	6	17	0
Colonies/cells plated out	$9,16 \times 10^{-7}$	$2,59 \times 10^{-6}$	-
Transf. efficiency	-	$8,65 \times 10^{-7}$	-

EL_1 Cell-Hi CN			
Conditions	2200 V	2200 V	2200 V
Plasmid amount (µg)	Neg.	3	3
Cells plated out	$1,87 \times 10^7$	$1,87 \times 10^7$	$1,87 \times 10^7$
Colonies grown	325	200	150
Colonies/cells plated out	$1,74 \times 10^{-5}$	$1,07 \times 10^{-5}$	$8,01 \times 10^{-6}$
Transf. efficiency	-	$3,56 \times 10^{-6}$	$2,67 \times 10^{-6}$

EL_sperm Cell-Hi CN					
Conditions	1800 V	1800 V	1800 V	1800 V carrier DNA	1800 V Carrier DNA
Plasmid amount (µg)	Neg.	4	1,5	4	1,5
Cells plated out	$1,75 \times 10^{-6}$	$1,75 \times 10^{-6}$	$1,75 \times 10^{-6}$	$1,75 \times 10^{-6}$	$1,75 \times 10^{-6}$
Colonies grown	31	0	107	0	21
Colonies/cells plated out	$1,77 \times 10^5$	-	$6,11 \times 10^{-5}$	-	$1,20 \times 10^{-5}$
Transf. efficiency	-	-	$4,08 \times 10^{-5}$	-	$8,00 \times 10^{-6}$

Table C.6: The average of all transformations by electroporation performed on *N. oceanica* CCMP1779 cells at different parameters (various voltages and plasmid DNA amounts) is given, in addition indicating the transformation parallel (EL_`number`). The efficiency average is presented for the transformations performed at the same conditions but on the cells growing in different growth media, Cell-Hi CN or f/2 medium. The standard deviation are available for these transformation samples. As shown in the table C.5 the transformation of the cells growing in f/2 medium resulted in significantly lower transformation efficiency value compared to cells growing in Cell-Hi CN medium causing the standard deviation to increase drastically for some samples. The transformation efficiency value marked bold is the highest efficiency achieved at the master project.

Transformation number	Transformation parameters	Average transformation efficiencies (colonies/cells/µg)	STD	STD %
EL_5	1400 V 4.5µg	$1,30 \times 10^{-6}$	$1,48 \times 10^{-6}$	113,8
EL_4	1400 V 4.5µg	$1,14 \times 10^{-6}$	$1,26 \times 10^{-6}$	110,0
EL_5	1400 V 1µg	$8,00 \times 10^{-6}$	$4,85 \times 10^{-6}$	60,6
EL_4	1400 V 1µg	$2,71 \times 10^{-6}$	$3,43 \times 10^{-6}$	126,5
EL_3	1800 V 4.1µg	$1,31 \times 10^{-7}$	-	-
EL_5	1800 V 1µg	$8,71 \times 10^{-6}$	$4,65 \times 10^{-6}$	53,3
EL_4	1800 V 1µg	$4,57 \times 10^{-6}$	-	-
EL_2	1800 V 1.5µg	$1,52 \times 10^{-6}$	-	-
EL_sperm	1800 V 1.5 µg	$4,08 \times 10^{-5}$	-	-
EL_sperm	1800 V 1.5 µg + 15µg sperm	$8,00 \times 10^{-6}$	-	-
EL_1	2200 V 3µg	$1,99 \times 10^{-6}$	$1,59 \times 10^{-6}$	80,0
EL_3	2200 V 1.5µg	$1,88 \times 10^{-7}$	-	-
EL_4	2200 V 1.2µg	$1,55 \times 10^{-6}$	$1,85 \times 10^{-6}$	119,7
EL_5	2200 V 1µg	$2,86 \times 10^{-7}$	-	-
EL_4	2200 V 1µg	$2,57 \times 10^{-6}$	-	-

Table C.7: The average of all transformations of *N. oceanica* cells with pSELECT100 plasmid is sorted in the groups by the voltage applied at electroporation and the used plasmid quantities ranging between “Low” (1-1.5 µg) and “High” (3-4.5 µg). The table is the summary of the table C.6. However, determination of the transformation efficiency-average of the group “1800V Low” did not include the value of the highest achieved transformation efficiency of $4,08 \times 10^{-5}$ colonies/cells/µg due to very high value significantly influencing the average of the transformation efficiency of this group.

Transformation conditions	Average of transformation efficiencies (colonies/cells/µg)	STD	STD%
2200V High	$1,99 \times 10^{-6}$	-	-
2200V Low	$1,15 \times 10^{-6}$	$1,13 \times 10^{-6}$	98,7
1800V High	$1,31 \times 10^{-7}$	$9,29 \times 10^{-8}$	70,7
1800V Low	$5,70 \times 10^{-6}$	$3,32 \times 10^{-6}$	58,2
1400V High	$1,22 \times 10^{-6}$	$1,12 \times 10^{-7}$	9,2
1400V Low	$5,36 \times 10^{-6}$	$3,74 \times 10^{-6}$	69,8

Table C.8: The average of all transformations of *N. oceanica* cells with pSELECT100 plasmid is sorted by the voltage applied at electroporation and the used plasmid quantities ranging between “Low” (1-1.5 µg) and “High” (3-4.5 µg). The table is the summary of the table C.6, including the highest achieved transformation efficiency of $4,08 \times 10^{-5}$ colonies/cells/µg. Comparing the standard deviations marked bold from table C.7 and C.8, the influence of the highest transformation efficiency of $4,08 \times 10^{-5}$ colonies/cells/µg on the average of the transformation efficiency of the group “1800V Low” is obvious.

Transformation conditions	Average of transformation efficiencies (colonies/cells/µg)	STD	STD%
2200V High	$1,99 \times 10^{-6}$	-	-
2200V Low	$1,15 \times 10^{-6}$	$1,13 \times 10^{-6}$	98,7
1800V High	$1,31 \times 10^{-7}$	$9,29 \times 10^{-8}$	70,7
1800V Low	$1,27 \times 10^{-5}$	$1,59 \times 10^{-5}$	125,4
1400V High	$1,22 \times 10^{-6}$	$1,12 \times 10^{-7}$	9,2
1400V Low	$5,36 \times 10^{-6}$	$3,74 \times 10^{-6}$	69,8

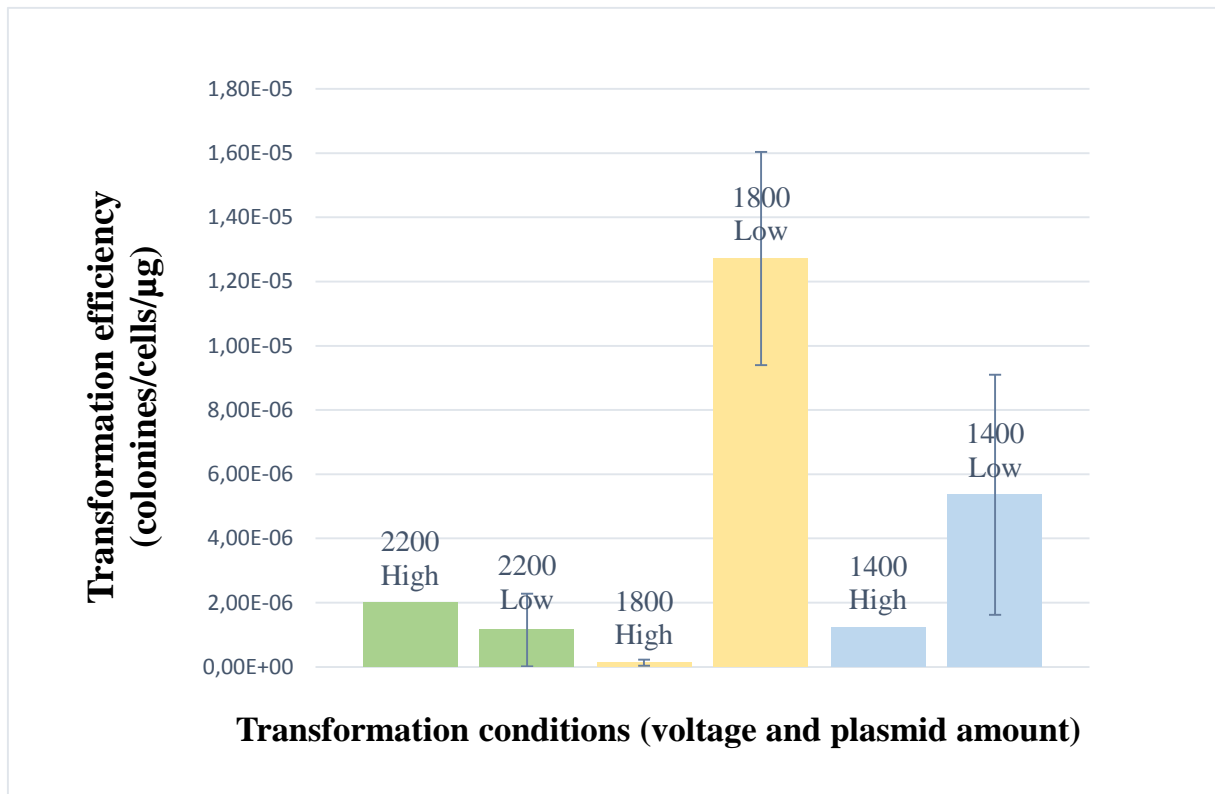


Figure C.1: Average of the transformation efficiencies based on various electroporation conditions applied at the transformation of *N. oceanica* cells. The most significant parameters determining transformation efficiency were the voltage applied at the electroporation and the amount of PCR-amplified transformation plasmid pSELECT100. The average of transformations where the cells were added either high (3 – 4.5 μg) or low (1 – 1.5 μg) amount of the PCR-amplified plasmid is shown. The average of transformation efficiency of the group “1800 V High” included the value of the highest transformation efficiency achieved during the master project, $4,08 \times 10^{-5}$ colonies/cells/μg. However, this value influence the average of this group to a large extent and therefore was excluded from the calculation of the conclusive average value.

Appendix D – Chapter V: Gibson Assembly

Part of the *N. oceanica* CCMP531 genome between *ycf54* gene and *secA* gene containing the DNA gap 2240 bp long (located between 55355 – 57596 bp). At exactly position 56285 – 56311 bp the DNA sequence (marked yellow) is least conserved and is a region for the potential insertion of the chloramphenicol resistance cassette of the plasmid pLit_chlL_chlor.

TAAGTAGCCAAAATAGATGGCTTTAA (26 bp long)

```
TTAAAACCTTCTTCAACTGGTTCTATTTTCGAATAAGAATTCCTTAGTTGCAAGTATAAAAATAATATTTTCATAAGAA
ATTATTTTCTTTAGTTGATAATTATTCCTCTTCTTGAGGATTTTTTAATTGTTGCAAGTGTCTGCTTTTGTGTACAAG
TGGTATCTTAGGATTTTTTATTATAAAATTATATAATACAAGCAATTATATACTAAAACAGCAAGACTTATAAATGC
TAAGGGTGATAAAAATAAAGTGATTTAAAAATAATAACCAATTAATAATAGTCCTGTTTTATTTGTAATTCGTATCT
TTGGACAAGATTTGTAAAGATGCTTATAGGTTCTTCTCTTTCCCTATATTTTAGTACATTCAGGTGTTTTACTAA
GTAATTACTAAAAGTATATCTTTAATTAGCTTGCTGCATTCAAAAATAGTTATTGCAATTTCTTGACTTAACCG
TAGACTATAATTTATCAATAAAAAGATAAATGCAATACTACCATTATAACCAAGTTTGTAGGGTAATTTTAAATGA
TTTATACCCTGTAGGAAATATAAGAAAATATGCAATAATAACCCAAAATTTGTACCATTTTATTATAACTATTTAT
TAACGGGTTACATATTCTAATTAAGTAGTAAGGAAAGGAATTTTTTCAAAAAATTTATTTGAAAACTACTTAC
AATTAACTCTTCATATTCTTGTATATATGGTACTAAAGATTGATTAGCTAAAAAAAATAAAAGGTATAAAAATATAT
TTTTAAAATAAATCCGATTTCGATTTAAATAGATTAATAAATTCCTTTTTATCAAAAATAGTCTCTAAACCTTAGCGA
TTTTACTAAAAAATCGTTAAGATTATGAATTATAAATTTAGAATAGCTGATTACCCATTTGAAAACTTACTATT
ATTGTATATACGGGTTGTAAGATTCAGTTTTTTATTCTTTTTATTAAATAAATCCAATAAAAAAATAAATTTTT
TTCAATTTTTATAAATTTATTTAAATTAAGTAGCCAAAATAGATGGCTTTAATTCTAAAAAATCTACTTTTATTTT
TTGAACTAAAAATTTTAACTTACTTACTTTTTTCGCGTATTATATAAATAAATTTAGTTTAGCTATGAAAATTTT
ATTTATATAAAACTGGCTCTTCAATTTTTGCCAACATTATGTTTATGAACGTATCTTGAAAAGTTTATTTGTTC
ATTAACCTTTTCATACTTTAAGATACTAAATTTTTTTATAGCTTGCTTAGATACGTTTAAACGAGCTTTATATTTT
TATATATAAGTTCTTAAATTGTTTATGATTATTAATAGATTTAATAGTTGTTAAATTATTAATTTGATCGTATTTT
ATGCTTTTCTTGGTCTAATTTTATAGAATTAATAATTACTTTAAGAATTTTTTGGACTTTTAAAGAAAAGTTTGTGA
CTTTCCCTCTATTGTATTATTGGATTGATTTTGTATATTCTCCATATGTTATTTTTTTATTTTGTAAACTTATTA
AAACACAAAAGTTTTTAAACGCTTTTTTAAAAAATATAAAAAGCATCAAACTTTGGTTTTTGGACTATATGAATTAT
AGAATGTTGTATAACTCTTCTTAGAAAGTCCTTTGTTTGTATGCAATTTTATAATCTAAGTTAATTAGAATAATAG
ACATGAAATTAATATTAGCGAAGCTTGTAAATATTTTTTATAAGTTTTACAAAGTTGCATTAACAAGTTAGTTAAAT
TTTTTCTTAATAAAAAGAAAATTAATGAGCTTCGTAAATGGAAAATTTTTAAAAGAGCTTTTAAGTATATTTTAA
AAAAGACATAATTTTCAACTAAGAGTTTTTTGTATCTTACATATTTTAAATAATAGATATATCAAGCTAAGAATAC
TTAATGCCTTTAATTTACTAAAACTTTAAAGTTAGTGTAGTAATTTTCTGGGTATAAAGAGTAGATTTTCTTT
GAAAATCGTATCTAATCATTTGTTTATTCTCAATTAGATCAACAAAGATTTGATCTAAAAATTTTTCTGTGTATGA
AT
```

Figure D.1: **DNA region of the *N. oceanica* chloroplast genome.** The region includes 1000 bp of left flanking region upstream for the most unconserved DNA sequence (marked yellow) and 1000 bp of right flanking region. The design of the primers (marked green) using IDT Primed Quest for subsequent PCR-amplification of the left flanking region of the chloroplast genome resulted in only one possible primer pair, which was unsatisfactory. The region excluded the most conserved DNA region (marked brown) also located near to the least conserved region. This would cause the deletion of this conserved DNA region after potential transformation with a plasmid. As the region is evolutionary significant and therefore stayed conserved through the *Nannochloropsis* species, the deletion of the region could be fatal for the cells.